MONOVALENT IONS AND GLUCOSE ABSORPTION IN GOLDFISH INTESTINE

T. ZUIDEMA

MONOVALENT IONS AND GLUCOSE ABSORPTION IN GOLDFISH INTESTINE

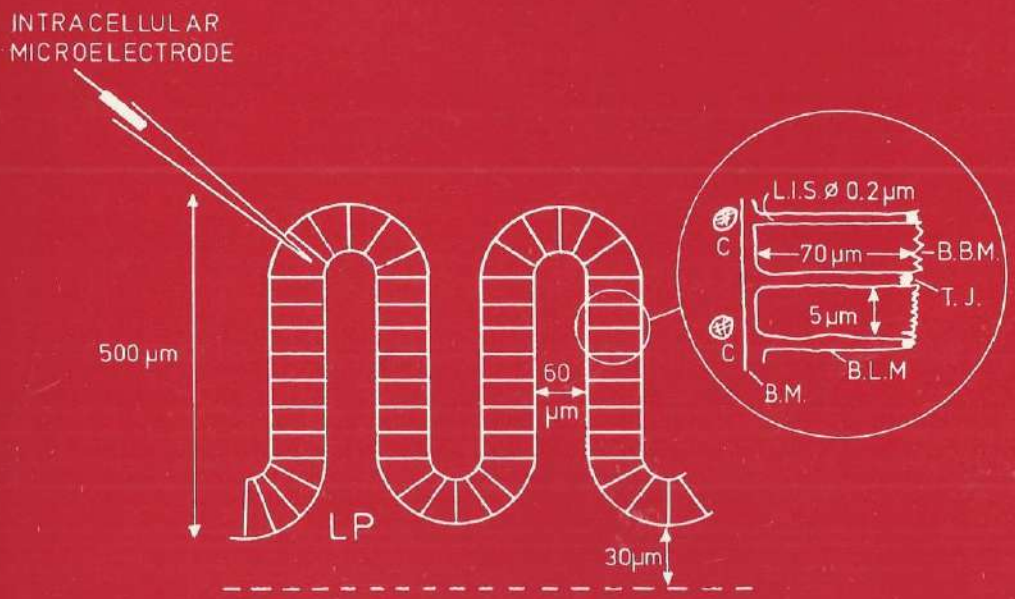

T. ZUIDEMA

MONOVALENT IONS AND GLUCOSE ABSORPTION IN GOLDFISH INTESTINE

ACADEMISCH PROEFSCHRIFT

ter verkrijging van de graad van doctor
aan de Universiteit van Amsterdam,
op gezag van de Rector Magnificus
prof. dr. S.K. Thoden van Velzen,
in het openbaar te verdedigen in de aula der
Universiteit (Oude Lutherse Kerk,
ingang Singel 411, hoek Spui) op
woensdag 4 november 1987 om 15.00 uur precies

door

Theodorus Zuidema

geboren te Rotterdam

Druk: Krips Repro Meppel
1987

Promotor: Prof. Dr. F.H. Lopes da Silva
Co-promotor: Dr. J. Siegenbeek van Heukelom

Dit onderzoek werd verricht op het Laboratorium voor Dierfysiologie, Universiteit van Amsterdam, en werd ondersteund door de Stichting voor Biofysica met financiële hulp van de Nederlandse Organisatie voor Zuiver Wetenschappelijk Onderzoek (ZWO).

Voorwoord.

Bij het verschijnen van mijn proefschrift heb ik er behoefte aan een aantal mensen, die aan de totstandkoming in enigerlei vorm hebben bijgedragen, nog eens zwart op wit te bedanken.

In de eerste plaats, Dr. J.Siegenbeek van Heukelom, beste Jan, jij bent nauw betrokken geweest bij alle fasen van het produktieproces. Jij hebt me onderricht in de beginselen van de membraanfysiologie, me geïnstrueerd bij het experimentele werk. In onze lange, soms moeizame diskussies, op het laboratorium of bij jou thuis is elk hoofdstuk, elk wild idee, elke formule gewikt en gewogen. Vaak heb je mij weer op het rechte spoor teruggebracht. Je hebt me niet alleen laten profiteren van je scherp analytisch inzicht en kennis van zaken, maar ook van je behendigheid met de tekstverwerking en je goed-georganiseerde literatuursysteem. Hartelijk dank voor acht jaar raad en daad.

Veel ben ik verschuldigd aan de andere leden van de werkgroep "membraantransport": In alfabetische volgorde, Henk Albus, Roel Bakker, Klaas Dekker, Jack Groot, Menno van der Ham, Maarten Kamermans, Ed Nijenhuis, Co van Riel en gedurende wat kortere tijd Dick Six. Ik heb veel geleerd van onze werk- en literatuurbesprekingen, onze informele diskussies en onze gezamenlijke bezoeken aan konferenties en workshops. Ik kijk daar met erg veel plezier op terug. Het experimentele en onderzoeksondersteunende werk van Klaas en Co wil ik graag apart noemen, evenals mijn intensieve samenwerking met Maarten wiens hoofdvakonderzoek bij de vakgroep Dierfysiologie deel uitmaakt van het werk dat hier vooral op mijn naam staat. Terecht staan hun namen ook boven de hoofdstukken 2, 3 en 4.

Prof. Dr F.H. Lopes da Silva, beste Fernando, dank voor je belangstelling, je vertrouwen in de goede afloop en je waardevolle adviezen bij het voorbereiden van voordrachten en artikelen. Het is een eer en genoegen bij jou te mogen promoveren.

Prof. Dr L.H. van der Tweel, geachte "baas", een belangrijk deel van mijn opleiding heb ik bij U genoten. Uw enthousiasme en veelzijdigheid leerden mij dat wetenschap behalve boeiend ook leuk kon zijn. Uw warme persoonlijkheid bepaalde de sfeer op het Laboratorium voor Medische Fysica, waar ik maar met moeite weg kon komen. Ik ben er nog steeds een beetje trots op uit Uw "school" afkom-stig te zijn. Ik ben er erg gelukkig mee dat U in de beoordelings-kommissie zitting hebt willen nemen en mijn

proefschrift zo grondig hebt willen bestuderen.

Ook de andere leden van de beoordelingskommissie, Prof. Dr K. van Dam, Prof. Dr H. van der Ende en Dr. C.H. van Os ben ik zeer erkentelijk voor hun bereidheid zich in mijn werk te verdiepen.

Binnen en buiten het laboratorium heb ik van de kennis en vaardigheden van velen gebruik mogen maken:

Prof. Dr. B.L. Roberts, dear Barry, the "spelling" error in Chapter IV was a "speling van het lot" and was introduced after you saw the manuscript. Your corrections and comments on spelling and grammar were very adequate.

Prof. Dr.J.Th.G. Overbeek en Prof. Dr. J.A.A. Ketelaar ben ik uitermate dankbaar voor hun bereidheid mee te denken en ons van advies te dienen toen wij ons overmoedig op het gladde ijs der elektrochemie begaven.

Ab van Rotterdam en Paul Diegenbach ben ik erkentelijk voor de tijd die zij in mijn wiskundige probleempjes wilden steken.

Hans van der Meyden en Simon van Mechelen zeg ik graag dank voor het verzorgen van veel van de illustraties.

Mede dankzij de bereidwilligheid en het vakmanschap van de mensen van de mechanische werkplaats, van de elektronische werkplaats, van de computerkamer en van de administratie konden de experimenten gedaan en dit boekje geschreven worden. Ik dank jullie allen heel hartelijk.

Lieve vader en moeder, U hebt U in Uw leven veel ontzegd om Uw kinderen een goede opleiding te kunnen geven. Van U hebben we geleerd af te maken, waar je eenmaal aan bent begonnen, ook als het langer duurt dan je had gedacht. Nu ook mijn proefschrift af is, realiseer ik mij dat het in belangrijke mate ook Uw werk was.

Lieve Annemarie, Aukje, Jelle en Minke, het is misschien wel eens moeilijk geweest voor jullie een echtgenoot en vader te hebben die zo nodig moest promoveren. Ik heb nu een baan minder, en jullie hebben recht op meer tijd en aandacht. Zonder jullie steun en geduld had ik dit nooit kunnen doen.

Monovalent ions and glucose absorption in goldfish intestine

Table of contents

Chapter 1

Introduction and historical background

Epithelial transport studies cover a wide field of research not only with respect to function and structure of epithelia but also with respect to their relation to other organs and to the whole animal. The mechanisms whereby epithelia transport nutrients, electrolytes and water against, often steep, gradients, while preventing undesirable backflux, have become a challenge for scientists of different disciplines and professional interest.

Many of these mechanisms were elucidated during the past decennia thanks to the introduction of new theoretical formalisms and experimental techniques in transport research. One of these techniques was the miniaturization by Walker [64] and others of ion-selective electrodes, making them small enough to be inserted without substantial damage into the interior of small cells [62].

1. Goldfish intestinal epithelium

The choice of a preparation usually brings both advantages and disadvantages. One of the advantages of goldfish intestinal epithelium to the electrophysiologist is that the underlying muscular tissue can be stripped off easily, leaving a folded but very uniform layer of intestinal cells with sufficient coherence and sturdiness to be mounted in an Ussing-type chamber for continual bilateral perfusion. In this set-up one or more microelectrodes can be inserted and kept in cells for often more than one hour so that responses to successive changes in fluid composition can be recorded from the same cell [2]. Also some disadvantages are associated with the preparation like the unstirred layers due to the folded structure of the epithelium, and the small exposure area of the columnar cells, which requires very fine tips of the electrodes. These tip sizes set limits to the characteristics of the microelectrodes, especially to the selectivity and dynamic behaviour of ion-selective electrodes [4].

One of the typical features of goldfish enterocytes is their long-drawn-out cylindrical geometry and the presence of a thin extracellular space encircling them and separating them from neighbouring cells (Fig.1).

This space, which is called 'lateral intercellular space' (l.i.s.) or 'interspace' takes up 4 to 8% of the tissue volume and is bounded by the lateral aspects of the 'basolateral membrane' which forms the

larger part of the total cellular membranes.

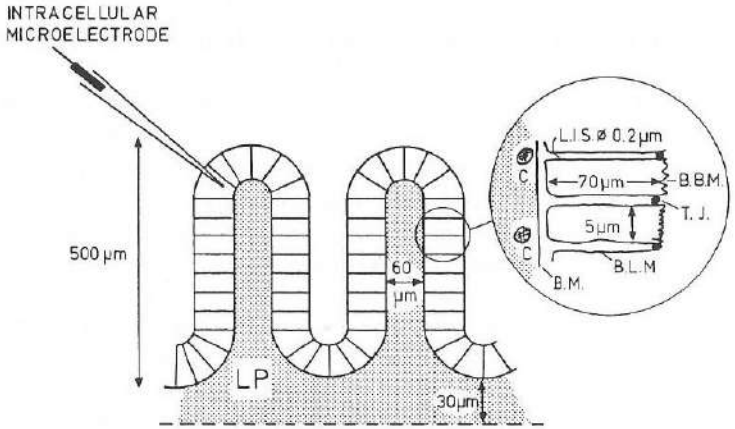

Fig. 1; Schematic representation of the dimensions of stripped intestinal preparation of the goldfish as well as the positioning of the intracellular microelectrode. For the experimental set-up see Fig. 8.
L.P.= lamina propria, L.I.S. = lateral intercellular space (or "interspace"), B.B.M. = brushborder membrane, B.M. = basement membrane, T.J. = tight junction, C. = capillary.

At the mucosal -or 'apical'- side it is bounded by the 'tight junctions' by which apposing cells are attached to each other, while the open end is directed towards the subepithelial space and faces the 'basal membrane'. This elongated geometry which is particularly striking in intestinal epithelia of teleosts [67] such as goldfish, gives rise to a number of phenomena which can be described as 'cable behaviour', not strictly in electrical sense [10] but rather in the electrodiffusional and osmotic sense. This type of behaviour, typical for long-drawn-out 'leaky' compartments transporting large amounts of solute and water, has been a source of controversy since the formulation of the osmotic gradient hypothesis by Diamond and Bossert in 1967 [15].

2. Backgrounds

2.1. Solute-linked water transport. The introduction of the phenomenological theory of non-equilibrium thermodynamics into membrane transport [35,37] was a step forward in recognizing and distinguishing fluxes and driving forces in membrane research and led to the understanding that water transport in epithelia is the passive consequence of osmotic gradients within the epithelium set up by active solute transport. The site of osmotic equilibration in absorptive epithelia was identified later by Diamond and Bossert [15,16] as the lateral intercellular space. They reformulated the so-called standing-gradient model that predicts solute accumulation at the apical side in the l.i.s. due to active transport and successive osmotic equilibration towards the serosal side (Fig. 2). According to this model the osmolarity of the effluent varies with the parameters of the system from nearly isotonic to hypertonic in comparison to the bathing solution.

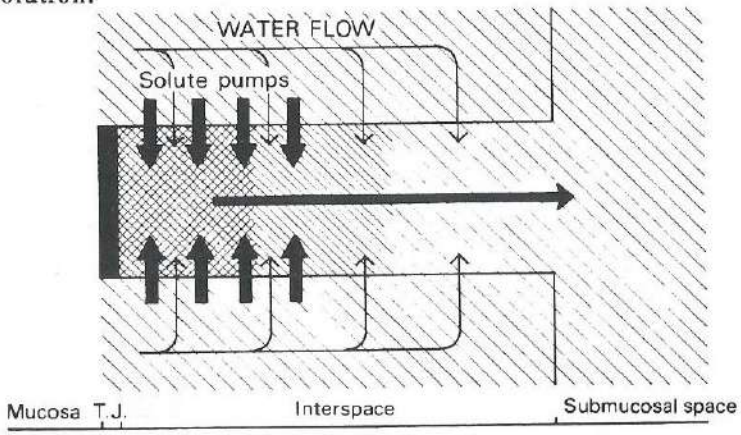

Fig. 2: Redrawing of the standing osmotic gradient model proposed by Diamond and Bossert [15].

Although in the original model the tight junction was assumed to be impermeable to ions and water, it was found in the following years that the tight junctions are more or less leaky to ions and water and therefore interfere with the solute-linked water transport [27]. This was the subject of considerable debate: the leakiness of the tight junctions would dissipate the osmotic gradients at the apical side of the interspace [50].

Besides the fact that accurate measurement of the water permeability of the mucosal barrier is impeded by unstirred layer effects [14] no generally accepted methods exist to distinguish between the membrane permeability and the junctional permeability for water. For that reason the validity of the standing gradient model or its alternatives should be settled by methods that measure directly or indirectly the osmolarity profile in the l.i.s. rather than by measuring water permeabilities. Attempts in this respect have been made by different groups using different techniques: dilution potentials [41], microprobe X-ray analysis [33] and ion-selective microelectrodes [13,57,70] but the results are still unequivocal.

2.2. Sodium-linked sugar and amino acid transport. In 1962 Crane [12] proposed an hypothesis that explains the interactions between sodium and non-electrolyte transport in intestinal and renal epithelia. His hypothesis, known as the sodium-gradient hypothesis, was extended by Schultz and Zalusky [52] to include effects on transepithelial potential and short-circuit current (Fig.3).

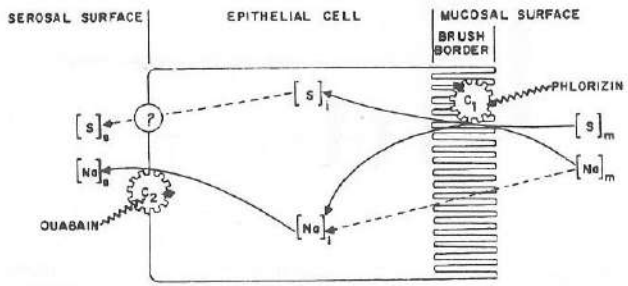

Fig. 3: Model for interaction between transmural transport of Na^+ and sugars by isolated rabbit ileum (From Schultz and Zalusky [51]).

The essential features of the model are:

i. a carrier-mediated coupled influx of sodium and organic solute across the mucosal membrane driven by the transmucosal sodium gradient;

ii. an active sodium extrusion, maintaining the sodium gradient, as well as facilitated diffusion of the organic solute, both across the basolateral membrane.

This model has, despite minor alterations, stood all theoretical and experimental challenges (for a review see e.g. [20]) and has been shown to hold not only for D-glucose (as in the original model) but also for other D-sugars, like D-galactose, and a great number of L-amino acids [1,2,24,38].

The absorption of organic solutes in intestine and kidney tubules is accompanied by a depolarization of the membrane [48,65] indicating that the entry step involves translocation of charge over the cellular membranes (which is called 'rheogenic transport'). Moreover, this depolarization was shown to be dependent on the concentration of sodium in the mucosal bathing solution. Therefore the electrochemical potential gradient for sodium was identified as the major driving force for coupled sodium/non-electrolyte influx. Since the sodium pump in the basolateral membrane was also assumed to be 'electrogenic' [8,66], as was confirmed later [29,69], the potential changes could be analysed in terms of an equivalent Thévenin circuit [48] comprising two current-generating elements in series shunted by a low resistance (as depicted in Fig. 4).

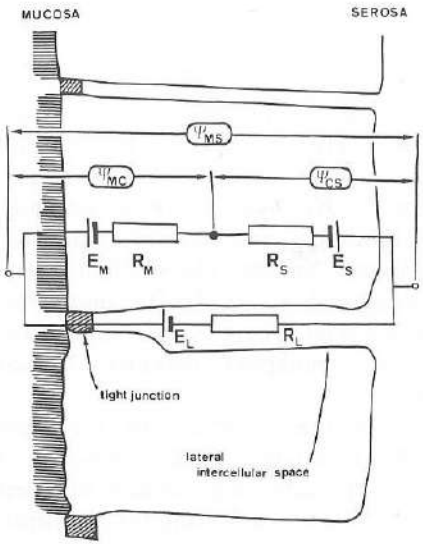

Fig. 4: Schematic representation of the equivalent Thévenin network for goldfish intestinal epithelium (see Glossary of symbols and notations).

Attempts to quantify this circuit description require assumptions about current-voltage relationships (e.g. linearity) and a detailed knowledge of lumped conductances and zero-current potentials of the components [1,26].

Data on conductances are not easily obtained from intestinal epithelia because they are folded. In contrast to flat sheets, eg. Necturus gallbladder epithelium, such structures do not allow two-dimensional cable analysis of the spread of intracellular current injection [24,46]. This is the more a handicap because in leaky epithelia the electrical properties of the shunt pathway (comprising the tight junctions and the interspace) and the basolateral membrane may easily lead to considerable underestimation of the resistance ratio of the apical and basolateral membrane (R_m/R_s) due to cable effects in the interspace [10]. Electromotive forces are idealized quantities obtained by circuit analysis or by calculation with the formal diffusion equations under zero current conditions and are not easily measured independently. Finally, whether the rheogenic events are coupled only chemically as in the original model [28,52] or also electrically [51] or indirectly by cell swelling [34] is still to be established. Without additional assumptions only steady states can therefore be analysed.

2.3. Chloride transport. In the sixties chloride was thought to follow the active transcellular flux of sodium passively and mainly paracellularly, being driven by the transepithelial potential set up by active sodium transport. By now there is considerable evidence that in most absorptive epithelia mechanisms exist for 'secondary active' anion transport energized by the electrochemical sodium gradient set up by active sodium extrusion, similar to those for glucose and amino acids [22,23,43]. In contrast, there is no compelling evidence for any 'primary active' anion transport directly linked to a source of metabolic energy [9].

The exact nature of the coupling to the electrochemical sodium gradient is not yet established with certainty and may even be different for different epithelia and under different conditions. Some authors, for instance, claim an obligatory coupling where a single carrier translocates one Na^+ ion to every Cl^- ion across the apical membrane [17,18,61], others suggest two separate transport systems, one exchanging Na^+ for H^+, the other Cl^- for HCO_3^- mediated by the intracellular production of H^+ and HCO_3^-, a mechanism originally suggested by Turnberg et al [63] for human ileum (e.g. [6,21,40]) and frequently called "double exchange mechanism".

Recently two groups postulated a Na^+-K^+-(2)Cl^--cotransport mechanism [30,42] to explain the effect of potassium on NaCl absorption, but this model needs further confirmation.

The mechanism of Cl^- exit from the cell is also subject to different opinions: Some authors suggest that the partial chloride conductance of the basolateral membrane is insufficient to permit exclusively electrodiffusional outflow and, therefore, they raise the possibility that the exit step of chloride is at least partly nonconductive, i.e. coupled by cotransport to a cation or by countertransport to another anion [11,32,45,53]. The analysis of Baerentsen et al [5], however, shows that the Cl^- conductance of the basolateral membrane may be largely underestimated by these authors since it is masked by both the potassium permeability of the basolateral membrane and the rheogenicity of the Na/K-pump.

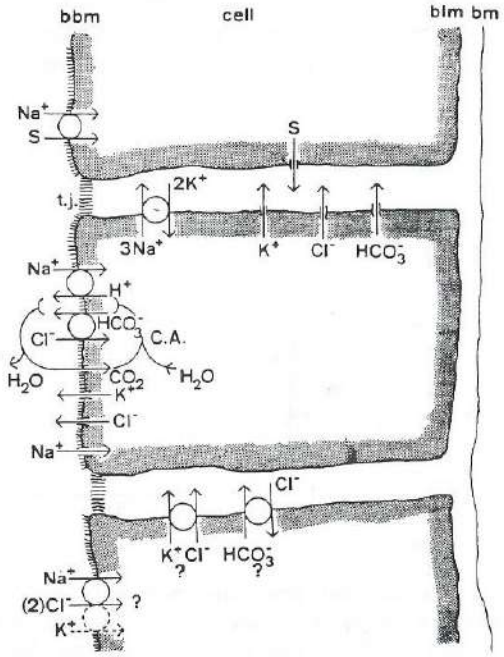

Fig. 5: Schematic representation of the electrodiffusional permeabilities and carrier mechanisms in goldfish enterocyte membranes as mentioned in the text (see also legends of Fig. 1).

Considering that the influx of sodium into the cell takes place predominantly across the apical membrane (mainly by secondary

active transport) and the efflux across the basolateral membrane (by the Na/K-pump), the question may be raised whether intracellular concentration gradients exist, especially since in the cell core with its high concentration of membranous organelles diffusion rates may be low. Indeed intracellular gradients have been reported [33,68] which were abolished by serosally-added ouabain.

3. Aims of this study

Relatively little electrophysiological work has been done on fish intestine. In fact the only intracellular potential measurements that have been reported are for plaice [36,44], winter flounder [17,60] and goldfish [1,2,9]. This is understandable since teleost intestinal cells are rather elongated and thereby can introduce 'cable phenomena' in cells and interspaces: a factor that cannot be neglected in model descriptions of active absorption by these leaky epithelia. For the same reason, however, they are suitable preparations for the study of those 'cable properties' and their relation to active absorption.

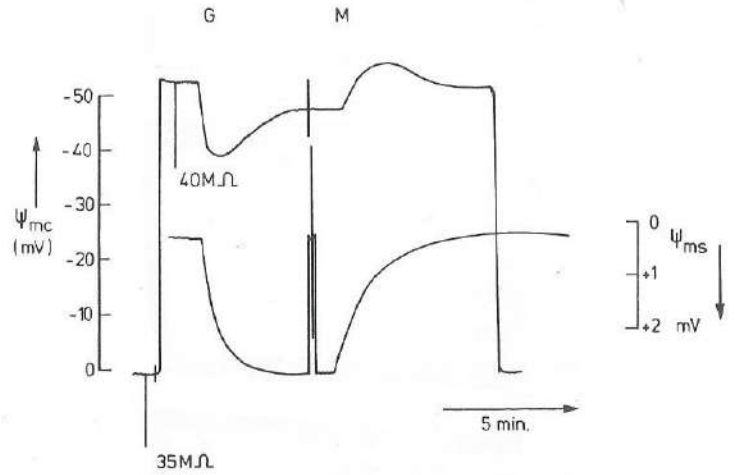

Fig. 6: Recording of the mucosal membrane potential (ψ_{mc}) and the transmural potential (ψ_{ms}) responses in goldfish intestine to mucosal addition (indicated as G) and removal (indicated as M) of glucose (for details see Albus et al [1:Fig.2]).

The transport mechanisms for water, non-electrolytes and chloride discussed above have been shown to be present in goldfish intestine [3,31,59]. Isoosmotic substitution of 28 mM of glucose for mannitol in the mucosal bathing solution, for instance, evokes a characteristic depolarization of the mucosal membrane of approx. 11.5 mV, followed by a slow partial repolarization of -6 mV [1]. Concurrently with the depolarization a serosa-positive transepithelial potential develops that reaches a steady state value of 2.0 mV during the repolarization phase of the membrane potential (Fig. 6).

These electrical phenomena form a beautiful illustration of the electrogenic version of the sodium-gradient hypothesis [1]: from analysis with the equivalent electrical circuit (Fig.4) it was concluded that the depolarization of the mucosal membrane is due in the first place to the rheogenic influx of sodium across the mucosal membrane in cotransport with glucose, while the repolarization phase is associated mainly with electrogenic processes occurring at the basolateral membrane involving the Na/K-pump. The first process, therefore, was described by a decrease in the mucosal membrane e.m.f. (E_m), the second, by a increase of the serosal membrane e.m.f. (E_s) (see Fig. 7).

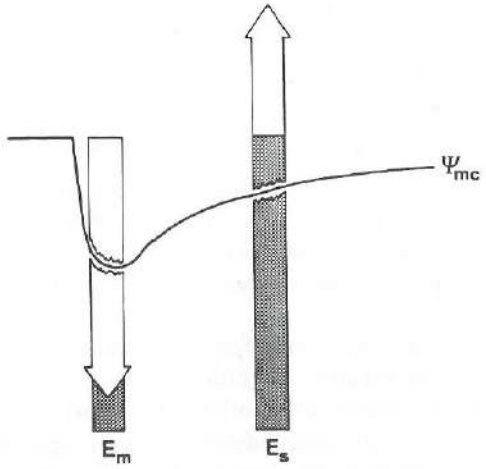

Fig. 7: The depolarization phase in the transmembrane glucose evoked response is mainly due to a decrease in E_m while the repolarization phase reflects the increase in E_s (see Fig. 4)

In the paper of Albus et al [1] it was already suggested that the increase in E_s does not solely reflect the enhanced action of the rheogenic Na/K-pump but also may contain the Nernst contribution of a reduced potassium concentration in the interspace. If that is true this has some important consequences for the analysis since it adds a

capacitive element to the equivalent circuit that cannot be neglected in analysing the transient phenomena. In that sense the present study is a follow-up of the work of Albus et al since it takes into account the role of the interspace in the glucose evoked responses of goldfish intestinal epithelium. Although a strict separation of all processes is not possible, a study of the time relationships under various experimental conditions will be shown to yield important information about the polarity and sequence of these processes. As well as serving as a useful test for the viability of the preparation, the glucose evoked potentials (GEP) provide information about the electrodiffusional properties of the plasma membranes. Measurement of ion activities, both intracellularly and extracellularly during glucose absorption, helps to identify the driving forces and coupling mechanisms between those processes.

In goldfish intestinal epithelium a net absorption of chloride is found which is abolished by serosally-added ouabain and bilateral sodium substitution [31]. This indicates a coupling to the active absorption of sodium. Since both the transepithelial potential and the shunt conductance for chloride are small most of the transepithelial chloride flux should be transcellular. From measurements of the intracellular chloride activity one can decide in which membrane the coupling mechanism is located. Substitution of sodium in the external medium does not affect the intracellular chloride concentration significantly, nor does chloride substitution affect the intracellular sodium concentration [31]. In contrast, these substitutions do induce considerable changes in intracellular pH and consequently suggest the existence of the double exchange mechanism mentioned above [49,63].

The answer to the question whether, and to which extent, the membranes are permeable to chloride is essential for establishing the need to postulate more and other transport mechanisms for chloride. The existence of such mechanisms is still speculative since they have not yet been identified by transport studies in vesicle preparations or by biochemical analysis. Considering this, the aims of the present study can be summarized as follows:

- to determine the permeation properties of the plasma membranes as well as the electrochemical driving forces across those membranes. This was done by analyzing intracellular and transepithelial potentials obtained with conventional and ion-selective microelectrodes both under control conditions and during unilateral and bilateral ion substitutions (Chapter III; [77]).
- to identify the compensatory fluxes during active rheogenic transport of sodium and glucose under open circuit conditions, as well as the coupling mechnisms between the mucosal cotransport system and the basolateral Na/K-pump. This was done by analysing transients in intracellular and interstitial potentials obtained under various conditions with normal and ion-selective microelectrodes after the onset of glucose absorption. (Chapter IV and VI; [75]).
- Measurement of intracellular ion activities brings along a number of methodological problems which are dealt with in the various chapters. Some emphasis is put on the problems encountered when working with large organic substitutes for chloride, such as gluconate and glucuronate (Chapter II; [71]).

4. Materials and techniques.

The materials and techniques used in this study are mostly described in the Materials & Methods sections of chapters II to V. A few additions, however, are considered indispensable.

4.1. Preparation and bathing solutions. Goldfishes of approx. 70 g were kept at 16-18 °C in low-copper tap water and were fed with Tetramin (TetraWerke, Mall, FRG). They were sacrificed by cutting the spine just behind the gills and subsequent decerebration. The intestines were removed and kept submersed in gassed saline solution. The first 10 cm behind the intestinal bulb was stripped free from underlying musculature by blunt dissection. Square pieces of 0.7 x 0.7 cm^2 were mounted, mucosal side upwards, in a Lucite chamber (Fig. 6). The exposed area was 0.20 cm^2. Both surfaces of the epithelium were continuously perfused with fresh solutions at a flow rate of about 2 ml/min. Experiments were performed at an ambient temperature of 18-20 °C. Bathing solutions were, unless otherwise specified, bicarbonate buffers and were continuously gassed with humidified 95% O_2 + 5% CO_2, maintaining a pH of 7.3. Their osmolarity was, if necessary, adjusted to 315 mOsm by addition of mannitol.

4.2. Experimental set-up. Intracellular recordings were obtained with glass microelectrodes prepared as follows: Glass tubing (Duran 50, ϕ_{out} = 8.0 - 8.1 mm; ϕ_{in} = 5.0 mm) with internal glass fiber (ϕ = 0.5 mm) was drawn with a Shimadzu glass drawing machine (GDM-1) to capillaries with an outer diameter of 1.23 $\pm$ 0.02 mm. After an appropriate cleaning procedure these were pulled to ultra-fine tips (0.1 - 0.3 μm) with the microelectrode puller described by Siegenbeek van Heukelom et al [55] and subsequently filled with 3M

KCl (tip resistance typically 20-25 MΩ) or liquid ion-exchanger in combination with an appropriate reference solution (see Chapter III and IV).

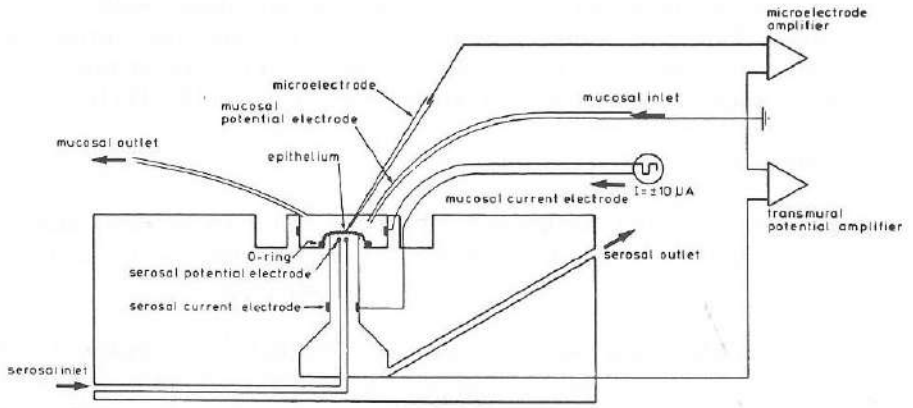

Fig. 8: Experimental set-up for measuring intracellular and transmural potentials. The current electrodes produce biphasic current pulses which allow the transepithelial resistance (R_{ms}) and the intracellular to transmural voltage divider ratio (R_m/R_s) to be measured.

Impalements were performed at an angle of approx. 40° with the preparation under low magnification microscopic control. The micropipettes were mounted in a Lucite holder [1] which contained control saline solution in contact with an Ag-AgCl electrode and was attached to a Leitz micromanipulator. Two microelectrodes could be manipulated independently; one of them could be driven by an Inchworm drive (Burleigh Instr. Inc., Rochester, NY, USA).

Double-barreled microelectrodes, consisting of a reference barrel and an ion-selective barrel were also constructed and tested. However, these were not satisfactory because the tips were either not fine enough to prevent cell damage, or they were not sufficiently selective for accurate intracellular activity measurements. Therefore we chose to use separate microelectrodes placed in nearby cells and discarded experiments in which a low number of impalements was obtained in the same tissue (less than three impalements with either

microelectrode). Except for the fact that single-barreled ion-selective microelectrodes are more selective, this procedure has the advantage that normal 3 M KCl filled micropipettes can be used as reference electrodes (which have a small tip potential, normally less than -3 mV). The sources of error are discussed below (Section 4.3). The microelectrodes were connected to high impedance electrometers (311 J, Analog Devices) in a circuit of our own design (cf [62]) and the guarding output was fed back to the case enveloping the microelectrode holder down to the surface of the mucosal bathing solution ("active guard"). Alternatively, the normal microelectrode was connected to a M-4A electrometer probe (W.P. Instruments Inc. New Haven CT U.S.A.) that allowed the tip resistance to be measured directly. Direct or differential signals, including the transepithelial potential, were recorded on a multipen recorder (Rikadenki Kogyo Co Ltd, Tokyo, Japan) and continuously displayed on both a dual beam oscilloscope (Gould OS 255) and a digital voltmeter (Fluke 8050A).

4.3. Ion-selective microelectrodes and liquid junctions. Ion-selective microelectrodes were tested in a set-up depicted in Fig. 9.

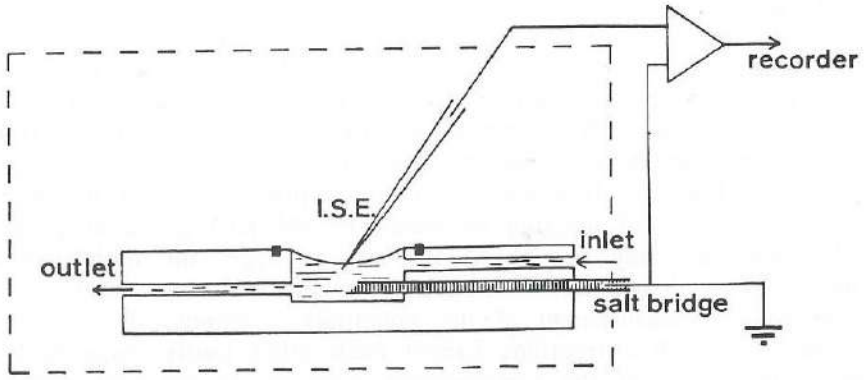

Fig. 9: Experimental set-up for testing and calibrating ion-selective electrodes (I.S.E.). The Faraday cage (----) is connected to the x1 output of the electrometer ("active guard").

The set-up was placed in a Faraday-cage which was connected to the guarding output of the electrometer (Keithley 610C) to reduce capacitive shunting of the high impedance electrodes. The reference electrode was an Ag-AgCl electrode connected to the test solution by a freshly cut agar bridge prepared with 3M KCl or physiological salt

solution. If a bridge of the latter type was used appropriate corrections were made for the difference in liquid junction potential at the agar bridge junction.

Potassium-selective (KLIX) and chloride-selective (CLIX) electrodes were calibrated in 100 mM, 8.5 mM and 0.80 mM solutions of KCl. Ion activities in these solutions are, according to the tables of Robinson and Stokes [47], and using the Guggenheim convention ($f_{\pm} = f_+ = f_-$), 77, 7.7 and 0.77 meq/l respectively. Selectivities were assessed with 100 mM solutions of uni-univalent salts of the interfering ions. Interference of bivalent ions on KLIX-electrodes was checked to be negligible by comparing Ca- and Mg-free saline solutions with control solutions.

Sodium-selective (NLIX) electrodes were calibrated in 200, 100, 20 and 2.0 mM solutions of NaCl and selectivities estimated with 100 mM of KCl, 2.5 mM of $CaCl_2$ and Ca-free saline solutions. Calculations of the slope constants and selectivity coefficients were done with the phenomenological equation of Nicolsky-Eisenman. In this equation (Eq. 6 in Chapter II) the contribution of a variable liquid junction potential at the salt-bridge junction of the reference electrode is usually ignored. Nevertheless even 3M KCl salt bridges can introduce liquid junction potentials of several mV [7,39,71], which, although hardly quantifiable, are certainly not negligible. The accuracy of the equation is therefore limited. Whether this accuracy would be improved generally by introducing corrections for those liquid junction potentials is however doubtful since:

- equations like the Henderson diffusion equation do not necessarily describe the liquid junction potentials of 3M KCl junctions properly (the boundary may not be of the mixture type, the mobilities are not constant throughout the whole concentration range, etc);
- independent measurement of the potentials is impossible;
- in practice such corrections cancel each other partly, espe-cially if the composition of the experimental solutions is not very different from the solutions used for calibration.

The latter consideration has led to the proposal of calibration procedures with mixed solutions [62] in which the question of the activity coefficients remains unanswered and free concentrations are estimated instead, not by calculation but with graphical methods.

From the Nicolsky-Eisenman equation it can be seen that relatively small errors in potential measurements lead already to substantial errors in apparent ion activity: 1 mV corresponds to a 4% change in ion activity. The standard error of the mean in our potential measurements is usually 1 to 2 mV and therefore of the same magnitude as the expected variation in liquid junction potentials under normal conditions. So under those conditions the inaccuracy in estimating apparent single ion activities would be probably 5 - 10%. Here we do not take into account that it is at least doubtful, although generally accepted, that a microelectrode tip behaves as a 3M KCl liquid junction in the intracellular environment (e.g. by cation selectivity hydrated glass tip; see [54]) and would not give rise to additional tip potentials inside the cell.

Also the estimation of single ion activities in physiological salt solutions containing large and slowly diffusing organic ions suffers from this duality between potential and single ion activity (Chapter II).

4.4 Glossary of frequently used symbols and notations.

Lumped electromotive forces and theoretical diffusion potentials (mV) are denoted E with subscript referring to the barrier or type of junction:

m for mucosal membrane **H** for liquid junction according
s for serosal membrane to Henderson equation
l for paracellular pathway $\mathbf{I^z}$ for type of ion-selective junction (Na^+, K^+ or Cl^-, etc.)

Potential differences (mV) between compartments are denoted by ψ with the following subscripts:

m for mucosal compartment **SB** for 3M KCl salt bridge
s for serosal compartment **R** for reference solution
c for intracellular compartment **T** for test solution

and are defined as $\psi_{xy} = \psi_y - \psi_x$.

$\Delta\psi$ refers to a potential change (mV) in response to an external stimulus (ion substitution, glucose addition, current) and is defined as $\Delta\psi = \psi(\text{time } 2) - \psi(\text{time } 1)$; ΔE is defined analogously.

specific lumped membrane resistances R (in $\Omega\,cm^2$) and conductances G (in mS/cm^2) are defined with respect to serosal area and carry subscripts as above. The surface amplification factor for mucosal to serosal area is 4.7 and is always included in the calculations.

ion activities are denoted $a_x I^z$, I referring to the ionic species, z to the charge number and x to the compartment; concentrations are given by $[I^z]_x$:

o for the bulk solution
i for the intracellular compartment

calculations.

ion activities are denoted $a_x I^z$, I referring to the ionic species, z to the charge number and x to the compartment; concentrations are given by $[I^z]_x$:

o for the bulk solution
i for the intracellular compartment
is for the lateral intercellular space
s for the submucosal compartment (interstitium)

in order to meet the conventions in electrochemical literature in Chapter II slightly different symbols are used: ϕ stands for ψ, U for either E or ψ and a_I for aI.

other, less frequently used, symbols are defined wherever they are used.

5. **Preliminary reports** of parts of this study are presented on international meetings of the European Intestinal Transport Group, the European Society for Comparitive Physiology and Biochemistry, the combined Dutch and Belgian Physiological and Pharmacological Societies, the combined Dutch and English Physiological Societies, the Institut National de la Santé et de la Recherche Medicale and are published as abstracts [56,57,72,73,74,76]. Chapters II, III and IV are published as full papers [71,75,77].

Acknowledgments: This work was supported by the Netherlands Foundation for Biophysics with financial aid of the Netherlands Organisation for Advancement of Pure Science (ZWO).

References

1. Albus H, Bakker R, Siegenbeek van Heukelom J (1983) Circuit analysis of membrane potentials changes due to electrogenic sodium-dependent sugar transport in goldfish intestinal epithelium. Pflügers Arch. **398**: 1-9
2. Albus H, Lippens F, Siegenbeek van Heukelom J (1983) Sodium-dependent sugar and amino acid transport in isolated goldfish intestinal epithelium: Electrophysiological evidence against direct interactions at the carrier level. Pflügers Arch. **398**: 10-17
3. Albus H, Siegenbeek van Heukelom J (1976) The electrophysiological characteristics of glucose absorption of the goldfish intestine as compared to mammalian intestines. Comp. Biochem. Physiol. **54A**: 113-119.

4. Armstrong WMcD, Garcia-Diaz JF (1980) Ion-selective microelectrodes: theory and technique. Federation Proc. **39**: 2851-2859
5. Baerentsen HJ, Christensen O, Thomsen PG, Zeuthen T (1982) Steady state and the effects of ouabain in the Necturus gallbladder epithelium: A model analysis. J. Membrane Biol. **68**: 215-225
6. Baerentsen H, Giraldez F, Zeuthen, T (1983) Influx mechanisms for Na^+ and Cl^- across the brushborder membrane of leaky epithelia: A model and microelectrode study. J. Membrane Biol. **75**: 205-218
7. Barry PH, Diamond JM (1970) Junction potentials, electrode standard potentials, and other problems in interpreting electrical properties of membranes. J. Membrane Biol.**3**: 93-122
8. Barry RJC, Eggenton J (1972) Membrane potentials of epithelial cells in rat small intestine. J Physiol (London) **227**: 201-216
9. Bonting SL, de Pont JJHHM, van Amelsvoort JMM, Schrijen JJ (1980) Transport ATPases in anion and proton transport. Ann. N. Y. Acad. Sci. **341**: 335-355
10. Boulpaep EL, Sackin H (1980) Electrical analysis of intraepithelial barriers. In: Current topics in membranes and transport, vol. 13. F.Bronner, A.Kleinzeller and E.Boulpaep, editors. p.169. Academic Press, New YorK.
11. Corcia A, Armstrong WMcD (1983) KCl cotransport: A mechanism for basolateral chloride exit in Necturus gallbladder. J. Membrane Biol. **76**: 173-182
12. Crane RK (1962) Hypothesis for mechanism of intestinal active transport of sugars. Federation Proc. **21**: 891-895
13. Curci S, Frömter E (1979) Micropuncture of the lateral intercellular spaces of Necturus gallbladder to determine space fluid K^+ concentration. Nature **278**: 355-357
14. Diamond JM (1979) Osmotic water flow in leaky epithelia. J. Membrane Biol. **51**: 195-216
15. Diamond JM, Bossert WN (1967) Standing gradient osmotic flow. A mechanism for coupling of water and solute transport in epithelia. J. Gen. Physiol. **50**, 2061-2083
16. Diamond JM, Bossert WN (1968) Functional consequences of ultra-structural geometry in "backwards" fluid-transporting epithelia. J. Cell Biol. **37**: 694-702
17. Duffey ME, Thompson SM, Frizzell RA, Schultz SG (1979) Intracellular chloride activities and active chloride absorption in the intestinal epithelium of winter flounder. J. Membrane Biol. **50**: 331-341
18. Duffey ME, Turnheim K, Frizzell RA, Schultz SG (1977) Intracellular chloride activities in rabbit gallbladder. Direct evidence for the role of the sodium-gradient in energizing "uphill" chloride transport. J. Membrane Biol. **32**: 229-245
19. Ellory JC, Evans MH, Heal JW, Smith MW (1972) Intracellular and trans-epithelial potential recording from the goldfish intestine. J. Physiol. (London) **226**: 29-30P
20. Freel RW, Goldner AM (1981) Sodium-coupled nonelectrolyte transport across epithelia: emerging concepts and directions. Am. J. Physiol. **241**: G451-G460
21. Friedman PA, Andreoli TE (1982) CO_2-stimulated NaCl absorption in the mouse renal cortical Thick Ascending Limb of Henle. Evidence for synchronous Na^+/H^+ and Cl^-/HCO_3^- exchange in apical plasma membranes.

J. Gen. Physiol. **80**: 683-711
22. Frizzell RA, Field M, Schultz SG (1979) Sodium-coupled chloride transport by epithelial tissues. Am. J. Physiol. **236**: F1-F8
23. Frizzell RA, Smith PL, Vosburgh E, Field M (1979) Coupled sodium-chloride influx across brush border of flounder intestine. J. Membrane Biol. **46**: 27-39
24. Frömter E (1972) The route of passive ion movement through the epithelium of Necturus gallbladder. J. Membrane Biol. **8**: 259-301
25. Frömter E (1979) Solute transport across epithelia: What can we learn from micropuncture studies on kidney tubules? J. Physiol. (London) **288**: 1-31
26. Frömter E (1982) Electrophysiological analysis of rat renal sugar and amino acid transport. I. Basic phenomena. Pflügers Arch. **393**:179-189
27. Frömter E, Diamond JM (1972) Route of passive ion permeation in epithelia. Nature New Biol. **235**: 9-13
28. Giraldez F (1984) Active sodium transport and fluid secretion in the gallbladder epithelium of Necturus. J. Physiol. **348**: 431-455
29. Graf J, Giebisch G (1979) Intracellular sodium activity and sodium transport in Necturus gallbladder epithelium. J. Membrane Biol. **47**: 327-355
30. Greger R, Schlatter E (1983) Properties of the basolateral membrane of the Cortical Thick Ascendig Limb of Henle's Loop of rabbit kidney. A model for secondary active chloride transport. Pflügers Arch. **396**: 325-334.
31. Groot JA (1982) Aspects of the Physiology of the Intestinal Mucosa of the Goldfish (Carassius Auratus L). Thesis University Amsterdam. MultiCopy Amsterdam
32. Guggino WB, Boulpaep EL, Giebisch G (1982) Electrical properties of chloride transport across the Necturus proximal tubule. J. Membrane Biol. **65**: 185-196
33. Gupta BL, Hall TA, Naftalin RJ (1978) Microprobe measurement of Na, K and Cl concentration profiles in epithelial cells and intercellular spaces of rabbit ileum. Nature **272**: 70-73
34. Hudson, R.L., Schultz, S.G. (1984) Sodium-coupled sugar transport: effects on intracellular sodium activities and sodium-pump activity. Science **224**: 1237-1239
35. Katchalsky A, Curran PF (1967) Non-equilibrium thermodynamics in biophysics. Harvard University Press.
36. Katz U, Lau KR, Ramos MMP, Ellory JC (1982) Thiocyanate transport across fish intestine (Pleuronectes platessa). J. Membrane Biol. **66**: 9 -14.
37. Kedem O, Katchalsky A (1961) A physical interpretation of the phenomenological coefficients of membrane permeability. J. Gen. Physiol. **45**: 143-179
38. Kohn PG, Smyth DH, Wright EM (1968) Effects of amino acids, dipeptides and disaccharides on the electrical potential across rat small intestine J. Physiol. (London) **196**: 723-746
39. Laprade R, Cardinal J (1983) Liquid junctions and isolated proximal tubule transepithelial potentials. Am. J. Physiol. **244**: F304-F319
40. Liedtke CM, Hopfer U (1982) Mechanism of Cl^- translocation across small intestinal brush-border membrane. II. Demonstration of Cl^--OH^--exchange and Cl^--conductance. Am. J. Physiol. **242**: G272-G280
41. Machen TE, Diamond JM (1969) An estimate of the salt concentration in the lateral intercellular spaces of rabbit gallbladder during maximal fluid transport. J. Membrane Biol. **1**: 194-213
42. Musch MW, Orellana SA, Kimberg LS, Field M, Halm DR, Krasny EJ, Frizzell RA (1982) Na^+-K^+-Cl^--cotransport in the intestine of a marine teleost. Nature **300**: 351-353
43. Nellans HN, Frizzell RA, Schultz SG (1973) Coupled sodium-chloride influx across the brushborder of rabbit ileum. Am. J. Physiol. **225**: 467-475.
44. Ramos MMP, Ellory JC (1981) Na and Cl transport across the isolated anterior intestine of the plaice Pleuronectes Platessa. J. Exp. Biol. **90**: 123-142.
45. Reuss L (1983) Basolateral KCl co-transport in a NaCl-absorbing epithelium.Nature **305**: 723-726
46. Reuss L, Finn AL (1975) Electrical properties of the cellular transepithelial pathway in Necturus gallbladder. J. Membrane Biol. **25**: 115-139.
47. Robinson RA, Stokes RH (1959) Electrolyte solutions. (2nd ed) Butterworth. London.
48. Rose RC, Schultz SG (1971) Studies on the electrical potential profile across rabbit ileum. Effects of sugars and amino acids on transmural and transmucosal electrical potential differences. J. Gen. Physiol. **57**: 639-663.
49. Sachs G, Faller LD, Rabon E (1982) Proton-hydroxyl transport in gastric and intestinal epithelia. J. Membrane Biol. **64**: 123-135
50. Sackin H, Boulpaep EL (1975) Models of coupling of salt and water transport. Proximal tubular reabsorption in Necturus kidney. J. Gen. Physiol. **66**: 671-733
51. Schultz SG (1977) Sodium-coupled solute transport by small intestine: a status report. Am. J. Physiol. **233**: E249-E254
52. Schultz SG, Zalusky R (1964) Ion transport in isolated rabbit ileum. The interaction between active sodium and active sugar transport. J. Gen. Physiol. **47**: 1043-1059
53. Shindo T, Spring KR (1981) Chloride movement across the basolateral membrane of proximal tubule cells. J. Membrane Biol. **58**: 35-42
54. Siegenbeek van Heukelom J (1971) Cell cummunication in epithelial systems. Thesis, Utrecht.
55. Siegenbeek van Heukelom J, Dijkstra K, Van Ingen H (1976) A versatile and reproducibly operating microelectrode puller. Med. Biol. Eng. **3**: 644-652.
56. Siegenbeek van Heukelom J, Zuidema T (1985) The influence of Ba^{2+} on membrane potential and K^+-induced depolarizations in goldfish intestinal epithelium. J. Physiol. (London) **366**: 92P
57. Siegenbeek van Heukelom J, Zuidema T, Kamermans M (1986) The role of the structure of epithelial compartments in transepithelial transport. In: Ion Gradient-Coupled Transport; INSERM Symposium No. 26, Editors: F. Alvarado and C.H. van Os, Elsevier Science Publishers B.V., Amsterdam.
58. Simon M, Curci S, Gebler B, Frömter E (1981) Attempts to determine the ion concentrations in the lateral spaces of Necturus gallbladder epithelium with microelectrodes. In: Benzon Symposium: Water Transport Across Epithelia. H.H. Ussing, N. Bindslev, N.A. Larssen and O. Sten-Knudsen, editors. Munksgaard, Copenhagen.
59. Smith MW (1964) The in vitro absorption of water and solutes from the intestine of goldfish, Carassius Auratus. J. Physiol. (London) **175**: 38-49
60. Smith PL, Welsh MJ, Stewart CP, Frizzell RA, Orellana SA, Field M (1981) Chloride absorption by the intestine of the winter flounder Pseudopleuronectes americanus: Mechanism of inhibition by reduced pH. Bull. Mount Desert Island Biol. Lab. **20**: 96-101
61. Spring KR, Kimura G (1978) Chloride reabsorption by renal proximal tubules of Necturus. J. Membrane Biol. **38**: 233-254
62. Thomas RC (1978) Ion-sensitive intracellular micro-electrodes. Academic

Press, New York, London, San Francisco.
63. Turnberg LA, Bieberdorf FA, Morowski SG, Fordtran JS (1970) Interrelationship of chloride, bicarbonate, sodium and hydrogen transport in human ileum. J. Clin. Invest. **49**: 557-567
64. Walker JL Jr (1971) Ion specific liquid ion-exchanger microelectrodes. Analytical Chemistry **43**: 89A-93A
65. White JF, McD Armstrong W (1971) Effect of transported solutes on membrane potentials in bullfrog intestine. Am. J. Physiol. **221**: 194-201
66. Wright EM (1966) The origin of the glucose dependent increase in the potential difference across the tortoise small intestine. J. Physiol. (London) **185**: 486-500
67. Yamomoto T (1966) An electron microscope study of the columnar epithelial cell in the intestine of fresh water teleosts: Goldfish (Carassius Auratus) and rainbow trout (Salmo Irideus). Z. Zellforsch. **72**: 66-87.
68. Zeuthen T (1978) Intracellular gradients of ion activities in the epithelial cells of the Necturus gallbladder recorded with ion-selective microelectrodes. J. Membrane Biol. **39**: 185-218
69. Zeuthen T (1981) On the effects of Amphotericin B and ouabain on the electrical potentials of Necturus Gallbladder. J. Membrane Biol. **60**: 167-169.
70. Zeuthen T (1983) Ion activities in the lateral intercellular space of gallbladder epithelium at low external osmolarities. J. Membrane Biol. **76**: 113-122
71. Zuidema T, Dekker K, Siegenbeek van Heukelom J (1985) The influence of organic counterions on junction potentials and measured membrane potentials. Bioelectrochem. Bioenerg. **14**: 479-494
72. Zuidema T, Groot JA, Siegenbeek van Heukelom (1981) Chloride transport in goldfish intestinal epithelium. 4th Meeting European Intestinal Transport Group, 30 aug. - 2 sept. Berlin.
73. Zuidema T, Kamermans M, Siegenbeek van Heukelom J (1983) The role of the intercellular compartment during glucose absorption. Interstitial and intracellular potassium activities in goldfish intestinal epithelium. Gastroenterol. Clin. Biol. **7**: 514
74. Zuidema T, Kamermans M, Siegenbeek van Heukelom J (1983) Interstitial and intracellular potassium activities during glucose absorption in goldfish intestinal epithelium. Arch. Int. Physiol. Biochim. **91**: P5.
75. Zuidema T, Kamermans M, Siegenbeek van Heukelom J (1986) Influence of glucose absorption on ion activities in cells and submucosal space in goldfish intestine. Pflügers Arch. **407**: 292-298
76. Zuidema T, Siegenbeek van Heukelom J, Kamermans M, Groot JA (1982) The transmembrane glucose evoked potential in goldfish Carassius Auratus intestinal epithelium and the role of the extracellular space. 4th conference of the European Society for Comparative Physiology and Biochemistry, Bielefeld (FRG) 8-11 September 1982.
77. Zuidema T, Van Riel JW, Siegenbeek van Heukelom J (1985) Cellular and transepithelial responses of goldfish intestinal epithelium to chloride substitutions. J. Membrane Biol. **88**: 293-304

Chapter II

830—THE INFLUENCE OF ORGANIC COUNTERIONS ON JUNCTION POTENTIALS AND MEASURED MEMBRANE POTENTIALS

T. ZUIDEMA, K. DEKKER and J. SIEGENBEEK VAN HEUKELOM

Department of Zoology, University of Amsterdam, Membrane Biophysics, Kruislaan 320, 1098 SM Amsterdam (The Netherlands)

(Revised manuscript received May 20th 1985)

SUMMARY

Cellular electrophysiological responses to substitution in the bathing media of Cl^- by large organic cations are shown to be dependent on the type of reference electrode. This is shown by measurements in goldfish enterocytes. Similarly, a potential change between a cation-sensitive electrode in the bathing medium and a 3 *M* KCl-filled agar bridge of about −4 mV is observed. Therefore, these cellular responses, measured with respect to either of these two electrodes as reference electrode, do not show the same result.

The concept of single ion activity measurement with ion-sensitive electrodes is discussed with respect to the extrathermodynamical assumption concerning the reference electrode.

INTRODUCTION

In membrane research the influence of ions on membrane transport processes is frequently evaluated by substituting these ions by large organic ions for which the cell membrane can be considered to be inpermeable. The continuous measurement of intracellular single ion activities with ion-sensitive microelectrodes during such substitutions can provide information about the coupling between ion-fluxes [1–8].

The measurement of single ion activities can be carried out only after introduction of an additional extrathermodynamical assumption concerning the contribution of the constituting ions to the mean ion activities [9–13]. The most common practice in membrane physiology is to assume that during a transition from one solution to another potential changes occurring near a 3 *M* KCl reference electrode are negligible or can be described by a Henderson diffusion equation [See equation (7)].

However, measuring K^+ activities with ion-sensitive microelectrodes in biological salt solutions containing 5.7 m*M* KCl, we found a shift in potassium signal of

-4.1 ± 0.3 mV ($n = 20$) when Cl^- was replaced iso-osmotically by glucuronate or gluconate (for the composition of the solutions see Experimental section). As this corresponds to an apparent drop from 4.2 meq/dm^3 to 3.5 meq/dm^3 it was decided to investigate the origin of this change. Two different but complementary explanations can account for this:

(A) The activity coefficients of the salt solutions have changed indeed, or

(B) the sensor or reference electrodes do not behave ideally.

Two independent ways to investigate which of these explanations is to be preferred are to measure the equivalent conductance as a function of concentration and the osmotic coefficients.

Whatever the correct explanation, the consequences for electrophysiological experiments can be important. If the effects are due to a reduction of the single ion activity coefficients *per se*, this already introduces changes in membrane potentials since these potentials are mainly determined by the ion activity gradients across the membranes, especially of K^+. If the effects are due to changes of the junction potentials near the reference electrodes, then the measured intracellular potentials should be corrected correspondingly. Finally, if artifactual behaviour of the potassium-selective microelectrode is the origin of the changes, the normal calibration and correction procedures for these electrodes are becoming irrelevant for this kind of experiments.

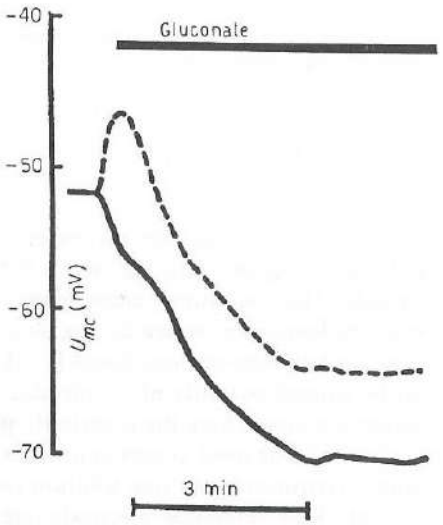

Fig. 1. Simultaneous recordings of the intracellular potential (U_{mc}) in a goldfish intestinal epithelial cell during chloride substitution by gluconate in the medium with either a potassium-sensitive electrode (— — —) or a 3 *M* KCl bridge as reference in the medium (———). Results obtained with a fine-tipped microelectrode as reference resemble the results obtained with the potassium-selective electrode (not shown).

Figure 1 shows strikingly how the membrane potential response [U_{mc}: cell interior with respect to the reference electrode in the luminal bathing medium (m)] of goldfish intestinal epithelial cells to chloride–gluconate substitutions depends on the choice of the reference electrode: a potassium-selective microelectrode or a 3 *M* KCl agar bridge (for details see Experimental and Results sections).

THEORETICAL CONSIDERATIONS AND EQUATIONS

(1) As for the activity coefficients, the convention frequently used in electrophysiology is that the single ion activity coefficients in uni-univalent electrolytes are related to the mean activity coefficient according to the so-called Bates–Guggenheim convention [11,14], stating for the rational activity coefficient (f)

$$f_+ = f_- = f_\pm \tag{1}$$

Between 1 and 100 m*M* the differences in molal activity coefficient, molar activity and rational activity coefficient [13] are insignificant compared to the accuracy normally required in electrophysiology ($\pm 0.5\%$) and are therefore neglected.

Deviations from equation (1) are described in the literature [11] as due to the difference in hydration of the two constituting ions.

The major factors determining the mean ion activity coefficients are ionic interaction and finite ion diameter and are accounted for in the extended Debye–Hückel theory by the equation (2) [13]

$$\log f_\pm = + \frac{\{A\,|z_+ z_-|\sqrt{c}\}}{1 + Ba\sqrt{c}} + bc \tag{2}$$

where a (in Å) is the distance of nearest approach of the ions in the electrolyte solution studied; z_+ and z_- represent the charge numbers of the cation and the anion, respectively, and c is the salt concentration in mol/dm^3. The quantities A and B follow from the theory and are for uni-univalent electrolytes: $A = 0.5115$ $M^{-1/2}$ and $B = 0.3291 \times 10^8$ cm^{-1} $M^{-1/2}$ at 25°C [13]; b is an adjustable parameter which represents non-quantified short range ionic interactions and equals 0.055 dm^3/mol for NaCl and 0.0202 for KCl [10,13,15]:

(2) If a is less than 2 Å there is reason to assume, according to the Association Theory of Bjerrum [13–15], that substantial ion association occurs above 10 meq/dm^3 (which is within the physiological range). As gluconate and glucuronate are known to associate strongly with Ca^{2+} [16] it is reasonable to look for similar effects in salt solutions of K^+ or Na^+.

(3) The quantity a appears also in the equation for the equivalent conductance [13]:

$$\Lambda_c = \Lambda_0 - \frac{(B_1\Lambda_0 + B_2)\sqrt{c}}{1 + Ba\sqrt{c}} \tag{3}$$

where Λ_c is the equivalent conductance (Ω^{-1} cm^2 eq^{-1}) at concentration c, Λ_0 the

extrapolated value of this quantity at $c = 0$; and $B_1 = 0.2300\ M^{-1/2}$ and $B_2 = 60.65\ \mathrm{cm^2\ \Omega^{-1}\ M^{-1/2}}$. Measurement of the equivalent conductance as a function of the concentration provides not only an estimate of a but also of Λ_0 from which the ionic mobilities can be derived.

(4) According to the Gibbs–Duhem relation (at constant temperature and pressure) the osmotic coefficient (φ) in a single salt solution is related to the same entities as in the previous equation by [13]

$$1 - \varphi = \frac{(2.3026\ A\,|z_+ z_-|\sqrt{c})\,\sigma(Ba\sqrt{c})}{3} - \frac{bc}{2} \tag{4}$$

where

$$\sigma(x) = \frac{3}{x^3}\left[1 + x - 2\ln(1+x) - \frac{1}{1+x}\right]$$

Therefore, if substantial ion association takes place this should be revealed by the osmotic coefficients. Obviously, in this type of determinations electrode artifacts are absent.

An equation has been derived by the Bates group which relates the deviation of the single ion activities from the mean ion activity with the hydration (h) and osmotic coefficient (φ) of the solution [11]

$$\log(f_+) = \log(f_\pm) + 0.00782(h_+ - h_-)c\varphi \tag{5a}$$

$$\log(f_-) = \log(f_\pm) + 0.00782(h_- - h_+)c\varphi \tag{5b}$$

If therefore a considerable difference between f_+ and $f_\pm$ is observed it might indicate strong hydration of the ions; in this case most likely the glucuronate ion.

(5) A great variety of ion-sensitive electrodes (i.s.e.) is available for measuring ion activities [7,8,11,12,17,18]. Interference by other ions is commonly expressed by the Nicolsky–Eisenman equation [12]:

$$U_i = U_{i,0} + s\log\left(a_i + \sum_j K_{i,j} a_j^{(|z_i/z_j|)}\right) \tag{6}$$

where U_i is the potential of the cell assembly, z_i, a_i are the charge number of the primary ion i and its activity in moles per $\mathrm{dm^3}$ in the test solution, z_j, a_j are the charge number of any interfering ion j and its activity in moles per $\mathrm{dm^3}$ in the test solution, $K_{i,j}$ is the selectivity factor: $K_{i,j}$ is a measure of the relative sensitivity of the sensor for the interfering ion j compared to the ion i that is to be detected, $U_{i,0}$ is the potential difference comprising a constant potential (for a given temperature and reference solution) and a variable liquid junction potential of the connecting reference electrode and s is the slope constant: theoretically $= 2.303.RT/z_i\mathscr{F} = 59.16$ mV/z_i at 25°C.

It is clear that the dependence of $U_{i,0}$ on the liquid junction potential near the reference electrode may introduce errors.

(6) In electrophysiology the reference electrodes are connected to the bathing media by means of agar bridges filled with 3 M KCl or biological salt solutions. Problems involved in the use of liquid junction type electrodes have been described earlier by Barry and Diamond [9] and, more recently, by Laprade and Cardinal [19] for solutions where cations were substituted. More specifically, from these studies it appears that liquid junctions which are not strictly of the bi-ionic or single-salt dilution type are badly defined and often time-dependent. The applicability of the original Henderson diffusion equation can be improved, especially for more concentrated solutions, with the introduction of single ion activity coefficients [9,12]:

$$U_H = U'' - U' = -\frac{RT}{\mathscr{F}} \frac{\sum_i z_i u_i (a_i' - a_i'')}{\sum_i z_i^2 u_i (a_i' - a_i'')} \ln \frac{\sum_i z_i^2 u_i a_i'}{\sum_i z_i^2 u_i a_i''} \tag{7}$$

where $\sum_i$ is the sum taken over all ions, U_H is Henderson's diffusion potential, U', U'' are the potentials in the compartments $'$ and $''$ with respect to a common ground, z_i is the charge number of ion i, including the sign of valence, u_i is the absolute mobility of ion i ($u_i = \lambda_i/\mathscr{F}$) and a_i', a_i'' are the single ion activities of ion i.

Even this equation can give rise to errors of up to several mV [9,19,20].

EXPERIMENTAL

Conductivity measurements

Using a conductivity meter (Philips PW 9501/01 with cell PR 9513, measuring frequency 2000 Hz, accuracy 0.5%) calibrated carefully with the NaCl data from the literature [13,15], we measured the equivalent conductance of the chloride salts of potassium, choline (*m.w.* of the unhydrated cation 120.2 dalton) and N-methyl-(D)-Glucamine (NMG, *m.w.* = 194.2 dalton), and the sodium or potassium salts of isethionate (*m.w.* of the unhydrated anion 125.1 dalton), thiocyanate (*m.w.* = 58.1 dalton), gluconate (*m.w.* = 195.2 dalton) and glucuronate (*m.w.* = 193.1 dalton). The equivalent conductance equation [equation (3)] was curve-fitted to the data with Λ_0 and a as fitting parameters.

The use of glucuronate or gluconate

Throughout this study a significant difference (Student's t test: $P < 0.05$) in measured parameters was never observed when Cl^- was replaced by gluconate or glucuronate (see, for instance, Table 1). Therefore both organic anions were used without discrimination and in the salts that were commercially available (potassium and sodium salts prepared from glucuronic acid and Na-glucuronate and Na-gluconate).

Single ion activities

Potassium activities in single and mixed salt solutions of KCl, K-glucuronate, NaCl and Na-glucuronate were measured with micropipettes filled with liquid

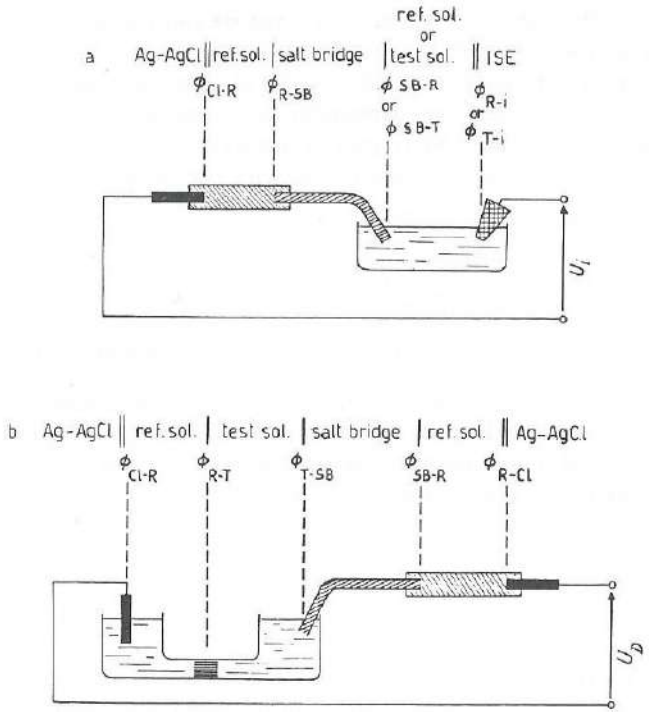

Fig. 2. Descriptions and diagrams of the measuring circuits for (a) ion potentials and (b) diffusion potentials. The convention for the direction of the interface potentials is right side positive. The symbols are placed under the interfaces they refer to.

ion-exchanger (WPI IE190: $s = 56.9 \pm 0.2$ mV/decade; $K_{K,Na} = 0.020 \pm 0.002$; $K_{K,Ca} = 0.015 \pm 0.006$) and with a glass miniature electrode (Microelectrodes Inc., Londonderry, Mass, U.S.A.) in a circuit according to Fig. 2a. Chloride activities in KCl, choline-Cl and NMG-Cl were measured with Ag|AgCl electrodes. Reference electrodes during calibration were freshly-cut 3 *M* KCl (in 3% agar) cannules connected to Ag|AgCl electrodes by 100 m*M* KCl bridges. The symbol for the interface potential of conductor B with respect to conductor A is ϕ_{A-B}.

When the test solution (T) is substituted for the reference solution (R) the change in circuit potential is given by:

$$\Delta U_i = U_i(\text{test}) - U_i(\text{ref}) = (\phi_{SB-T} + \phi_{T-i}) - (\phi_{SB-R} + \phi_{R-i}) \tag{8a}$$

where U_i is defined by equation (6).

Introducing the differences $\Delta\phi_i = \phi_{T-i} - \phi_{R-i}$ and $\Delta\phi_{SB} = \phi_{SB-T} - \phi_{SB-R}$ one gets:

$$\Delta U_i = \Delta\phi_i + \Delta\phi_{SB} \tag{8b}$$

Diffusion potentials

Diffusion potentials (U_{diff}) were measured between 100 m*M* organic salt solutions and a 100 m*M* KCl reference solution in the circuit depicted in Fig. 2b. The circuit potential is given by:

$$U_{diff} = \phi_{R-T} + \phi_{T-SB} + \phi_{SB-R} = U_H - \Delta\phi_{SB} \tag{9}$$

which is the sum of three junction potentials. ϕ_{R-T} is a bi-ionic potential and can be equated with the Henderson diffusion equation (7): U_H.

Osmotic measurements

Osmotic coefficients of 100 m*M* salt solutions were determined with two osmometers, one using the freezing point depression method (Precision Systems, Micro-osmometers), the other using the vapor pressure reduction method (Wescor, 5100 C). The accuracy of calibration was typically 2 mosmoles/dm^3. The correct functioning of the osmometers was verified by measuring the osmotic coefficients of potassium nitrate (0.858 ± 0.002 and 0.855 ± 0.003, respectively) and potassium acetate (0.913 ± 0.003 and 0.919 ± 0.003, respectively). These values are in accordance with the data from Robinson and Stokes [13].

Intracellular measurements

The intracellular potential measurements shown in the introduction (see Fig. 1) were taken in goldfish enterocytes during chloride–gluconate substitutions. Originally the tissue was bathed with a standard solution [21] containing 117.5 m*M* NaCl, 5.7 m*M* KCl, 25 m*M* $NaHCO_3$, 2.5 m*M* $CaCl_2$, 1.2 m*M* $MgSO_4$, 1.2 m*M* NaH_2PO_4 and 27.8 m*M* glucose (315 ± 3 mosmoles/dm^3). The solutions were gassed with an humidified mixture of 5% O_2 + 95% CO_2: pH = 7.3. All Cl^- (127.1 meq/dm^3) is substituted by gluconate (117.5 meq/dm^3) and SO_4^{2-} (4.8 meq/dm^3). The solution was adjusted to 315 mosmoles/dm^3 with 14 m*M* mannitol. The experimental set-up and the tissue preparation, allowing the impalement of the epithelial cells with microelectrodes, are on the whole the same as described earlier [21]. The reference bath electrodes were 3 *M* KCl agar bridges connected to the Ag|AgCl electrodes by a standard salt bridge, similar to the one shown in Fig. 2a. The mucosal bath electrode was connected to the ground of the electronic equipment. A potassium-selective microelectrode was placed in the mucosal bath near the cells impaled by the normal microelectrode. When the potassium-selective microelectrode was used as a reference electrode the measurements were obtained as the differential potential change between the intracellular microelectrode and the extracellular potassium-selective electrode (cf. Fig. 3a) both with respect to the mucosal bath electrode.

Since biological media, as used here, are electrochemically extremely complex and no theoretical descriptions are available to explain the observed change in ion-sensi-

tive electrode response, the conclusions drawn from the other parts of this paper cannot be related directly to these types of solutions. However, they might provide an indication to what procedure is best in correcting for the observed changed.

Statistics

Average results are presented ± Standard Error of the Mean (s.e.m.). If errors are presented in calculated results these are only related to the errors in the experimentally determined parameters.

RESULTS

Conductivity measurements

Table 1 shows the limiting equivalent conductivities and the a values derived from the conductivity measurements. Note the agreement in λ_0 of SCN^- measured with K^+ or Na^+ as counterion. The λ_0 values of glucuronate ions of different salts show some scatter, but this is mainly due to the way the solutions are produced (see legend to Table 1). According to Bjerrum's theory there is some indication that ion association may occur with the ions gluconate, glucuronate, choline and NMG.

With equation (2), taking a from Table 1 and assuming $b = 0.0202$, one can calculate $f_\pm$ for these solutions; as they will be needed elsewhere in the calculations, here we only give $f_\pm(\mathrm{KCl}) = 0.768 \pm 0.003$ and $f_\pm(\text{K-glucuronate}) = 0.740 \pm 0.002$ for the salt solutions at 100 mM concentration; at 10 mM concentration these values become 0.901 ± 0.001 and 0.896 ± 0.001, respectively.

TABLE 1

The function $\Lambda_c = \Lambda_0 - \{(0.230\ \Lambda_0 + 60.65)\sqrt{c}/(1 + 0.3291\ a\sqrt{c})\}$ fitted to the measured equivalent conductivities for the concentrations 1, 2, 5, 10, 20, 50 and 100 meq/dm³. The accuracy in the concentration was 0.2% or better. Temperature was 25.0 ± 0.2°C; the quantity a is calculated in Angström units. S.d. is the standard deviation for the measured points (Λ_{obs}) from the fitted curve (Λ_c): s.d. = $\{\Sigma(\Lambda_c - \Lambda_{obs})^2/n\}^{1/2}$. For the calibration of the conductivity meter the data for NaCl from the literature were used: $(NaCl)_{lit}$. To obtain λ_0 of the organic ions (last column) the λ_0 of Na^+, K^+ or Cl^- (resp. 50.10, 73.50 or 76.35 Ω^{-1} cm² eq^{-1}) were subtracted from the limiting equivalent conductivity of the salts. All substances were of analytical purity (Sigma, Aldridge or Merck). Sodium glucuronate from Sigma (a) was compared with the sodium and potassium salts of D-glucuronic acid titrated to pH 8.2 by NaOH or KOH adjusted previously by succinic acid (b, c). Small differences in limiting equivalent conductivity values were found

Substance	Λ_0 (Ω^{-1} cm² eq^{-1})	a (Å)	s.d. (Ω^{-1} cm² eq^{-1})	λ_0 (Ω^{-1} cm² eq^{-1})
$(NaCl)_{lit}$	126.4	4.2	0.04	–
$(NaCl)_{obs}$	126.2	4.3	0.3	–
KCl	150.0	3.7	0.4	–
NaSCN	114.9	4.7	0.4	64.8
KSCN	139.4	4.3	0.2	65.9
Na-glucuronate (a)	78.6	2.3	0.2	28.5
Na-glucuronate (b)	76.9	2.4	0.3	26.8
K-glucuronate (c)	98.8	2.1	0.2	25.5
Na-gluconate	77.9	2.3	0.4	27.8
Na-isethionate	91.3	3.6	0.3	41.2
Choline–Cl	114.4	1.9	0.4	37.9
NMG–Cl	100.1	1.7	0.2	23.7

Single ion activities

Table 2a presents the potentials measured with potassium-selective electrodes with respect to the reference electrode (3 M KCl) when K^+ was replaced by Na^+ at constant ionic strength in the presence of either chloride or glucuronate. It is clear that glucuronate introduces a deviation in potassium signal of approximately 4 mV, but leaves the slope (s) constant and the selectivity ($K_{K,Na}$) of the electrode system unaffected. Similar deviations but of opposite sign were observed with chloride-sensitive microelectrodes in NMG–Cl and choline Cl solutions (unpublished observa-

TABLE 2

Average circuit potentials in a circuit according to Fig. 2a measured with single-barreled potassium-sensitive microelectrodes and 3 M KCl salt bridge

(a) Potentials in mixtures of KCl and NaCl are compared with those in mixtures of K-glucuronate and Na-glucuronate. The potentials measured in Cl-containing solutions are presented as U_K, taking the value in 100 mM KCl as reference value. The difference in potential between the glucuronate- and the corresponding chloride-containing solutions is presented as ΔU_K. The values in columns 1 and 2 related to the amount of cations present in the solution

Cations		Anions	
Na (meq/dm³)	K (meq/dm³)	Cl U_K (mV)	glucuronate ΔU_K (mV)
0	100	0	−4.1 ± 0.2
90	10	−54.8 ± 0.6	−3.7 ± 0.4
99	1	−86.2 ± 3.2	−4.3 ± 0.4
100	0	−95.8 ± 4.0	−5.1 ± 0.5

(b) Electrodes responses ΔU_K during dilution of KCl of K-glucuronate in decadic steps in activity using mean activity data from the literature [13]. The same dilutions in concentration were made for K-glucuronate. The value in the first column relates to the concentration of the salt, the value in the second to the estimated mean activity expressed for KCl. The value for 100 mM KCl is taken as reference

Salt concentration (mM)	Estimated K activity (meq/dm³)	KCl ΔU_K (mV)	K-glucuronate (ΔU_K (mV)
100.0	77	0	−3.8 ± 0.4
8.50	7.7	−56.5 ± 0.2	−57.8 ± 0.2
0.80	0.77	−114.3 ± 0.3	−114.4 ± 0.4

tions). From Table 2b it follows that s changes apparently from 57.2 to 55.3 mV/decade, but at the lowest concentration the potassium signals are the same.

Artifacts of the ion-selective microelectrodes due to counterion interference by imperfect sealing [12] or failure of co-ion exclusion [1] are unlikely as a potassium-sensitive glass electrode (ΔU_K in Table 3) and an Ag|AgCl electrode (ΔU_{Cl} in Table 3) measured essentially the same values as the liquid ion-exchanger microelectrodes irrespective of whether lyotropic ions (thiocyanate, choline) or lyophobic ions (glucuronate and NMG) were substituted. In addition, the fact that larger tip diameters of the microelectrodes (> 3 μm) did not alter the results also pleads against imperfect sealing [1]. Therefore there is no reason to assume that specific electrode artifacts of the sensor electrodes are involved. As stated previously, however, ΔU_K and ΔU_{Cl} do include the changes in liquid junction potential near the salt bridge: $\Delta\phi_{SB}$.

In addition, ΔU_K was measured during similar substitutions with 10 mM salt solutions: $\Delta U_K = -1.1 \pm 0.1$ mV ($n = 3$).

Diffusion potentials

Diffusion potentials measured at 25°C across a porous plug between KCl, K-glucuronate, choline chloride or NMG–Cl are presented as U_{diff} in Table 3. These experimental diffusion potentials include the non-symmetrical liquid junction potentials at the 3 M KCl junctions: $-\Delta\phi_{SB}$. The theoretical diffusion potentials calculated with the modified Henderson equation (7) for the liquid junctions between the 100 mM KCl and the test solutions are presented as U_H. The ionic mobilities used in this calculation were derived from the λ_0 values in Table 1 with $u = \lambda_0/\mathcal{F}$ and the activities calculated with the a values from this table and equations (1) and (2).

At 10 mM the change KCl → K-glucuronate induced a change U_{diff} of −9.4 mV ($n = 3$). This is not significantly different from the value −9.9 mV at 100 mM concentration.

TABLE 3

(a) Changes in ion potentials (ΔU_K or ΔU_{Cl}) due to the switch from a 100 mM KCl reference solution to a 100 mM test solution measured in a circuit according to Fig. 2a and diffusion potentials (U_{diff}) according to Fig. 2b. The value U_H is the theoretical diffusion potential for the liquid junction between a 100 mM KCl solution and the test solution calculated with equation (7) at 25°C, assuming $f_+ = f_- = f_\pm$ [cf. equation (2)]. (b) The same as in (a) but with 10 mM concentrations. Potassium potentials (U_K) were measured with a potassium-sensitive miniature glass electrode and chloride potentials (U_{Cl}) with an Ag|AgCl electrode. Diffusion potentials (U_{diff}) were measured across a porous plug. All salt bridges were freshly cut 3 M KCl agar bridges

Cation	Anion	ΔU_K (mV)	ΔU_{Cl} (mV)	U_{diff} (mV)	$f_\pm$	U_H (mV)
(a) 100 mM						
K	Cl	0	0	0	0.768	0
K	glucuronate	−3.78 ± 0.08	–	−9.90 ± 0.03	0.740	−10.5
Choline	Cl	–	3.08 ± 0.08	6.10 ± 0.11	0.736	6.8
NMG	Cl	–	3.40 ± 0.12	9.01 ± 0.03	0.732	10.1
(b) 10 mM						
K	Cl	0	0	0	0.901	0
K	glucuronate	−1.1 ± 0.1	–	−9.4 ± 0.3	0.896	−10.5

Osmolarity

Comparison of the data of KCl, K-glucuronate, choline chloride and NMG–Cl did not show any significant differences in the osmotic coefficients either with the vapour pressure osmometer or with the freezing point depression osmometer. The small differences in these data are within the accuracy of calibration (see Table 4). Using the parameter a from Table 1, Bjerrum's theory would predict an association of 6 to 8% in the solutions under investigation, which corresponds to roughly 3 to 4% reduction in osmolarity (*i.e.* 6 to 8 mosmoles/dm^3). The data, therefore, do not support clearly the idea that ion association occurs in these electrolyte solutions. In the same table are compiled the values of φ calculated from Table 1 with equation (4). Clearly all values are in the same range and the influence of the value for K-glucuronate is too small to be observable during such measurements.

Intracellular potential measurements

Figure 1 shows mucosal membrane potentials (U_{mc}) in a goldfish intestinal epithelial cell during chloride–gluconate substitutions: the dashed tracings represent the responses when a potassium-selective microelectrode was used as reference

TABLE 4

Osmolarities of the studied potassium and chloride salts determined with a Freezing Point Osmometer (FP) and a Vapour Pressure Osmometer (VP). The differences observed are within the accuracy of calibration typical for the instruments (±2 mosmoles/dm^3)

Cation	Anion	Osmotic coefficient		
		FP	VP	calculated
100 mM				
K	Cl	0.919 ± 0.002	0.911 ± 0.002	0.927
K	glucuronate	0.919 ± 0.002	0.902 ± 0.002	0.911
Choline	Cl	0.910 ± 0.002	0.905 ± 0.002	0.908
NMG	Cl	0.928 ± 0.002	0.914 ± 0.003	0.906
10 mM				
K	Cl	–	–	0.967
K	glucuronate	–	–	0.965

electrode. It can be seen that U_{mc} first depolarizes and subsequently hyperpolarizes. In the other tracings where the reference electrode was a normal 3 M KCl salt bridge, the initial positive deflection is absent and the total hyperpolarization in U_{mc} is also about 6 mV larger. Averaged over 20 determinations the deviation was 4.1 ± 0.3 mV.

DISCUSSION

The conclusion derived from the osmotic measurements is that there is no reason to assume that ion association is an important factor in the solutions of the studied organic salts.

Since different types of ion-sensitive electrodes all produced essentially the same results, it is not likely that specific artifacts of these electrodes are involved. In addition, one can conclude that the observed effects not only apply to K^+ but also to Na^+ and are in fact roughly the same (see Table 2).

From the conductivity measurements of the organic salts it can be concluded that in the 10 to 100 mM range, ionic interactions affect the activities or the mobilities of the ions as the distance of nearest approach (a) in equation (3) is smaller than the value expected from the sum of the radii of the constituting ions.

Relating λ_0 to the diffusion coefficient at infinite dilution D_0 [13] one finds $D_0 = 0.72 \pm 0.02\ 10^{-5}$ cm^2 s^{-1} as compared to glucose $D = 0.67\ 10^{-5}$ cm^2 s^{-1}. From D_0 one can calculate the radius (r) of the glucuronate ion ($D = kT/4\pi\eta r$) and finds $r \simeq 5$ Å. The discrepancy between a (2.1 Å) and the sum of the ion radii (about 7 Å) might indicate that these anions are not spheroid or that the charge is not located in the centre of the ion. Another choice of b cannot accomodate this discrepancy.

As for the potential measurements, one can still choose either the extrathermodynamical assumption that the ion activities changed or that the diffusion potentials near the junctions changed. This can easily be shown by adding the left and right hand sides of equations (8) and (9) to:

$$U_{diff} + \Delta U_i = U_H + \Delta\phi_i \qquad (10)$$

The left handside of equation (10) contains only experimentally observed values while the right handside contains U_H and $\Delta\phi_i$, which only depends on f_+. Both assumptions can now be assessed by applying them to the results.

Assuming that changes in cation activity coefficient (f_+) equal the mean activity coefficient ($f_\pm$) one finds $U_H = U_{diff} + \Delta U_K + 0.9$ mV from the experiments. Alternatively, applying the modified Henderson diffusion equation one finds $U_H = -10.5$ mV for 100 mM potassium salt solutions. This calculated value and the experimentally determined value differ by 2.4 mV, which therefore is the additional potential change near the liquid junction. The best explanation for this change is that the mobilities of K^+ and Cl^- are changed in the junction by the presence of a relatively high concentration of large organic ions which behave slightly similar to a micellar suspension in the suspension effect [22,23]. If this explanation applies here indeed, the effects are expected to occur in most types of liquid junctions where large organic ions are included. Thus the difference between the diffusion potential U_{diff}

and the calculated Henderson potential (U_H) could be relatively small because the artifacts near the junctions with the salt bridge ($-\Delta\phi_{SB}$) and the reference solution cancel each other partly (see Fig. 2b and Table 3). The deviations are best observable when ΔU_i is measured with an ion-sensitive electrode with respect to a junction type reference electrode in which case presumably $\Delta U_i \simeq \Delta\phi_{SB}$.

The other assumption, that the activity coefficients changed, can be assessed by analyzing $\Delta\phi_i$, assuming that the unmodified Henderson diffusion equation can be applied to the junction near the reference electrode. $\Delta\phi_{SB}$ for 100 mM is -1.32 mV and for 10 mM it is -0.38 mV. With equation (8) one can now calculate the f_+ in 100 mM and 10 mM K-glucuronate. If $f_+(KCl) = f_-(KCl) = f_\pm(KCl)$, then in K-glucuronate f_+ at 100 mM is 0.698 ± 0.001 and at 10 mM f_+ is 0.876 ± 0.001. With equation (5) one can calculate from this that the glucuronate ion in the 100 mM solution should have a hydration number of approximately 37 (assuming that this value for K^+ is 2 [11]). It is left open whether one wants to consider this as a physically realistic value. It might be possible that other theories — like the discrete lattice theory — when fully developed, will provide an answer to this question. Using the found value of 37 to calculate f_+ in the 10 mM solution one finds $f_+ = 0.891$.

Up to now it was tried in this discussion to contrast the differences in results depending on the assumption made. If the electrode processes are predominant they account for about -2.4 mV in U_K and nearly nil in U_{diff}. If the activity change is predominantly the origin of the measured ΔU_K, f_+ should drop from 0.768 to 0.698 upon KCl → K-glucuronate substitution, in 100 mM solutions. There is, however, no theoretical reason to exclude the possibility that the substitution introduced an effect that influences both the activity of the counterion and the junction potentials near the electrodes with transference. In any case, an explanation that would only assume that the activity coefficient changed is not very likely, as can be deduced from the following arguments based on the application of equation (10). The right hand terms in this equation both depend on the activity of K^+ in the solution. Therefore one can solve simultaneously $\Delta\phi$ with equation (6) and U_H with equation (7), both as functions of f_+, and try to find the value f_+ (and $f_- = f_\pm^2/f_+$) where equation (10) is fulfilled. This occurs when f_+ is about 0.55, which is an unrealistically low value.

As far as it is allowed to make statements about single ion activities, the conclusion from this analysis is that though it cannot be excluded that the ion activity coefficients of the ions decrease when their counterions are large organic ions, it is not the only effect. Processes occuring near the reference salt bridge must be included in the explanation of the potential changes observed in circuits where these organic ions are used.

This is illustrated in Fig. 3, where transients were recorded using the circuit of Fig. 2a. The reference solution (R) was a standard salt solution and the sensor electrode (ISE) a potassium-selective microelectrode.

In tracing (a) a 3 M KCl agar bridge was used as reference electrode: in (b) a 3 M KCl microelectrode (tip diameter smaller than 0.5 μm and with a tip resistance of 20

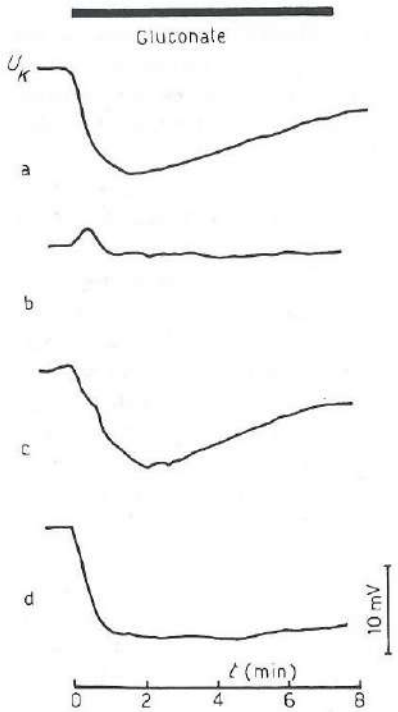

Fig. 3. Recordings of the transient potentials in a circuit according to Fig. 2a when the test solution was changed from a standard Ringer solution to a chloride-free Ringer solution. For all measurements a potassium-sensitive microelectrode was used as sensor electrode. Different reference electrodes were used: (a) a 3 *M* KCl agar bridge (the steady state value after 15 min was −4.2 mV); (b) a 3 *M* KCl-filled microelectrode; (c) a 3 *M* KCl-filled microelectrode with broken tip; (d) a standard Ringer salt bridge.

MΩ), in (c) a 3 *M* KCl microelectrode with broken tip and in (d) a standard salt solution agar bridge. One sees that the first and third transient are slow and only reach their steady state value asymptotically. Standard salt agar bridges produce better results, being fast and reproducible [see recording(c)]. This is probably because the salt solution junction approximates the bi-ionic type (which is normally well-defined and stable [9]). The recording with the microelectrode (b) in Fig. 3 shows only a small transient, but the magnitude of this transient is not very reproducible. This different behaviour is clearly related to the extremely small surface of the tip opening, as breaking off the tip gives recording (c). It cannot be decided whether this is directly or indirectly due only to this extremely small surface or also to the greater importance of the charged glass capillary surface surrounding the junction, thus influencing electrokinetically the diffusional parameters for cations and anions in this junction.

Standard salt agar bridges, if accurately corrected for the liquid junction potential, seem well suited for steady state measurements. For transients, however, one

should preferably choose reversible ion-selective electrodes. Although this is recognized by many investigators, who therefore use Ag|AgCl reference electrodes during cation substitutions [9,19], it is not yet common practice for anion substitutions. Here we show that one should be extremely cautious using 3 *M* KCl salt bridges for accurate electrical measurements during anion substitutions, especially when transients are to be measured in which case the errors may be even as large as 12 mV. Inherently, in both approaches an extrathermodynamical assumption is still hidden: either that near the 3 *M* KCl reference electrode no potentials are developed or that the cation activity did not change. By using cation-sensitive reference electrodes during anion substitutions one can overcome the transient problems, as we illustrated in Figs. 1 and 3. The selection of the most suitable cation-selective reference electrode depends partially on its selectivity to divalent cations, because these ions may be associated to a large extent in chloride-free solutions [16]. Applying both assumptions to the analysis of data from biological research might show to what extent these assumptions influence the outcome.

ACKNOWLEDGEMENTS

We thank Prof. Dr. J.Th.G. Overbeek and Prof. Dr. J.A.A. Ketelaar for critical reading of earlier versions and constructive suggestions and Dr. P. Diegenbach for help with the fitting procedure. This work was supported by the Netherlands Foundation for Biophysics with financial aid of the Netherlands Organisatior for Advancement of Pure Science (ZWO).

REFERENCES

1 W.McD. Armstrong and J.F. Garcia-Diaz, Fed. Proc. Fed. Am. Soc. Exper. Biol., 39 (1980) 2851.
2 M.E. Duffey, K. Turnheim, R.A. Frizzell and S.G. Schultz, J. Membr. Biol., 32 (1979) 229.
3 H. Freiser (Editor), Ion-selective Electrodes in Analytical Chemistry, Plenum Press, New York, London, 1978, Vol. 1.
4 L. Reuss and T.G. Grady, J. Membr. Biol., 51 (1979) 15.
5 A.P. Sharp and R.C. Thomas, J. Physiol. (London), 312 (1981) 71.
6 K.R. Spring and G. Kimura, J. Membr. Biol., 38 (1978) 233.
7 R.C. Thomas, Ion-sensitive Intracellular Microelectrodes, Academic Press, New York, London, San Francisco, 1978.
8 R.C. Thomas and C.J. Cohen, Pflügers Arch., 390 (1981) 96.
9 P.H. Barry and J.M. Diamond, J. Membr. Biol., 3 (1970) 93.
10 H.S. Harned and B. Owen, The Physical Chemistry of Electrolytic Solutions, Rheinhold, New York, 1964.
11 N. Lakshminarayanaiah, Membrane Electrodes, Academic Press, New York, San Fransisco, London, 1976.
12 P.C. Meier, F. Lanter, D. Ammann, R.A. Steiner and W. Simon, Pflügers Arch., 393 (1982) 23.
13 R.A. Robinson and R.H. Stokes, Electrolyte Solutions, Butterworth, London, 1959.
14 G. Kortüm, Treatise on Electrochemistry, Elsevier, Amsterdam, 1965.
15 J. O'M. Bockris and A.K.N. Reddy, Modern Electrochemistry, Plenum Press, New York, 1973.
16 G.R.J. Christoffersen and L.H. Skibsted, Comp. Biochem. Physiol., 52A (1975) 317.
17 R.M. Garrels in Glass Electrodes for Hydrogen and Other Cations, Principles and Practise, G. Eisenman (Editor), Dekker, New York, 1967, p. 344.

18 J.L. Walker, Jr., Anal. Chem., 43 (1971) 89A.
19 R. Laprade and J. Cardinal, Am. J. Physiol., 244 (1983) F304.
20 D.A. MacInnes, The Principles of Electrochemistry, Dover, New York, 1961.
21 H. Albus, R. Bakker and J. Siegenbeek van Heukelom, Pflügers Arch., 398 (1983) 1.
22 J.Th.G. Overbeek, J. Colloid Sci., 8 (1953) 593.
23 J.Th.G. Overbeek in Progress in Biophysics and Biophysical Chemistry, J.A.V. Butler and J.T. Randall (Editors), Butterworth, London, 1956, Vol. 6, p. 57.

Chapter III

Cellular and Transepithelial Responses of Goldfish Intestinal Epithelium to Chloride Substitutions

T. Zuidema, J. W. van Riel, and J. Siegenbeek van Heukelom
Department of Zoology, Membrane Biophysics, University of Amsterdam, 1098 SM Amsterdam, The Netherlands

Summary. In goldfish intestine chloride was substituted by large inorganic anions (gluconate or glucuronate) either mucosally, serosally or bilaterally. Changes in intracellular activities of chloride (a_iCl^-), sodium (a_iNa^+) and potassium (a_iK^+), pH_i, relative volume, membrane and transepithelial potentials, transepithelial resistance and voltage divider ratio were measured. Control values were: a_iCl^- = 35 meq/liter, a_iNa^+ = 11 meq/liter and a_iK^+ = 95 meq/liter. During bilateral substitution the latter two did not change while a_iCl^- dropped to virtually zero.

Mucosal membrane potentials (ψ_{mc}) were: control, −53 mV; serosal substitution, −51 mV; bilateral substitution, −66 mV; while during mucosal substitution a transient depolarization occurred and the final steady state ψ_{mc} was −66 mV.

During control and bilateral substitution the transepithelial potentials (ψ_{ms}) did not differ from zero. During unilateral substitutions ψ_{ms} was small, in the order of magnitude of the errors in the liquid junction potentials near the measuring salt bridges.

During bilateral substitution pH_i increased 0.4 pH units. Cellular volume decreased during mucosal substitution to 88% in 40 min; after serosal substitution it transiently increased, but the new steady-state value was not significantly above its control value.

Three minutes after mucosal substitution an a_iCl^- of approx. 10 meq/liter was measured.

Chemical concentrations of Na, K and Cl were determined under control conditions and bilateral substitution. Cl concentrations were also measured as a function of time after unilateral substitutions.

The data indicate an electrically silent chloride influx mechanism in the brush border membrane and an electrodiffusional chloride efflux in the basolateral membrane. A substantial bicarbonate permeability is present in the basolateral membrane. The results are in agreement with the observed changes in membrane resistances, volume changes and pH changes.

Key Words intracellular ion activity · K^+ · Na^+ · Cl^- · HCO_3^- · intestinal epithelium · intercellular space · goldfish

Introduction

Henin and Smith [27] were the first to report that ψ_{mc} in rabbit colonic mucosa hyperpolarized after mucosal chloride omission. Later this effect was also found in other intestinal preparations, especially those bathed in bicarbonate salt solutions [14, 26, 30]. Hyperpolarizations in bicarbonate-free situations were smaller or insignificant [37, 43, 54]. In *Necturus* proximal tubule and gallbladder ψ_{mc} even depolarized when chloride was substituted in bicarbonate-free solutions. Guggino et al. [25], however, showed that after bilateral or serosal chloride substitution a hyperpolarization occurred which was dependent on bicarbonate and was abolished by serosal SITS (4-acetamido-4′-isothiocyanatostilbene-2,2′-disulfonic acid) application.

The chloride conductances of both the apical and basolateral membrane of proximal tubule and gallbladder are usually estimated low [25, 39, 40, 46]. Some of the limitations of these studies were corrected for recently by Fisher [16] who carefully measured the transient diffusion potentials across the subepithelial connective tissue and minimized the influence of electrical changes at the apical barrier. His results support the earlier conclusions.

Baerentsen et al. [4], however, pointed out that the chloride permeability of the basolateral membrane is masked by the large potassium permeability and the rheogenic contribution of the Na/K pump and is therefore easily underestimated. Also subsequent changes in intracellular chloride activity tend to mask the depolarizing effects of chloride substitutions. Especially the latter effects may be important in intestinal epithelia, whose villus or fold structure gives rise to considerable unstirred layers and consequently delayed responses. Moreover, the columnar shape of the enterocytes and the long and narrow interspace bounding the basolateral membrane make it necessary to treat the interspace as a separate compartment in the analysis [15].

The purpose of the present study was to obtain information about the chloride conductance of the plasma membranes of goldfish intestinal epithelium. To this end we performed an analysis of potential changes and changes in intracellular activities in re-

sponse to chloride substitutions. In contrast to the aforementioned studies in gallbladder and proximal tubule we conclude that the basolateral membrane of goldfish enterocytes possesses a substantial chloride permeability.

Part of this study was presented at the 4th Conference of the European Society for Comparative Physiology and Biochemistry, 1982 [24].

Materials and Methods

Preparation and Experimental Set-up for Intracellular Measurements

Preparation of the tissue and experimental set-up have been described earlier [1, 48].[1]

Bathing Solutions

The standard salt solution had the following composition (in mM): NaCl, 117.5; KCl, 5.7; $NaHCO_3$, 25; NaH_2PO_4, 1.2; $CaCl_2$, 2.5; $MgSO_4$, 1.2; and mannitol, 27.8. Solutions were gassed with humidified 95% O_2 + 5% CO_2. In the chloride-free solutions the sodium salts of glucuronate (Sigma Chemicals) and gluconate (Merck-Schuchardt) were used as substitutes for chloride; in these solutions KCl and $CaCl_2$ were substituted by K_2SO_4 and $CaSO_4$, respectively, and balanced osmotically by addition of 14 mM of mannitol. No different results were found between solutions where gluconate or glucuronate were used as substitute.

Assays of Intracellular pH and Extracellular Space

Intracellular pH and extracellular space were determined as described by Groot [21, 22]. Free floating strips of intestinal mucosa were preincubated several times in fresh solutions of the desired composition for at least 30 min before incubation in radioactive solutions. The solutions were stirred by continuous flow of humidified gas (95% O_2 + 5% CO_2). After 30 to 45 min the strips were removed, gently blotted on Whatman (#1) filter paper and weighed in tarred aluminium weighing boats (Heraeus) on a Mettler ME 30 microbalance. Radioactivity was measured in a liquid scintillation counter (Packard Tricarb 2660) with Instagel® (Packard) as scintillation mixture. The extracellular space was calculated from the distribution ratio of ^{3}H-labeled PEG (4000 D) between tissue and medium and was normally 15% of the tissue volume [*cf.* 21, 36, 54, 55]. This value is assumed to be constant during the experiments. Intracellular pH was estimated from the distribution ratio of ^{14}C-labeled DMO (5,5-dimethyloxazolidine-2,4-dione) according to Waddell and Butler [53].

The radioactivity in the solutions was about 10^6 dpm/ml. Experiments were carried out at 20°C.

Assay of Intracellular Na, K, Cl Concentrations and Water Content[2]

Ion and water content in free-floating strips were analyzed as described by Groot [21]. For the determination of the intracellular Cl concentration and water content after unilateral Cl substitution mucosal strips were mounted as flat sheets on tissue holders, leaving an exposed area of 0.2 cm^2 [23]. The holders were clamped between two Lucite chambers with gassed solutions of the desired composition.

At chosen intervals the tissue was punched out of the holders, gently blotted with Whatman (#1) filter paper and weighed as described above. Dry weight was determined after drying for at least 2 hr at 105°C. The dried tissue was extracted in 0.1 N HNO_3 for at least 2 hr. Then chloride was determined with a Micro Chlor-o-counter (Marius, Utrecht, Netherlands).

Ion-Sensitive Microelectrodes[3]

Although the steady-state ψ_{mc} in this study varied from −40 to −70 mV, the differences between individual cells of the same preparation are small, normally less than 5 mV. In order to reduce the errors due to this variability, the average of 3 to 8 individually measured membrane potentials was taken as the reference value for calculation of the steady-state intracellular activities.

Construction, calibration and application of both normal and ion-sensitive microelectrodes are described elsewhere.[4] For the Cl^--sensitive microelectrodes a liquid membrane (WPI-IE 170) was used. A slope constant of 54.9 ± 0.2 mV/decade in Cl^- activity was found (n = 30), while the selectivity coefficients were $K_{Cl,HCO_3} = 0.16 \pm 0.01$ (n = 12), $K_{Cl,gluconate} = 0.04 \pm 0.01$ (n = 12) and $K_{Cl,HPO_4} < 0.10$ [3, 34].

In the solutions used for chloride substitution experiments the apparent chloride ion activity was 6.8 meq/liter; as the salt solution contained 25 mM $NaHCO_3$ one can calculate that 3.2 meq/liter can be attributed to HCO_3 taking into account an activity coefficient of 0.76.

The intracellular HCO_3^- activity is calculated from pH_i values obtained as described above with the assumption that pCO_2, CO_2 solubility and activity coefficients in the cell and the bathing solutions are the same.

Measuring Artifacts Due to the Use of Large Organic Anions

During calibration when control solutions were changed to glucuronate and gluconate salt solutions a shift of about −4.1 mV with respect to the reference salt bridge was measured with potassium-selective microelectrodes. This shift varied almost linearly with the concentration of the substituting organic anions, but slope constant or selectivity of the electrodes were not affected. The deviation can be caused by changes in the liquid junction potential near the reference salt bridge or by a reduction in single cation activities of sodium and potassium. On theoretical grounds it is impossible to discriminate between these two alternatives [8, 31, 34, 60]. A full account of the possible causes and consequences of this deviation is given in a separate paper [60].

As normally ψ_{mc} is defined as the potential change sensed by the microelectrode upon penetration of the cell membrane, the reference potential taken is the one measured by the microelectrode in the mucosal bath solution. Accordingly, corrections are made when ψ_{mc}, measured during ion substitutions, is used for calculations of permeability ratios (*see* Table 5).

ψ_{ms} is normally measured with agar salt bridges, mostly 3 M KCl. The shift has no consequences for bilateral substitutions, when it occurred at both sides of the epithelium. Corrections are needed, however, for the shift during unilateral substitutions [8, 31, 60], in order to calculate the transepithelial potential changes.

As plasma membranes and the tight junctions are cation-selective, the reading of a cation-selective electrode in the mucosal bath was chosen as the reference. If the shift of −4.1 mV is, indeed, due to a change in cation activity in the bathing solutions, this is the best way to account in the analysis for the membrane responses to this change. A number of experiments was carried out even using the potassium-sensitive microelectrode directly as reference electrode (Fig. 1). By placing the tip of this electrode near the cells penetrated by the measuring microelectrode, potential artifacts by diffusional delays in unstirred layers are minimized [16].

Finally, the sodium-selective liquid membrane in the microelectrode had a high sensitivity to Ca^{2+} [12, 34], which was present in the solution in a concentration of 2.5 mM. As in gluconate and glucuronate solutions a substantial part of Ca^{2+} is associated to these anions [10], an average additional deviation was found of −6.3 mV, corresponding to approx. 70% of the calcium being associated. Since neither addition nor omission of $CaSO_4$ in chloride-free solutions alters the membrane potential significantly [*cf.* 16, 25] the chloride-free solutions were not adjusted by increasing the calcium activity.

Statistics

The presented steady-state values are the average of the measured values. Transient responses were measured at distinct time intervals with respect to the preceding steady-state values and averaged. All values are given ± SEM.

[1] Zuidema, T., Kamermans, M., Siegenbeek van Heukelom, J. Basolateral potassium redistribution in goldfish intestine induced by glucose absorption. *Pflügers Arch.* (*submitted*).

[2] Throughout this paper ionic activities are denoted $a_x I$, chemical concentrations $[I]_x$; I ionic species, z charge number and x intracellular compartment (i) or bathing solution (o).

[3] *See* footnote 2.

[4] *See* footnote 1.

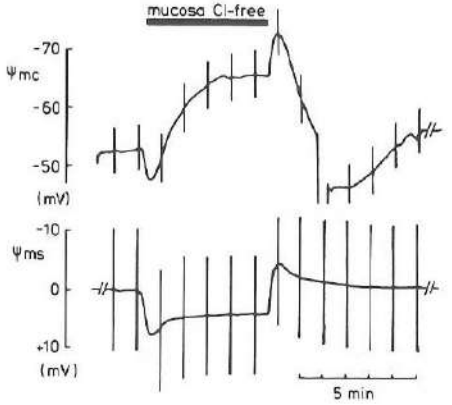

Fig. 1. Typical recordings of ψ_{mc} and ψ_{ms} during mucosal chloride-gluconate substitution. In these recordings a potassium-selective microelectrode was used as reference electrode

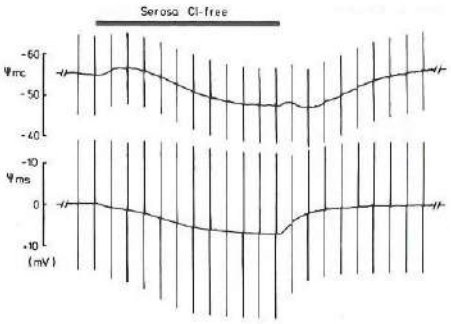

Fig. 2. Typical recordings of ψ_{mc} and ψ_{ms} during serosal chloride gluconate substitutions. Mucosal reference electrode and serosal voltage electrode were connected to the bath by Ringer agar bridges

Results

Electrical Responses to Chloride Substitutions

Mucosal Substitutions

In Fig. 1 representative recordings are shown of the responses to mucosal chloride substitution of ψ_{mc} and ψ_{ms} both with respect to a potassium-sensitive microelectrode in the mucosal bath. The initial depolarization of ψ_{mc} is followed by a hyperpolarization. In eight identical determinations we found an average peak depolarization of ψ_{mc} of +4.7 ± 0.5 mV followed by a hyperpolarization of −10.0 ± 0.6 mV. In contrast, ψ_{sc} (defined as $\psi_{sc} = \psi_{mc} - \psi_{ms}$) did not depolarize at any time. The initial change in ψ_{ms} was +5.9 ± 0.5 mV, while the steady-state potential change was + 2.9 ± 0.5 mV (equivalent with −1.2 mV with respect to a 3 M KCl agar bridge).

Serosal Substitutions

Typical changes in ψ_{mc} and ψ_{ms} due to serosal chloride substitution are shown in Fig. 2. The serosal voltage electrode was formed by a salt bridge filled with standard salt solution, thus introducing a large liquid junction potential in series with the transepithelial potential. The small initial upward deflection in ψ_{mc} (2.8 ± 0.5 mV) is most likely induced by the shunt diffusion potential which develops more quickly and introduces, by voltage dividing, a hyperpolarization of several mV.

Table 1. Electrical responses to chloride substitutions

$N = 33$	Control	Mucosal	Serosal	Bilateral
ψ_{mc} (mV)	−52.4 ± 0.7	−65.7 ± 1.2	−51.4 ± 1.6	−66.6 ± 1.3
ψ_{ms} (mV)	0.0 ± 0.1	−1.2 ± 0.3	−2.5 ± 0.6	−0.2 ± 0.1
R_{ms} (Ωcm^2)	17.8 ± 0.5	16.9 ± 0.8	21.9 ± 1.1	20.3 ± 0.9
R_m/R_s	1.48 ± 0.08	1.49 ± 0.14	1.24 ± 0.16	1.11 ± 0.25
n	58	19	17	22

Steady-state membrane potentials and transepithelial potentials during control, mucosal, serosal or bilateral chloride substitution situations. Control values are pooled averages of the individual controls of the mucosal, serosal and bilateral substitutions. N is the number of preparations, n is the number of measurements.

Table 2. Intracellular ion activities

Ion	ψ_{mc} (mV)	a_iI (meq/liter)	$(a_iI)_{eq}$ (meq/liter)	N, m, n
Control				
Na^+	−50.6 ± 1.3	11.1 ± 1.1	800	11, 60, 61
K^+	−53.6 ± 1.7	95.1 ± 3.2	36	14, 68, 60
Cl^-	−55.7 ± 1.4	35.3 ± 1.4	10.4	15, 74, 78
Bilateral				
Na^+	−64.8 ± 1.4	15.5 ± 3.3	1240	5, 21, 24
K^+	−69.8 ± 2.8	93.1 ± 3.0	60	5, 21, 26
Cl^-	−70.2 ± 1.0	(7.0 ± 0.3)[a]	0	5, 21, 27

Steady-state membrane potentials (ψ_{mc}) and intracellular ion activities (a_iI) of goldfish enterocytes during perfusion with normal Ringer (control) and during bilateral perfusion with Cl^--free solutions. The ion activities are calculated as described in Materials and Methods.

[a] The apparent a_iCl^- under chloride-free conditions and normalized to 0.

$(a_iI)_{eq}$ is the intracellular activity expected if electrochemical equilibrium would exist across the cellular membrane.

Averages were taken over the number of epithelia investigated (N); m is total number of impalements with voltage-sensing electrodes; n is total number of impalements with ion-sensitive microelectrodes. ψ_{mc} averaged over all bilateral determinations was 68.5 mV.

Table 1 gives the steady-state values of ψ_{mc} and ψ_{ms} during control, mucosal, serosal and bilateral chloride substitution. In this table ψ_{ms} was taken with respect to a 3 M KCl salt bridge. The transepithelial resistance R_{ms}, simultaneously determined, is also presented. From the apparent voltage divider ratio in the cell and across the epithelium: $\Delta V_{mc}/\Delta V_{ms}$, that was measured simultaneously, the apparent ratio R_m/R_s (*see also* Table 1) was calculated as described earlier [1] using a correction for the different resistivity of the chloride-free solutions (112 Ωcm *vs.* 64 Ωcm). Both R_{ms} and R_m/R_s do not change significantly after mucosal replacement of chloride ($P > 0.1$). However, after serosal or bilateral chloride substitution R_m/R_s decreases by 20–30% and R_{ms} increases by approx. 15%.

Steady-State Membrane Potentials and Intracellular Ion Activities[5]

Whereas in the gluconate solutions an apparent a_oCl^- was measured of 6.8 meq/liter, in the cell an apparent a_iCl^- is measured of 7.0 ± 0.3 meq/liter (27 cells). Therefore, this a_iCl^- was calibrated to be zero.

In Table 2 the steady-state ψ_{mc} values are given under control conditions and during prolonged bilateral chloride substitution together with the average intracellular activities of Na^+, K^+ and Cl^-. In addition, the intracellular equilibrium ion activity (a_iI_{eq}) is given for each ion. Clearly the experimentally determined a_iK^+ and a_iCl^- are above electrochemical equilibrium while a_iNa^+ is far below. This is commonly found in leaky epithelia like gallbladder [20, 42], proximal tubule [51] and intestine [2, 11, 19, 28, 30, 49, 54, 56, 58, 59]. Under Cl^--free conditions the membrane potential hyperpolarizes so that the equilibrium activities of the cations increase by 75–80%, while the equilibrium activity of chloride is zero.

Moreover, the data show that replacement of chloride does not significantly affect the intracellular cation activities, which is in agreement with the cation activity measurements of Lee and Armstrong [32] (in bullfrog intestine) and White [54] (in *Amphiuma* intestine).

Change in Cell Water and Intracellular pH Induced by Bilateral Cl^- Substitution

As glucuronate is a relatively impermeable anion, the most likely candidate for an exchange with intracellular Cl^- is HCO_3^-. Therefore one must expect an increase in pH_i according to the Henderson-Hasselbalch equation:

$$pH = pK' + \log(HCO_3^-) - \log(CO_2). \quad (1)$$

Indeed, such an increase is found in goldfish intestine [22, 24].

[5] *See* footnote 2.

Table 3. Ion content, cell water and pH

Salt solution	NaCl	Na-glucur	P
Cell water (kg H_2O/kg dry wt)	3.19 ± 0.06	2.97 ± 0.04	<0.01
Na^+ content	146 ± 7	140 ± 7	NS
Na^+ conc.	46 ± 2	47 ± 2	NS
K^+ content	479 ± 9	465 ± 6	NS
K^+ conc.	151 ± 3	157 ± 3	NS
Cl^- content	193 ± 6	30 ± 3	<0.001
Cl^- conc.	61 ± 2	10 ± 1	<0.001
pH_o	7.45 ± 0.02	7.53 ± 0.01	
pH_i	7.14 ± 0.03	7.64 ± 0.02	<0.001
$pH_i - pH_o$	−0.31 ± 0.04	+0.11 ± 0.02	<0.001

Influence of Cl^--free incubation solution on cell water, ion content, ion concentration, pH_i and difference between pH_i and pH_o in free floating strips of goldfish intestinal epithelium. Determinations were executed in 30 strips from 3 animals.

The effect of Cl^--free solutions on intracellular concentrations resembles the changes in intracellular activities measured with ion-selective microelectrodes (Tables 2 and 3). In paired experiments the cation content and concentration remained unchanged within experimental accuracy, while cell water decreased with 7% and ($pH_i - pH_o$) increased with 0.42 pH units.

From these data one can calculate that the HCO_3^- activity increased from 8.9 meq/liter to 23.5 meq/liter; these are the values used for correction of the chloride-selective microelectrodes for intracellular interference of HCO_3^-. With this information one can calculate that the total interference of all other anions in the cell under control conditions is equivalent with 7.0 − 0.16 × (23.5 − 8.9) = 4.7 meq/liter Cl^-.

Changes in Cell Water after Unilateral Chloride Substitutions

Figure 3 shows the changes in cell water (kg H_2O/kg dry wt) after mucosal Cl^- substitution (filled symbols) and serosal substitution (open symbols). After mucosal substitution cell water decreased by 12%, and after serosal substitution it increased transiently and returned to a value not significantly different from control.

Changes in Intracellular Chloride Activity and Concentration after Mucosal Chloride Substitution[6]

Figure 4 shows the changes in a_iCl^- after mucosal substitution. The average initial rate of change is

[6] *See* footnote 2.

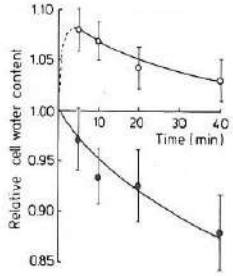

Fig. 3. Responses of relative cell water content to mucosal (●; $n = 9$) and serosal (○; $n = 18$) chloride substitutions as a function of time after the substitution

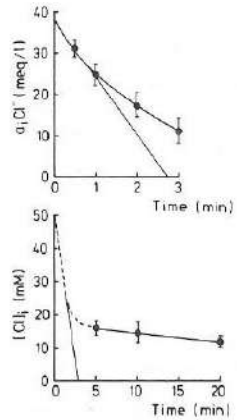

Fig. 4. Intracellular chloride activity (a_iCl^-) and concentration [Cl^-]$_i$ as a function of time after mucosal substitution by gluconate (at $t = 0$ min). Note the difference in time scale.

Upper curve: a_iCl^- averaged over recordings where ψ_{mc} and ΔE_{Cl} were simultaneously recorded in two cells closely apart. The slope of the straight line corresponds to a rate of change of 0.25 meq/liter · sec.

Lower curve: [Cl^-]$_i$ averaged over 8 to 12 mucosal strips from three fishes. The interrupted part of the curve is obtained by transformation of the upper curve using an apparent activity coefficient of 0.76 (*see* text) and allowing for the different time scale

approximately 0.25 meq/liter · sec. a_iCl^- decreased within 3 min to approximately 10 meq/liter, and was still decreasing. This value is already nearly the electrochemical equilibrium value for chloride across the basolateral membrane (6.5 meq/liter). After 3 min it became impossible to keep both microelectrodes in their respective cells, most likely because of cell shrinkage.

Table 4. Influence of bicarbonate on membrane potential and pH_i

$[NaHCO_3]$ (mM)	ψ_{mc} (mV)	$(pH_i - pH_o)$	a_iHCO_3 (meq/liter)
4	−30.5 ± 0.5	0.10 ± 0.03	3.7
10	−45.2 ± 2.1	0.13 ± 0.02	9.8
25	−58.8 ± 2.3	−0.19 ± 0.04	11.8
62.5	−71.4 ± 1.6	−0.34 ± 0.03	32.5

Membrane potentials, intracellular to extracellular pH differences and estimated intracellular HCO_3 activity as a function of $NaHCO_3$ concentration in the bathing solutions.

The decrease of the cellular chloride content was measured for longer times. During these determinations the chloride concentration in the extracellular space is assumed to be equal to that in the serosal bathing solution. The ratio of a_iCl^- and $[Cl^-]_i$ in control solutions was 0.76. Applying this ratio to the other determinations of $[Cl^-]_i$ one finds that the data of a_iCl^- and $[Cl^-]_i$ correspond reasonably and the final steady state in Cl^--free solutions is 9.2 meq/liter, which is nearly the equilibrium value of a_iCl^- across the basolateral membrane (6.5 meq/liter).

Membrane Potentials and Estimated Intracellular Bicarbonate Activity

In Table 4 measurements are presented of ψ_{mc} and transmembrane pH gradients in four different HCO_3^- buffers. These solutions were obtained by substituting 37.5 mM out of 127.1 mM Cl^- and the 25 mM HCO_3^- already present in the solution, by mixtures of HCO_3^- and gluconate having a total concentration of 62.5 mOsm. With increasing $NaHCO_3$ concentration the pH of the salt solution (pH_o) increased. ψ_{mc} hyperpolarized and pH_i increased, but less than pH_o. From $(pH_o - pH_i)$ $a_iHCO_3^-$ was calculated under the same assumptions as above using the Eq. (1).

Analysis and Discussion

For the analysis, the obtained data, corrected for liquid junction potentials as described in Materials and Methods, are lumped in one set in Table 5. Data in parentheses are estimates made as interpolations between experimentally determined values. The simplifying derivatives and assumptions which have been made for the analysis are discussed in paragraphs 1 to 4.

1. Equivalent Electrical Network

The equations of the equivalent electrical network related to our preparation [1] are:

$$\psi_{mc} = (R_s + R_i) \cdot E_m/R_T + R_m \cdot (E_s + E_i)/R_T \quad (2a)$$

and

$$\psi_{ms} = R_i \cdot (E_m - E_s)/R_T + (R_m + R_s) \cdot E_i/R_T \quad (2b)$$

where R refers to specific membrane resistances (Ωcm^2), E to electromotive forces (mV), subscript m to the brush border membrane, s to the basolateral membrane and i to the shunt pathway. R_T is defined as $R_T = R_s + R_m + R_i$. The theoretical zero-current potentials E are assumed to satisfy the Goldman-Hodgkin-Katz equation extended to include the phenomenological permeabilities of the four major ions (Na^+, K^+, Cl^- and HCO_3^-) and the contribution of a rheogenic Na/K pump [29, 57].

As the relative shunt conductance $g_{shunt} = (R_m + R_s)/R_T = 0.95$ [1] it can easily be shown[7] that by substitution of ψ_{ms} for E_i in Eq. (2a) an error is introduced of less than 2.5%. Therefore the influence of E_i in ψ_{mc} will be equated with the value of ψ_{ms}.

In control situation and during bilateral substitution $\psi_{ms} = 0$:

$$\psi_{mc} = (R_s + R_i)E_m/R_T + R_mE_s/R_T = \psi_{sc} = E_a. \quad (3)$$

With this equation one can relate the influence of electrogenic events, occurring either only mucosally (ΔE_m) or basolaterally (ΔE_s), to a potential change of the enterocyte membrane potential ($\psi_{sc} = \psi_{mc}$) as if it were an unpolarized or apolar cell (E_a) provided that the voltage divider ratio is known. This applies also the rheogenic contribution of the Na/K pump in the basolateral membrane ($\Delta E_{s,pump}$) and to the unilateral electrodiffusional permeabilities (*see* Appendix B).

The rheogenic contribution of the Na/K pump to E_a ($\Delta E_{a,pump}$) is calculated with the equation that compares the Goldman-Hodgkin-Katz equation with a pump ratio $r = 3/2$ (Na : K = 3 : −2) and 1 (Na : K = 1 : −1) [*cf.* 57]:

$$\Delta E_{a,pump} = RT/F \cdot \ln\{L[M + (r-1)a_oK^+]/M[L + (r-1)a_iK^+]\}. \quad (4)$$

R, T and F have their usual meaning, L and M are defined in Appendix A. Consequently $\Delta E_{s,pump} = (R_T/R_m) \cdot \Delta E_{a,pump}$.

2. HCO_3^- Permeability

After bilateral chloride substitution the total cation activity did not diminish, though Cl^- is, within the accuracy of the experimental error, completely washed out of the cell (*see* Table 3). To preserve electroneutrality, other negative charges must have replaced Cl^- in the cell and the most likely substitute is HCO_3^-. The observed pH_i changes are in agreement with an $a_iHCO_3^-$ increase of 14.6 meq/liter. Since HCO_3^- can easily substitute for Cl^-, a substantial pathway through the membranes for HCO_3^- exists.

Bicarbonate changes in the media induce membrane potential changes that do not allow a calculation of P_{HCO_3}/P_K since they are more than Nernstian (Table 4). These results could be explained by a pH- or HCO_3^--sensitive P_K of the cell membrane as proposed by Reuss et al. [41] and Halm et al. [26]. Unilateral substitutions suggest that the basolateral membrane possesses mainly the HCO_3^- or H^+ permeability [*cf.* 9, 18], as in chloride-free media mucosal substitution of the bicarbonate buffer by a Tris-Hepes buffer causes a hyperpolarization while serosal substitution causes a depolarization.

3. P_{Na} in Basolateral Membrane is Negligible

The electrodiffusional sodium permeability of the basolateral membrane in leaky epithelia is generally estimated low [41, 44, 50]. The direct influence of unilateral sodium substitutions on ψ_{mc} are disturbed by large transepithelial diffusion potentials and possibly by changes in pH_i altering the permselectivity of the mucosal membrane [26, 41]. Bilateral substitutions of sodium by NMDG (N-methyl-D-glucamine) in our preparation led to a sharp increase in R_m/R_s ratio (from 1.36 ± 0.29 to 3.28 ± 0.35, $n = 5$). Therefore we assume that $(P_{Na}/P_K)_b$ is negligible.

4. The Influence of $E_i = 0$

In the bilaterally substituted situation the observation that $\psi_{ms} = 0$ and the assumption that $E_i = 0$ lead to the conclusion that E_m and E_s are equal (*cf.* Eq. (1)). As E_s includes the rheogenic contribution of the pump ($\Delta E_{s,pump}$), the potential in the basolateral membrane due to electrodiffusional fluxes (GHK equation) must be smaller than the potential calculated similarly for the mucosal membrane.

Equally, in control situation ψ_{ms} does not differ significantly from zero [1]. An increased osmolarity in the interspace with respect to the bathing media (e.g., 8 mOsm; [52], will only introduce a contribution of −0.55 mV. This value would introduce in the analysis an increase of about 4 mV for E_s and a decrease of 6 mV for E_m. This leads to a contradiction with experimental results, as will be discussed in paragraph 7.

[7] From Eq. (2b) one derives that

$$E_i = \psi_{ms} - R_i(E_m - E_s - E_i)/R_T.$$

Insertion of ψ_{ms} instead of E_i in Eq. (2a) introduces an error of the magnitude

$$R_m \cdot R_i(E_m - E_s - E_i)/R_T^2.$$

Repeated insertion of ψ_{ms} for E_i leads to a series expansion (with $x = R_i/R_s$)

$$\psi_{sc} = E_m - (R_s/R_T) \cdot (E_m - E_s - E_i) \cdot (1 - x + x^2 - \ldots)$$
$$\psi_{mc} = E_m - (R_s/R_T) \cdot (E_m - E_s - E_i)/(1 + x).$$

The error is therefore

$$\varepsilon(\psi_{mc}) = x \cdot (R_s/R_T) \cdot (E_m - E_s - E_i)/(1 + x).$$

Insertion of $R_m/R_T = 0.55$, $x = R_i/R_T = 0.05$ and the estimate $E_m - E_s < 50$ mV gives $\varepsilon < 2.5\%$.

Table 5. Data lumped for the analysis

	Control	Mucosal	Serosal	Bilateral
ψ_{mc} (mV)	−53	−64	−51	−66
ψ_{ms} (mV)	0	+2.9	−6.6	0
a_iK^+ (meq/liter)	95	(94)	(94)	93
a_iNa^+ (meq/liter)	11	(14)	(14)	16
a_iCl^- (meq/liter)	35	10[a]	26[a]	0
a_iHCO_3 (meq/liter)[b]	9	(20)[c]	(13)[c]	24
R_m (Ωcm^2)	18	18	21	21
R_m/R_s	1.4	1.4	1.0	1.1

Steady-state membrane potentials, transepithelial potentials, intracellular ion activities, under control conditions, and after mucosal, serosal and bilateral chloride substitution. The values in parentheses are interpolated between the values found in control situations and when bilaterally chloride was substituted.

[a] Values obtained by multiplying the intracellularly determined concentration with 0.76 (*see* text).

[b] Calculated from pH_i values (*see* text).

[c] Interpolation under the assumption that the increase is proportional to the decrease in chloride concentration.

Membrane resistances and shunt resistance under control condition are calculated under the assumption that the relative shunt conductance is 0.95, so that $R_m = 210\ \Omega cm^2$, $R_s = 150\ \Omega cm^2$ and $R_i = 18.9\ \Omega cm^2$.

Table 6. Membrane permeabilities and electromotive forces

A.	Brush border membrane	Basolateral membrane	Tight junction	
P_K (10^{-6} cm/sec)	37	34	124	
P_{Cl}/P_K	0.21	0.59	0.20	
P_{Na}/P_K	0.025	0	0.80	
P_{HCO_3}/P_K	0	0.23	ND	
B.	Control	Mucosal	Serosal	Bilateral
E_m (mV)	(−53)	−60	−56	(−66)
E_s[a] (mV)	(−53)	$-59 + \Delta E_{s,pump}$	$-38 + \Delta E_{s,pump}$	(−66)
R_m/R_s	(1.4)	1.4	1.1	1.1

A. Permeabilities for potassium of the three main barriers in the epithelium: The brush border membrane, basolateral membrane and tight junction are given in absolute values related to the serosal area (0.2 cm^2). The permeabilities of Cl^-, Na^+ and HCO_3^- are with respect to the potassium permeability. ND: Not determined.

B. Electromotive forces across the mucosal and the serosal membrane, and voltage divider ratio calculated with the Goldman equations with permeabilities from Table 6*A* and activities from Table 5. Values used to obtain the permeabilities of Table 6*A* are placed in brackets.

[a] The value E_s contains a contribution of the Na/K pump ($\Delta E_{s,pump}$) which is estimated as −9 and −8 mV during resp. control and bilateral substitutions. The value for unilateral substitutions is estimated to be −8.5 mV.

5. Solution of the Goldman-Hodgkin-Katz Equation

Essentially the problem of the analysis is to solve two sets of Goldman-Hodgkin-Katz equations [45] to satisfy the condition that $E_m = E_s$ using the measured values for the ion activities under different conditions. The equations used are presented in Appendices A and B.

During bilateral substitutions the term representing the chloride contribution can be put to zero. This provides a possibility of calculating the relative sodium permeability in the mucosal membrane and for bicarbonate in the basolateral membrane. In order to estimate $\Delta E_{s,pump}$ the permeability ratios weighed by the ratios as described in Appendix B were substituted in the Goldman-Hodgkin-Katz equation for the apolar cell. Comparison of the GHK equations with and without the rheogenic contribution of the Na/K pump (Eq. (4); $r = 3/2$ and $r = 1$) yields another set of equations which permits the unknown parameters to be solved [57]. The resulting relative permeability ratios are presented in Table 6*A* (first and second column), $\Delta E_{s,pump}$ is approximately −9 mV in the control situation and approximately −8 mV in chloride-free media.

From the values of R_m and R_s (Table 5) the absolute potassium permeability of the membranes can be calculated (Table 6*A*) with the equation for the slope conductance (g) derived from the GHK equation (*cf.* [45]):

$$g = F^2 P_K / RT\{[\xi \ln \xi (M - L)]/(1 - \xi)^2 + (M\xi - L)/(1 - \xi)\} \quad (5)$$

where $\xi = \exp(\psi F/RT)$; the meaning of M and L is described in Appendix A.

6. Unilateral Substitutions

With the values of Table 6*A* and reasonable estimates for the intracellular ion activities (presented in parentheses in Table 5) we can predict E_m, E_s and R_m/R_s for the unilateral substitutions. These are given in Table 6*B*. Assuming that $\Delta E_{s,pump}$ is not very different from the values found above the predicted values of the electrical parameters are rather accurate (*cf.* Table 5).

In previous papers [7, 47] the relative permeabilities of the tight junction for goldfish intestine were estimated as: $P_{Cl}/P_{Na}/P_K = 0.25 : 1 : 1.25$ (Table 6*A*, third column). Using these values to calculate E_l after unilateral chloride substitution one finds $\Delta E_l = 4.8$ mV assuming for the tight junction $(P_{gluc}/P_K)_{tj} = 0$. Whereas ψ_{ms} due to serosal substitutions can be fitted within experimental accuracy with this value the steady-state ψ_{ms} due to mucosal chloride substitution (+2.9 mV) cannot. The transient value at 40 sec (+5.9 ± 0.5 mV; *see* Fig. 1) might still be in the range.

On the other hand, R_{ms} does not change during mucosal chloride substitutions, suggesting that the tight junction permeabilities for chloride and gluconate are not very different. As a tentative conclusion one may infer that initially $(P_{gluconate})_{tj}$ is still low ($\psi_{ms} = 5.9$ mV) but that it increases due to the substitution ($\psi_{ms} = 2.9$ mV). As yet there is no good explanation for this biphasic response of ψ_{ms}. A possible explanation might be that, though the osmolarity of the solutions used were alike, the difference in permeability introduced water flows, so that the diffusional junction between chloride and gluconate solutions does not occur exclusively in the tight junction. ψ_{ms} may be the result of liquid junction potentials due to a gradual change in composition of the solution in mucosal unstirred layer and in the interspace from the tight junction to the basement membrane. Especially during serosal substitution the high rate of transcellular chloride transport entering the interspace may enhance this effect.

The increase in R_{ms} during serosal or bilateral substitution is probably mainly due to the increase in resistivity of the interspace fluid which according to the dimensions of the interspace and the higher resistivity of the gluconate salt solution is expected to be 3–4 Ωcm^2.

7. Testing of the Assumptions

In the analysis it was assumed that P_{Na} and P_K of the apical membrane do not change during chloride substitutions. Earlier a $P_{Na}/P_K = 0.072$ was reported [47] with the assumption that the apical membrane is impermeable for chloride. Insertion of the presently found P_{Cl} in the old data shows then that $(P_{Na}/P_K)_m$ agrees with the value presented here. The present results are more likely as a fit, for the old value would require a decrease of $(P_{Na}/P_K)_m$ by a factor of three during bilateral chloride substitution.

According to Eq. (2*b*) small changes in E_l can only occur when considerable changes in E_m and E_s compensate for these changes in E_l, given the experimental fact that $\psi_{ms} = 0$ during control and bilateral substitutions. Consequently, the ion permeabilities determining E_s and E_m must also change considerably. For example, if, due to a hyperosmolarity of 8 mOsm in the interspace, $E_l = -0.55$ mV, the resultant increase in E_m of 4 mV can only be explained with a twofold increase of $(P_{Cl}/P_K)_m$ or a fourfold increase of $(P_{Na}/P_K)_m$. The decrease in E_s of 6 mV can then be explained with a smaller $(P_{Cl}/P_K)_s$. These different permeability values would cause an increase in R_m/R_s ratio after bilateral chloride substitution of 15–20%, whereas a decrease was observed (*cf.* Eq. (5)). So the assumption that E_l is negligible is not unwarranted.

8. Electroneutral Chloride Transport in the Brush Border Membrane

In control solutions a_iCl^- is above electrochemical equilibrium and $[Cl^-]_i$ is below chemical equilibrium. When Cl^--influx from the mucosal side was stopped by mucosal Cl^--omission, a_iCl^- dropped within 3 min to nearly the electrochemical equilibrium value over the basolateral membrane (10 *vs.* 6.5 meq/liter). As $[Cl^-]_i$ reduced further after 3 min, it is most likely that a_iCl^- reduces even below 10 meq/liter. Clearly, under control conditions most Cl^--influx through the mucosal membrane is electroneutral. Electroneutral entry mechanisms only exist when the chloride fluxes are coupled to those of other ions. This coupling is not necessarily completely electroneutral (i.e., may have a ratio differing from 1 : 1). If a direct coupling to Na^+ influx, as first proposed by Nellans et al. [35] (*see also* Refs. 13, 16), exists in goldfish intestine, it cannot be inhibited by furosemide or bumetanide. More likely Cl^- is coupled by countertransport to OH^- or HCO_3^- and via pH_i indirectly to Na^+, since not only chloride substitution causes alkalinization, but also Na^+ substitution causes cell acidification [22, 24]. The large transepithelial Cl fluxes (0.92 ± 0.14 nM/cm^2 sec) [6, 7] cannot occur paracellularly as the transepithelial potentials are small and the paracellular chloride conductance is not sufficient. Therefore an electroneutral transport mechanism is indispensable to explain the findings. Apparently in goldfish intestine this mechanism is located in the brush border membrane. It consists, most probably, of the dual-exchange mechanism ($Na^+/H^+ + Cl^-/HCO_3^-$) suggested by Turnberg et al. [52] for human ileum [5, 33].

One can get an impression of the ease with which Cl^- passes through the mucosal membrane by calculating the chloride conductance needed to explain the mucosal efflux after mucosal chloride substitution. The observed initial rate of decrease of 0.25 meq/liter · sec can only be explained with a value about four times as large as the total cell membrane chloride conductance.

9. The Basolateral Anion Conductances

The basolateral chloride conductance is high and is responsible for nearly all chloride permeability in the apolar cell. As mentioned above it still has a transport capacity which is lower than the electroneutral influx mechanism. This is supported by the observation that during serosal chloride substitutions the $[Cl^-]_i$ dropped less than during mucosal substitutions (*see* Table 5). It is also the reason why

during mucosal chloride substitution the relative cell volume decreases while during serosal substitutions it does not. The electrodiffusional permeability of the brush border membrane for chloride is so low that it is easily overlooked for two reasons. First: If 3 M KCl salt bridges are used as reference electrodes [60] the depolarization of the mucosal membrane is obscured by the shift of −4.1 mV to be expected for the cation-selective membrane in analogy to the shift observed with a potassium-sensitive microelectrode. Second, the reduction of a_iCl^- will lead to hyperpolarization overriding the depolarization. The initial depolarization after mucosal chloride substitution reflects the chloride permeability of both the mucosal membrane and the tight junction and is a weighed superposition of the depolarization of E_m, a hyperpolarization of E_s and a serosa-positive shunt diffusion potential.

The basolateral chloride permeability is approximately 20×10^{-6} cm sec^{-1} representing more than 30% of the total basolateral membrane conductance. This is the major reason why R_m/R_s decreases by serosal chloride substitution.

10. Conclusions for the Active Salt Transport of the Epithelium

In conclusion: the goldfish enterocyte possesses an electroneutral influx mechanism of chloride in the brush border membrane and a large chloride permeability in the basolateral membrane. The effective diffusional impedance of the basolateral membrane is higher than that of the brush border membrane, so that the cellular chloride activity is more influenced by the mucosal chloride activity than by the serosal activity.

If the stoichiometry of the mucosal coupling is 1 : 1 an extremely profitable configuration is present in the enterocyte since the energetics for uphill transport of chloride into the cell are minimized, as by this coupling no energy is necessary to overcome the electrical part (i.e., ψ_{mc}) of the electrochemical gradient. At the basolateral side this electrical part is used in a favorable way as here the chloride efflux is only coupled to other ions through the electrical gradient (principle of electroneutrality).

We thank Dr. B.I.. Roberts for his comments on the paper and correcting the English spelling and grammar and H. van der Meyden for the illustrations. The work was supported by the Netherlands Foundation for Biophysics with financial aid of the Netherlands Organisation for Advancement of Pure Science (ZWO).

References

1. Albus, H., Bakker, R., Siegenbeek van Heukelom, J. 1983. Circuit analysis of membrane potentials changes due to electrogenic sodium-dependent sugar transport in goldfish intestinal epithelium. *Pfluegers Arch.* **398**:1–9
2. Armstrong, W.McD., Bixenman, W.R., Frey, K.F., Garcia-Diaz, J.F., O'Regan, M.G., Owens, J.L. 1979. Energetics of coupled Na^+ and Cl^- entry into epithelial cells of bullfrog small intestine. *Biochim. Biophys. Acta* **551**:207–219
3. Armstrong, W.McD., Garcia-Diaz, J.F. 1980. Ion-selective microelectrodes: Theory and technique. *Fed. Proc.* **39**:2851–2859
4. Baerentsen, H.J., Christensen, O., Thomsen, P.G., Zeuthen, T. 1982. Steady states and the effects of ouabain in the *Necturus* gallbladder epithelium: A model analysis. *J. Membrane Biol.* **68**:215–225
5. Baerentsen, H., Giraldez, F., Zeuthen, T. 1983. Influx mechanisms for Na^+ and Cl^- across the brush border membrane of leaky epithelia: A model and microelectrode study. *J. Membrane Biol.* **75**:205–218
6. Bakker, R., Dekker, K., Zuidema, T., Groot, J.A. 1982. Transepithelial Cl-transport in goldfish *Carassius auratus* intestinal mucosa and the effect of theophylline on fluxes and electrophysiology. 4th Conference of the European Society for Comparative Physiology and Biochemistry, Bielefeld (FRG) September 8–11, 1982
7. Bakker, R., Groot, J.A. 1984. cAMP-mediated effects of ouabain and theophylline on paracellular ion selectivity. *Am. J. Physiol.* **246**:*G*213–*G*217
8. Barry, P.H., Diamond, J.M. 1970. Junction potentials, electrode standard potentials, and other problems in interpreting electrical properties of membranes. *J. Membrane Biol.* **3**:93–122
9. Burckhardt, B.C., Frömter, E. 1981. Bicarbonate and hydroxylion permeability of the peritubular cell membrane of rat renal proximal tubular cells. *Pfluegers Arch.* **389**:*R*40
10. Christoffersen, G.R.J., Skibsted, L.H. 1975. Calcium ion activity in physiological solutions: Influence of anions substituted for chloride. *Comp. Biochem. Physiol.* **52A**:317–322
11. Cremaschi, D., James, P.S., Meyer, G., Rossetti, C., Smith, M.W. 1984. Developmental changes in intra-enterocyte cation activities in hamster terminal ileum. *J. Physiol. (London)* **354**:363–373
12. Dagostino, M., Lee, C.O. 1982. Neutral carrier Na^+- and Ca^{2+}-selective microelectrodes for intracellular application. *Biophys. J.* **40**:199–207
13. Duffey, M.E., Turnheim, K., Frizzell, R. A., Schultz, S.G. 1979. Intracellular chloride activities in rabbit gallbladder: Direct evidence for the role of the sodium-gradient in energizing "Uphill" chloride transport. *J. Membrane Biol.* **42**:229–245
14. Ellory, J.C., Ramos, M., Zeuthen, T. 1979. Cl^--accumulation in the plaice intestinal epithelium. *J. Physiol. (London)* **287**:12*P*
15. Field, M., Karnaky, K.J., Smith, P.L., Bolton, J.E., Kinter, W.B. 1978. Ion transport across the isolated intestinal mucosa of the winter flounder, *Pseudopleuronectes americanus*: I. Functional and structural properties of cellular and paracellular pathways for Na and Cl. *J. Membrane Biol.* **41**:265–293
16. Fisher, R.S. 1984. Chloride movement across basolateral membrane of *Necturus* gallbladder epithelium. *Am. J. Physiol.* **247**:*C*495–*C*500
17. Frizzell, R.A., Field, M., Schultz, S.G. 1979. Sodium-coupled chloride transport by epithelial tissues. *Am. J. Physiol.* **236**:*F*1–*F*8
18. Frömter, E. 1979. Solute transport across epithelia: What can we learn from micropuncture studies on kidney tubules? *J. Physiol. (London)* **288**:1–31
19. Garcia-Diaz, J.F., O'Doherty, J., Armstrong, W.McD. 1978. Potential profile, K^+ and Na^+ activities in *Necturus* small intestine. *Physiologist* **21**:41
20. Giraldez, F. 1984. Active sodium transport and fluid secretion in the gall-bladder epithelium of *Necturus*. *J. Physiol. (London)* **348**:431–455
21. Groot, J.A. 1981. Cell volume regulation in goldfish intestinal mucosa. *Pfluegers Arch.* **392**:57–66
22. Groot, J.A. 1982. Aspects of the Physiology of the Intestinal Mucosa of the Goldfish (*Carassius auratus* L). MultiCopy, Amsterdam
23. Groot, J.A., Albus, H., Siegenbeek van Heukelom, J. 1979. A mechanistic explanation of the effect of potassium on goldfish intestinal transport. *Pfluegers Arch.* **379**:1–9
24. Groot, J.A., Dekker, K., Van Riel, J.W., Zuidema, T. 1982. Intracellular ion concentrations and pH of stripped mucosa of goldfish (*Carassius auratus*) intestine in relation to Cl^- transport. 4th conference of the European Society for Comparative Physiology and Biochemistry, Bielefeld (FRG), September 8–11, 1982
25. Guggino, W.B., Boulpaep, E.L., Giebisch, G. 1982. Electrical properties of chloride transport across the *Necturus* proximal tubule. *J. Membrane Biol.* **65**:185–196
26. Halm, D., Krasny, E., Frizzell, R.A. 1982. Apical membrane potassium conductance in flounder intestine: Relation to chloride absorption. *Bull. Mount Desert Island Biol. Lab.* **21**:88–93
27. Henin, S., Smith, M.W. 1976. Electrical properties of pig colonic mucosa measured during early post-natal development. *J. Physiol. (London)* **262**:169–187
28. Hudson, R.L., Schultz, S.G. 1984. Sodium-coupled sugar transport: Effects on intracellular sodium activities and sodium-pump activity. *Science* **224**:1237–1239
29. Jacquez, J.A., Schultz, S.G. 1974. A general relation between membrane potential, ion activities and pump fluxes for symmetric cells in a steady state. *Math. Biosci.* **20**:19–26
30. Katz, U., Lau, K.R., Ramos, M.M.P., Ellory, J.C. 1982. Thiocyanate transport across fish intestine (*Pleuronectes platessa*). *J. Membrane Biol.* **66**:9–14
31. Laprade, R., Cardinal, J. 1983. Liquid junctions and isolated proximal tubule transepithelial potentials. *Am. J. Physiol.* **244**:*F*304–*F*319
32. Lee, C.O., Armstrong, W.McD. 1972. Activities of sodium and potassium ions in epithelial cells of small intestine. *Science* **175**:1261–1264
33. Liedtke, C.M., Hopfer, U. 1982. Mechanism of Cl^- translocation across small intestinal brush-border membrane: II. Demonstration of Cl^--OH^- exchange and Cl^- conductance. *Am. J. Physiol.* **242**:*G*272–*G*280
34. Meier, P.C., Lanter, F., Ammann, D., Steiner, R.A., Simon, W. 1982. Applicability of available ion-selective liquid membrane microelectrodes to intracellular ion activity measurements. *Pfluegers Arch.* **393**:23–30
35. Nellans, H.N., Frizzell, R.A., Schultz, S.G. 1973. Coupled sodium-chloride influx across the brushborder of rabbit ileum. *Am. J. Physiol.* **225**:467–475
36. Okada, Y., Irimajuri, A., Inouye, A. 1976. Intracellular ion concentrations of epithelial cells in rat intestine. Effects of external K and uphill transports of glucose and glycine. *Jpn. J. Physiol.* **26**:427–440
37. Okada, Y., Sato, T., Inouye, A. 1975. Effects of potassium ions and sodium ions on membrane potential of epithelial cells in rat duodenum. *Biochim. Biophys. Acta* **413**:104–115
38. Os, C.H. van, Wiedner, G., Wright, E.M. 1979. Volume flows across gallbladder epithelium induced by small hydrostatic and osmotic gradients. *J. Membrane Biol.* **49**:1–20
39. Reuss, L. 1979. Electrical properties of cellular transepithelial pathway in *Necturus* gallbladder: III. Ionic permeability of the basolateral cell membrane. *J. Membrane Biol.* **47**:239–259
40. Reuss, L. 1983. Basolateral co-transport in NaCl-absorbing epithelium. *Nature (London)* **305**:723–726
41. Reuss, L., Cheung, L.Y., Grady, T.P. 1982. Mechanisms of cation permeation across apical cell membrane of *Necturus* gallbladder: Effects of luminal pH and divalent cations on K^+ and Na^+ permeability. *J. Membrane Biol.* **59**:211–224
42. Reuss, L., Weinman, S.A. 1979. Intracellular ionic activities and transmembrane electrochemical potential differences in gallbladder epithelium. *J. Membrane Biol.* **49**:345–362
43. Rose, R.C., Schultz, S.G. 1971. Studies on the electrical potential profile across rabbit ileum: Effects of sugars and amino acids on transmural and transmucosal electrical potential differences. *J. Gen. Physiol.* **57**:639–663
44. Sackin, H., Boulpaep, E.L. 1981. Isolated perfused salamander proximal tubule: II. Monovalent ion replacement and rheogenic transport. *Am. J. Physiol.* **241**:*F*540–*F*555
45. Schultz, S.G. 1980. Basic principles of membrane transport. *In*: IUPAB Biophysics Series 1, Cambridge University Press, Cambridge-London-New York-New Rochelle-Melbourne-Sydney
46. Shindo, T., Spring, K.R. 1981. Chloride movement across the basolateral membrane of proximal tubule cells. *J. Membrane Biol.* **58**:35–42
47. Siegenbeek van Heukelom, J. 1978. The electrical characteristics of the absorptive goldfish intestinal epithelium. *Gastroent. Clin. Biol.* **2**:329
48. Siegenbeek van Heukelom, J., Van den Ham, M.D., Albus, H., Groot, J.A. 1981. Microscopical determination of the filtration permeability of the mucosal surface of the goldfish intestinal epithelium. *J. Membrane Biol.* **63**:31–39
49. Smith, P.L., Welsh, M.J., Stewart, C.P., Frizzell, R.A., Orellana, S.A., Field, M. 1981. Chloride absorption by the intestine of the winter flounder *Pseudopleuronectes americanus*: Mechanism of inhibition by reduced pH. *Bull. Mount Desert Island Biol. Lab.* **20**:96–101
50. Spring, K.R., Giebisch, G. 1977. Tracer Na fluxes in *Necturus* proximal tubule. *Am. J. Physiol.* **232**:*F*461–*F*470
51. Spring, K.R., Kimura, G. 1978. Chloride reabsorption by renal proximal tubules of *Necturus*. *J. Membrane Biol.* **38**:233–254
52. Turnberg, L.A., Bieberdorf, F.A., Morowski, S.G., Fordtran, J.S. 1970. Interrelationship of chloride, bicarbonate, sodium and hydrogen transport in human ileum. *J. Clin. Invest.* **49**:557–567
53. Waddell, W.J., Butler, T.C. 1959. Calculation of the intracellular pH from the distribution of 5,5-dimethyl-2,4-oxazolidinedione (DMO). Application to skeletal muscle of the dog. *J. Clin. Invest.* **38**:720–729
54. White, J.F. 1976. Intracellular potassium activities in *Amphiuma* small intestine. *Am. J. Physiol.* **231**:1214–1219
55. White, J.F. 1977. Activity of chloride in absorptive cells of *Amphiuma* small intestine. *Am. J. Physiol.* **232**:*E*553–*E*559
56. White, J.F. 1980. Bicarbonate-dependent chloride absorption in small intestine: Ion fluxes and intracellular chloride activities. *J. Membrane Biol.* **53**:95–107
57. Zeuthen, T. 1981. On the effects of amphotericin B and ouabain on the electrical potentials of *Necturus* gallbladder. *J. Membrane Biol.* **60**:167–169
58. Zeuthen, T., Monge, C. 1976. Electrical potentials and ion activities in the epithelial cell layer of the rabbit ileum in vivo. *In*: Ion and Enzyme Electrodes in Biology and Medicine. M. Kessler et al., editors. p. 345. Urban and Schwarzenberg, Munich
59. Zeuthen, T., Ramos, M., Ellory, J.C. 1978. Inhibition of

active chloride transport by piretanide. *Nature (London)* **273**:678–680

60. Zuidema, T., Dekker, K., Siegenbeek van Heukelom, J. 1985. The influence of organic counterions on junction potentials and measured membrane potentials. *Bioelectrochem. Bioenerg. (in press)*

Received 30 May 1985; revised 20 August 1985

Appendix A

E_m and E_s are both of the type $(RT/F) \cdot \ln(M/L)$ (according to the Goldman-Hodgkin-Katz equation). With the simplifying assumptions from the Discussion one can write:

$$M_m = a_o K^+ + (P_{Na}/P_K)_m \cdot a_o Na^+ + (P_{Cl}/P_K)_m \cdot a_i Cl^- \quad (A1)$$

$$L_m = a_i K^+ + (P_{Na}/P_K)_m \cdot a_i Na^+ + (P_{Cl}/P_K)_m \cdot a_o Cl^- \quad (A2)$$

$$\psi_{mc} = E_m = RT/F \cdot \ln(M_m/L_m) \quad (A3)$$

$$M_s = a_o K^+ + (P_{Cl}/P_K)_s \cdot a_i Cl^- + (P_{HCO_3}/P_K)_s \cdot a_i HCO_3^- \quad (A4)$$

$$L_s = a_i K^+ + (P_{Cl}/P_K)_s \cdot a_o Cl^- + (P_{HCO_3}/P_K)_s \cdot a_o HCO_3^- \quad (A5)$$

$$E_s - \Delta E_{s,pump} = RT/F \cdot \ln(M_s/L_s) \quad (A6)$$

$\Delta E_{s,pump}$ is the rheogenic contribution of the basolaterally located Na/K pump to E_s.

Appendix B

The membrane potential of the unpolarized or apolar cell, E_a, is, like E_m and E_s, of the type $(RT/F) \cdot \ln(M/L)$ and according to Eq. (3) E_a can also been written as:

$$E_a = p \cdot E_s + (1 - p) \cdot E_m \quad (B1)$$

where $p = R_m/R_T$.

Taking only the "M"-terms one obtains:

$$\ln M_a = p \ln M_s + (1 - p) \ln M_m. \quad (B2)$$

Taking $A = a_o K^+$, $B = (P_{Cl}/P_K)_s \cdot a_i Cl^- + (P_{HCO_3}/P_K)_s \cdot a_i HCO_3^-$ and $C = (P_{Na}/P_K)_m \cdot a_o Na^+ + (P_{Cl}/P_K)_m \cdot a_i Cl^-$ (*cf.* Eqs. (A1) and (A4)), one can rewrite this equation as

$$\ln M_a = \ln(A + C)\{(1 + (B - C)/(A + C)\}^p \quad (B3)$$

and series expansion of the last right-hand term gives

$$\ln M_a = \ln(A + C)\{(1 + p(B - C)/(A + C) + p(p - 1)[(B - C)/(A + C)]^2/2 + \ldots\}$$

which reduces in first approximation to

$$\ln M_a = \ln A(1 + pB/A + (1 - p)C/A). \quad (B4)$$

A similar equation for the "L" terms can be derived. This shows that in the overall equation $E_a = (RT/F)\ln M_a/L_a$ the contributions of the mucosal and serosal permeabilities in both the nominator (M_a) and denominator (L_a) should be weighed with the same ratios that also determine the contributions of E_m and E_s in E_a.

Influence of glucose absorption on ion activities in cells and submucosal space in goldfish intestine

T. Zuidema, M. Kamermans, and J. Siegenbeek van Heukelom

Department of Zoology, Membrane Biophysics, University of Amsterdam, Kruislaan 320, NL-1098 SM Amsterdam, The Netherlands

Abstract. Mucosal glucose addition evokes in goldfish intestinal epithelium a fast depolarization of the mucosal membrane potential ($\Delta\Psi_{mc} = 12$ mV) followed by a slower repolarization ($\Delta\Psi_{mc} = -7$ mV). The intracellular sodium activity, a_iNa^+, rises from 13.2 ± 2.4 meq/l by 6.7 ± 0.5 meq/l within 5 min, a_iCl^- rises about 3 meq/l above the control value of 37.7 ± 2.2 meq/l, while a_iK is constant (97.7 ± 7.4 meq/l). The potassium activity measured in the submucosal interstitium near the basal side of the cells (a_sK^+) is 5.2 ± 0.2 meq/l in non-absorbing tissue compared to 4.2 meq/l in the bathing solution and shows a transient increase due to glucose absorption (1.1 ± 0.1 meq/l).

In chloride-free media $a_sK^+ = 4.2 \pm 0.1$ meq/l and Ψ_{mc} hyperpolarizes by -13 mV. The depolarization due to glucose absorption increases ($\Delta\Psi_{mc} = 14.1 \pm 1.4$) and the repolarization ($\Delta\Psi_{mc}^{repol}$) disappears. In addition, a_iNa^+ rises from 16.3 ± 2.4 meq/l by 9.9 ± 1.5 meq/l within 5 min, a_iK^+ remains constant and equal to the value in chloride containing solutions (88.5 ± 2.8 meq/l); a_sK^+ increases transiently (1.1 ± 0.1 meq/l).

Serosal Ba^{2+} (5 mM) depolarizes Ψ_{mc} ($+14.2 \pm 1.0$ mV) and abolishes the repolarization. Increased serosal or mucosal potassium activity depolarizes Ψ_{mc} and abolishes the repolarization.

These effects are discussed in terms of changes of ion activities, the basolateral potassium conductance, the influence of intracellular Ca^{2+}, the functional state of the Na/K-pump, and modulation of membrane permeabilities by extracellular potassium.

Key words: Intracellular ion activity – Interspace – Na^+ – K^+ – Cl^- – Ba^{2+} – Glucose absorption – Intestine – Goldfish

Introduction

Several electrophysiological analyses of the glucose or amino acid-induced intracellular and transepithelial potential changes in intestine and in proximal convoluted tubule have recently been published [1, 3, 10, 14, 17, 20, 21, 27, 29, 30, 32, 33, 46]. Whereas Fromter and co-workers [14, 32, 33] restricted themselves to the changes in rat proximal tubule during the first 100 s, the other reports [1, 3, 10, 17, 20, 21, 27, 29, 30, 46] studied in more detail the changes that occurred over longer periods. The geometry of the proximal tubule allows a reduction of the unstirred layers so, that a time resolution of approximately 0.2 s could be achieved [14]. In intestinal epithelia [1, 3, 17, 20, 21, 46] having a more folded structure such a time resolution is not possible.

First the membrane potential (Ψ_{mc}) depolarizes ($\Delta\Psi_{mc}^{depol}$) and later it repolarizes ($\Delta\Psi_{mc}^{repol}$) but to a lesser extent. In the goldfish the repolarization can be fully and quickly inhibited by the cardiac-glycoside ouabain (0.1 mM; [1]). All research groups conclude that the mucosal application of monosaccharides or amino acids introduces an additional conductive pathway in the brush border membrane. Some groups have concluded that the repolarization is caused by an increase of the basolateral potassium conductance t_K^{bl} [17, 20, 21, 27, 28, 30, 35, 46]. This increase of t_K^{bl} might be caused by cell swelling [28], or intracellular Ca^{2+}-changes [9]. Other groups attribute the repolarization to the enhanced action of the Na/K-pump [1, 3, 10]. A correlation between basolateral potassium conductance and the action of the Na/K-pump has been shown in several epithelia [13, 35]. Albus et al. [1, 3] suggested that the repolarization is associated with the action of the Na/K-pump and that this dependency must be twofold: firstly by the electrogenic nature of the pump itself and secondly by changes in potassium activity in the interspace. The average activity of potassium in the interspace, $a_{is}K^+$, was calculated to rise initially to about 9 mM and then to drop to about 5 mM [36]. The present paper presents data on ion activity changes induced by glucose absorption, in order to obtain further insight into these processes in goldfish stripped intestinal epithelium. Parts of this work have been presented as abstracts [39, 40, 50, 51].

Methods

Preparation and experimental set-up. The preparation of the tissue and the experimental set-up have been described before [1–3, 38]. Serosal and mucosal perfusion and electrode arrangements were made such that unstirred layers were minimized. Serosal and mucosal voltage electrodes were salt bridges filled with standard Krebs-Henseleit solution and connected to an Ag-AgCl half-cell. The epithelium is folded in a herringbone structure with protruding folds of approximately 500 µm height and 200 µm diameter; given the dimensions of the enterocytes (height 70 µm, diameter 5 µm) it is clear that about 60 µm width of underlying tissue

is still present in the folds (see Fig. 1). The extracellular space is 16% of the tissue volume while the interspace is estimated as 4–8%, taking its width as 0.2 μm [18].

Bathing solutions. The control bathing solution used in this study is a standard bicarbonate Krebs-Henseleit solution [2] with osmolarity 315 ± 2 mOsm and pH 7.3 at 20° C. When applied mucosally, glucose was isoosmotically (27.8 mM) substituted for mannitol.

Sodium salts of glucuronate (Sigma Chemicals, St. Louis, MO, USA) and gluconate (Merck Burckhardt, Darmstadt, FRG) were used as substitutes for chloride for the chloride-free solutions: in these solutions KCl and $CaCl_2$ were substituted by K_2SO_4 and $CaSO_4$ respectively, and balanced osmotically by mannitol.

In barium containing salt solutions 10 mM NaCl was substituted by 5 mM $BaCl_2$ and the $MgSO_4$ substituted by $MgCl_2$. The reduction in osmolarity of the solutions caused by these substitutions was compensated for by the addition of mannitol.

Microelectrodes. Glass-filamented microelectrodes were made with an electrode puller of our own design [37]. Filled with 3 M KCl they have a tip resistance between 20 and 30 MΩ measured in a standard Krebs-Henseleit solution.

Single-barrelled liquid ion-exchanger microelectrodes were prepared using the following technique:

1. Micropipettes, pulled as above were dipped into either a 0.2% solution of Aquasil (Pierce Chemical Comp., Rockford, IL, USA) in water or in a 3% solution of trimethylchlorosilane (TMCS, Pierce Chemical Comp., Rockford, IL, USA) in carbon-tetrachloride. The Aquasil treated microelectrodes were cured in an oven for several hours at 100° C.

2. The silanized tip was immersed into a liquid ion-exchanger until a column of 150–200 μm was sucked up by capillary action.

3. Then the barrel was back-filled with an aqueous solution of either 200 mM KCl (KLIX) or 200 mM NaCl (NaLIX) and all air bubbles were removed by local heating.

4. Before calibration, the completed electrode was allowed to stabilize for at least 1 h with the tip immersed in a solution identical to the filling solution. The electrodes were calibrated in pure and mixed solutions of KCl and NaCl before and after the experiments.

The reference electrode was a 3 M KCl agar bridge connected to an Ag-AgCl half-cell. The responses of this circuit to decadic changes in activity of the selected ion and the responses to complete substitutions of the selected ion by the major interfering ions (Separate Solution Method, [5]) were measured at 18° C. Slope constants (S) and selectivity coefficients ($K_{i,j}$) were assessed with the Nicolsky-Eisenman equation [31]. All relevant data for the ion-exchangers used in this study are shown in Table 1.

During the experiments the selectivity of the liquid ion-exchanger microelectrodes tended to decrease slightly, possibly because organic material adhered to the electrode tip. As the slope constant was not affected, proper corrections could be made.

Criteria for correct impalements with normal microelectrodes were mentioned elsewhere [1]. Because the potentials recorded by ion-sensitive microelectrodes are sometimes small the following criteria for correct impalements were adopted:

1. an abrupt change in potential upon advancing the electrode which leads to a stable potential (within 2 mV) for at least 1 min;

2. a voltage divider ratio for transepithelial current pulses similar to that measured with normal microelectrodes at the same place in the same tissue.

Since the enterocytes do not tolerate impalement by electrodes with tip diameters larger than 0.2–0.3 μm we did not try to measure intracellular ion activities with double-barreled microelectrodes, but always used separate ion-sensitive and open-tip microelectrodes. In our opinion, this approach is justified by the fact that the membrane potentials measured in different cells of the same tissue show little variation and seem to represent a homogeneous population [1, 3]. Systematic errors in the determination of intracellular activities from membrane potentials and ion potentials introduced by unstirred layers were minimized by measuring both signals simultaneously in nearby cells.

Impalements were carried out with a Burleigh Inchworm (Burleigh Instr. Inc., Fishers, NJ, USA) mounted on a Leitz micromanipulator.

Electrical potentials and ion activities. The apparent ion activity of the selected ion is calculated from the signals recorded by the ion-sensitive and the voltage electrodes. Interference by other ions was corrected for using the selectivity coefficients of the particular electrode and the average intracellular activity of the co-ions [5].

The contributions of interfering ions are below the level of detection in case of a_iK^+. In the bathing solutions, and most probably also in the interstitium, the average contribution of sodium is approximately 1.8 meq/l, and of Ca^{2+} and Mg^{2+} is 0.3 meq/l.

Corrections for interference in the measurements of the sodium-selective microelectrodes by intracellular potassium, using the average value found with potassium-selective microelectrodes (95 meq/l) were properly executed.

Whereas the standard error in the mean of ($\Delta E_i - \Delta\psi_{mc}$) was usually about 2 mV it introduces a proportional error of approximately 8% in the observed ion activities. Therefore ion fluxes from a large compartment with a high concentration into a smaller compartment with a low concentration may induce substantial activity changes in the small compartment, while the changes in the larger one are below the level of detection. For example a change of 4 meq/l K^+ in the cell (80% of the tissue volume) would correspond, when extruded only into the interspace, with a change in the opposite direction of 20–40 meq/l in that space (4–8% of the tissue volume). In this study, therefore, firm conclusions can be drawn only for activity measurements made in those compartments where the steady state activities of the particular ions are low: a_iNa^+ and a_sK^+.

The interspace, which is only 0.2 μm wide in our preparation, is not accessible to microelectrodes. Instead we measured therefore the potassium activity in the top of the intestinal folds just basal to the cells (a_sK^+; see Fig. 1).

The values of a_sK^+ were determined with respect to the macroscopic scrosal electrode. When a normal microelectrode was pierced through the epithelial layer into the top of the fold in the same way as the potassium sensitive electrode (see Fig. 1), it recorded the same electrical potential changes as the serosal voltage electrode (maximal difference 0.4 mV; average maximal difference 0.11 ± 0.06 mV; n = 16). The voltage deflections induced by transepithelial current pulses (I_{ms} = ± 10^{-4} A; cf. [1]) were identical for a normal microelectrode and a potassium-selective microelectrode (time constant less than 0.1 s) in the same position. These results support the validity of the determination of a_sK^+. Interference introduced during Cl^--gluconate substitutions on the potassium signal has been evaluated and analyzed elsewhere [49]; corrections were made accordingly.

Electronics. Amplifiers of our own design (inputstage Analog Devices 311 J, cf. [45], pp. 76, 77) or a Keithley 610 B electrometer were used for calibration measurement; both had input impedances greater than 10^{14} Ω. The ion-sensitive microelectrode had an active guard and all experiments were carried out in an earthed Faraday cage. The outputs were recorded on a multipen recorder (Rikadenki R-10-14).

Determination of cell water and ion content during Ba^{2+}-exposure. The methods used for determining cell water and ion content were standard and are described earlier [18, 19].

Statistics. The presented steady state values are the means of the measured values; transient responses were measured at distinct time intervals with respect to the preceding steady state values and averaged. All values are given ± SEM. The number of determinations is six or more, unless otherwise stated.

Table 1. Data on liquid ion-exchanger microelectrodes used in this study. Slope constants (S) and selectivities (K_{ij}) were measured at 18° C by the Separate Solution Method [5]. $(aI)_{app}$ represents the apparent activity of ion I in normal salt solution (i.e. including the interference by other ions). In parentheses are given the number of determinations. Data on Chloride sensitive electrodes are presented elsewhere [52]

Liquid membrane	Selected ion	S (mV/ decade)	K_{ij}	$(aI)_{app}$ (meq/l)
ETH 227	Na^+	58.1 ± 0.6	K^+: 0.031 ± 0.003 (24) Ca^{2+}: 2.1 ± 0.1 (20)	145.4 ± 1.1 (25)
WPI-IE 190	K^+	56.9 ± 0.2	Na^+: 0.020 ± 0.002 (27) Ca^{2+}: 0.015 ± 0.004 (3) Mg^{2+}: 0.009 ± 0.004 (4)	6.70 ± 0.14 (29)

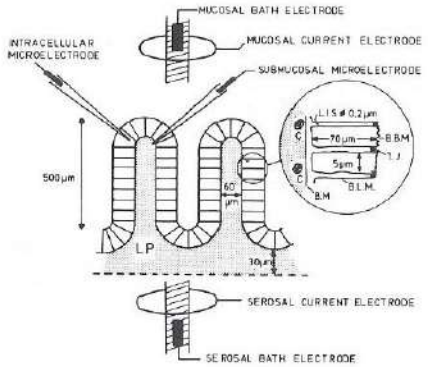

Fig. 1. Schematic representation of the electrode configuration and the microelectrode positioning in the intestinal preparation. Microelectrodes are either conventional 3 M KCl filled or liquid membrane microelectrodes. Bath potential electrodes are connected via salt bridges and the current injecting electrodes are chlorided silver wires. *L.P.* = lamina propria, *L.I.S.* = lateral intercellular space ("interspace" in the text), *B.B.M.* = brush border membrane, *B.M.* = basement membrane, *T.J.* = tight junction, *C.* = capillary

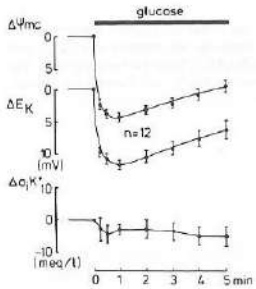

Fig. 2. Average transients at the onset of glucose absorption recorded simultaneously with open-tip microelectrodes (ψ_{mc}) and potassium sensitive microelectrode (ΔE_K) from two nearby cells. The lower trace representing the average Δa_iK^+ calculated from individual recordings as described in materials and methods. The average steady state values before glucose addition were: ψ_{mc} = −56.2 ± 2.6 mV, ΔE_K = 11.0 ± 2.4 mV, a_iK^+ = 97.7 ± 7.4 meq/l. All averages are given ± SEM; n represents the number of recordings

Results

Transient intracellular ion activities in control and chloride-free solutions

The influence of glucose addition to the mucosal control solutions on a_iK^+ is shown in Fig. 2. a_iK^+ decreased by 5 ± 3 meq/l (n = 12). This decrease is not significant ($P > 0.1$) nor is it significantly different from 6.7 meq/l, the amount of cation loss needed to compensate for the increase in a_iNa^+ (see Fig. 4).

Recordings of intracellular chloride activity show a small increase probably because of the depolarization of the membrane potential (see Fig. 3).

In Fig. 4 the averages of simultaneous recordings of $\Delta\psi_{mc}$ and ΔE_{Na} in response to mucosal glucose addition in control (n = 12; dotted line) and chloride-free solutions (n = 18; drawn line) are shown. The changes in intracellular sodium activity (Δa_iNa^+) calculated from these recordings are presented in the third panel. a_iNa^+ increased by

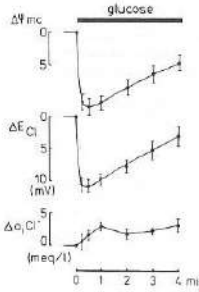

Fig. 3. Average transients at the onset of glucose absorption recorded simultaneously with open-tip microelectrodes (ψ_{mc}) and chloride sensitive microelectrode (ΔE_{Cl}) from two nearby cells. The lower trace representing the average $\Delta a_i Cl^-$ calculated from individual recordings as described in materials and methods. The average steady state values before glucose addition were: $\psi_{mc} = -51.4 \pm 2.4$ mV, $\Delta E_{Cl} = 33.2 \pm 1.7$ mV, $a_i Cl^- = 37.7 \pm 2.2$ meq/l. All averages are given $\pm$ SEM; $n = 5$

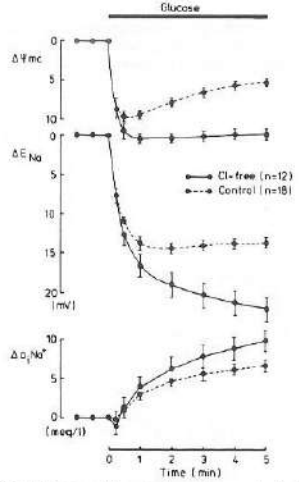

Fig. 4. Averaged transients at the onset of glucose absorption recorded simultaneously with open-tip (ψ_{mc}) and sodium-sensitive microelectrodes (ΔE_{Na}) measured in control solutions (*dotted lines*) and chloride-free solutions (*solid lines*). The average steady state values before glucose addition were in control solutions $\psi_{mc} = -51.6 \pm 1.3$ mV, $\Delta E_{Na} = -108.7 \pm 2.8$ mV, $a_i Na^+ = 13.2 \pm 2.4$ meq/l. In chloride free solutions these values were $\psi_{mc} = -60.8 \pm 1.4$ mV, $\Delta E_{Na} = -102.9 \pm 3.1$ mV, $a_i Na^+ = 16.3 \pm 2.4$ meq/l

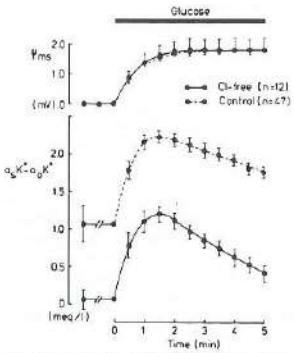

Fig. 5. Averaged transient recording at the onset of glucose absorption of the transepithelial potential (*upper graph*), and the submucosal potassium activity with respect to the bath-aK^+ ($a_sK^+ - a_oK^+$; *lower graph*), in control solutions (*dotted lines*) and in chloride-free solutions (*solid lines*)

6.7 $\pm$ 0.5 meq/l in control solutions whereas in chloride-free solutions after 5 min it had increased by 9.9 $\pm$ 1.5 meq/l and was still increasing.

In these figures the response of ψ_{mc} to glucose addition is characteristic of goldfish enterocytes. The steady state values of a_iNa^+ and a_iK^+ in control solutions are 13.2 $\pm$ 2.4 meq/l and 97.7 $\pm$ 7.4 meq/l, respectively. Both values are in the range reported for different intestinal preparations [4, 6, 21, 34, 48] and other leaky epithelia (e.g. [16]). Chloride-substitution increased a_iNa^+ by 4 meq/l and did not affect a_iK^+ significantly. As in normal solutions, a_iK^+ in chloride free solutions did not change significantly in response to mucosal glucose addition.

Submucosal potassium activities in control and chloride-free media

Figure 5 shows the changes in ψ_{ms} and the submucosal potassium activity change (a_iK^+ with respect to a_oK^+) in response to glucose under control (dotted line) and chloride-free conditions (solid line). The steady state a_sK^+ in control solutions was 5.2 $\pm$ 0.2 meq/l ($n = 14$) which is significantly above the bath activitiy a_oK^+ (4.2 meq/l). In the chloride-free experiments a_sK^+ is not significantly different from the a_oK^+ and the transient elevation of a_sK^+ is of shorter duration.

The elevated a_sK^+ in control solutions is not caused by cell damage since the increment persists and does not occur during chloride substitutions. Moreover, the average ψ_{mc} measured simultaneously in cells near the tip of the ion-selective microelectrode was -58.8 ± 1.2 mV ($n = 24$), what is not lower than generally measured in the enterocytes under control conditions (-53 mV). In addition, when measured in the control solutions, a_sCl^- and a_sNa^+ remained steady in the same time interval. Though these last determinations are less critical they, also, exclude the possibility that other factors might be the origin of the observed changes in a_sK^+.

The effect of serosal Ba^{2+} addition on the K^+-permeability of the basolateral membrane

Mucosal Ba^{2+} addition had no effect on the membrane potential or the repolarization. Serosal addition of Ba^{2+} depolarizes ψ_{mc} by 14.2 $\pm$ 1.0 mV [39] while responses to subsequent potassium elevations at either the mucosal or the serosal side are significantly reduced. This is interpreted as a reduction in potassium permeability of the basolateral membranes [9, 39].

Table 2. Data of tissue water (kg/kg dry weight), Na^+, K^+ and Cl^- content (mmoles/kg tissue H_2O) and $[Na^+]_i$, $[K^+]_i$ and $[Cl^-]_i$ (mmoles/l) in strips freely floating in glucose-free media. The average dry weight was approximately 3 mg for all determinations; the number of determinations is 6. The significance: P (determined by Student's t-test) is indicated as n.s.: > 0.05: not significant; *: < 0.05; **: < 0.01 and ***: < 0.001. The analysis of K^+-concentration is given in the text

	Control	Ba^{2+}	P
Tissue-water	3.04 $\pm$ 0.04	3.32 $\pm$ 0.03	***
Na^+-content	117 $\pm$ 6	169 $\pm$ 9	**
Na^+-conc.	38 $\pm$ 1	50 $\pm$ 2	***
K^+-content	480 $\pm$ 9	483 $\pm$ 10	n.s.
K^+-conc.	157 $\pm$ 4	145 $\pm$ 4	
Cl^--content	186 $\pm$ 7	227 $\pm$ 8	**
Cl^--conc.	61 $\pm$ 3	68 $\pm$ 2	n.s.

The chemically determined cell water, Na^+-, K^+- and Cl^--content of the enterocytes in glucose-free Ba^{2+}-containing medium as compared to control glucose-free salt solutions are given in Table 2. The content of Na^+ and Cl^- and the cell water increased due to Ba^{2+} treatment; $[K^+]_i$ decreased by about 8% ($0.1 > P > 0.05$); $[Na^+]_i$ increased.

Suppression of the repolarization by experimental procedures

A typical recording of an experiment with an increased serosal potassium activity suppressing $\Delta\psi_{mc}^{repol}$ is shown in Fig. 6A. Mucosal and serosal potassium elevations are equally effective. Therefore we conclude that elevation of both serosal and mucosal potassium activity can increase $a_{is}K^+$ to a value somewhere between the mucosal and serosal value.

In the presence of serosal Ba^{2+} $\Delta\psi_{mc}^{depol}$ was slightly reduced but $\Delta\psi_{mc}^{repol}$ was virtually absent (Fig. 6B). Control glucose-evoked responses were measured before and after exposure to barium to be sure that tissue deterioration was not the origin of the suppression.

Bilateral Cl-substitutions induce a hyperpolarization of ψ_{mc} (-13 mV) but the repolarization is suppressed (Fig. 6C).

All recordings shown in Fig. 6 are representative for the influence of elevated K^+ ($n = 6$), serosal Ba^{2+} addition ($n = 9$) and chloride substitution ($n = 30$).

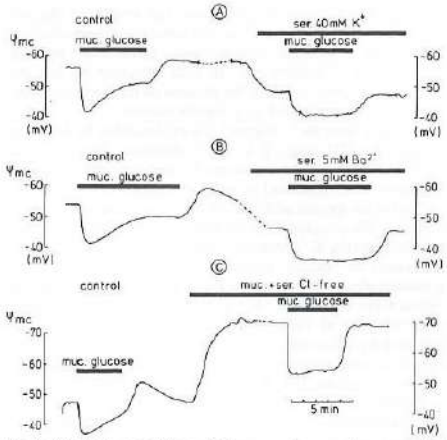

Fig. 6. Typical recordings of transmembrane glucose evoked potentials (ψ_{mc}) from one cell under control conditions (*left* side of the figure) and when the basolateral potassium efflux is affected by (*right* side of the figure): **A** Elevation of serosal potassium concentration (40 mM KCl substituted for NaCl, which may be equivalent with a change of about 20 meq/l in a_iK^+; see text). **B** Serosal addition of 5 mM $BaCl_2$ (substituted for NaCl). **C** Bilateral substitution of all chloride by gluconate. Note that in this trace the right hand ψ_{mc}-scale is shifted by -4.1 mV in order to account for offset potentials at the surface of the 3 M KCl reference salt bridge

Discussion

Most explanations for the repolarization ($\Delta\psi_{mc}^{repol}$) seen to occur on addition of monosaccharides or amino acids to the mucosal solution found in the literature are based on an increase in basolateral potassium conductance (t_K^{bl}; cf. [9, 17, 20, 27, 29, 30]) as the main reason. This increase may be due to cell swelling [21, 28], to an increase in the conductance of Ca^{2+}-activated K-channels [9], or related to an increased activity of the Na/K-pump [7, 10]. Stimulation of the Na/K-pump can be brought about by increase of a_iNa^+ [15, 25, 41, 42].

The data presented here show an increased a_iNa^+ and a transiently elevated a_sK^+. We have not measured t_K^{bl} [29], but an increase in t_K^{bl} can explain many of our observations. If this increase occurred during the depolarization phase or the early repolarization phase it would explain, together with the depolarized state of the cell, the transient increase of a_sK^+. The efflux of potassium that leads to this increase in a_sK^+ of 1 meq/l, is certainly beyond detection with a K^+-sensitive microelectrode in the cell [17].

The permanent elevated a_sK^+ in normal salt solutions is amazing, as one would expect that the potassium activity at the basolateral side of the enterocytes would be lowered because of the absorption from this space alone of K^+ by the Na/K-pump. Sustained elevated potassium activities, however, have also been reported in other tissues [11, 24]. Even routine clinical laboratory determinations of this value indicate that in serum an aK^+ is found that is elevated with respect to the blood plasm [22]. Therefore we conclude that it is not unusual to find such values, though the exact mechanism explaining it is not clear. The steady state a_sK^+ in Cl^--free solutions is not elevated, even after careful corrections in this value for the interference by gluconate ions [49].

The amount of glucose-induced a_iNa^+-elevation is similar to that obtained during similar experiments in frog kidney tubule [29], Necturus proximal tubule [26] and Necturus intestine [21] (though in these experiments the steady state increment was not significant). A small increase of a_iCl^- was also observed. Two mechanisms could induce these changes as there is a considerable Cl^--permeability in the basolateral membranes and a coupled Na^+/H^+ and Cl^-/HCO_3^- exchange system in the brush border membrane [52]. The small changes in a_iCl^-, and also in a_iK^+, have not been further investigated.

If the modulation of t_K^{bl} is also the origin of the repolarization in our preparation, the absence of a repolarization during increased extracellular potassium activity (Fig. 6a) can be understood. In that situation t_K^{bl} has increased sufficiently to make the process of transient increase too small to be measured as a repolarization.

Our data with Ba^{2+} support the explanation by Hudson and Schultz [21] that t_K^{bl} is Ba^{2+}-sensitive. We reported earlier [39] that depolarizations evoked by elevations of potassium in the mucosal or serosal medium could equally be affected by serosal addition of Ba^{2+} (but not by mucosal addition). We concluded from those observations that the site of action (the K^+-conductive pathway in the basolateral membrane) is equally sensitive to mucosal and serosal potassium elevations, because the l.i.s is equally accessible to potassium ions from the mucosal and serosal medium. From the data of Table 2 one can conclude that Ba^{2+} in itself already influences cell volume regulation. Some of our data are comparable with those from Brown and Sepúlveda [9], but the technical differences are too large to make a good comparison possible.

The influence of Ba^{2+} on $[Na^+]_i$ is larger than on $[K^+]_i$. This observation is not easily understood, if Ba^{2+} acts only through t_K^{bl}. Possibly coupling of t_K^{bl} with the Na/K-pump could be the origin of such influence [35].

Cellular and transepithelial responses to Cl^- substitution have been reported elsewhere [52] showing that the hyperpolarizing response to Cl^--substitution is mainly due to a disappearance of a considerable chloride conductance in the basolateral membranes. Cl^--free solutions repress $\Delta\psi_{mc}^{depol}$, but lead to an equal or larger $\Delta\psi_{mc}^{depol}$ (see Fig. 6C). It is likely that the depolarization increases because the membrane chloride conductance that can shunt electrical influx associated with the glucose response, is now absent. Abolition of the repolarization may be due to the fact that t_K^{bl} is indirectly already increased in Cl^--free solutions, before the glucose evoked changes occur. The underlying mechanism would be that the elevated a_iNa^+ increases a_iCa^{2+}, should a Na^+/Ca^{2+}-exchange be present. This rise in intracellular Ca^{2+} might open a basolaterally located Ca^{2+}-sensitive K-permeability, thus increasing in its turn t_K^{bl} [9].

It is clear that all coupled Na^+ influx enters the cells through the brush border membrane; it is also clear that most of the Na^+ leaves the cell through the Na/K-pump of which the enzyme molecules are found homogeneously distributed over the basolateral membranes of the cells. The goldfish enterocyte is a rather elongated epithelial cell: the length-diameter ratio of the cell is about 14 that of the interspace 350![1].

If massive ion handling through the lateral membranes occurs from the cell to the interspace, this can influence the concentrations of the ions considerably. In particular a_iNa^+ and $a_{is}K^+$ can change readily in relative terms because they are low. The two facts about the Na^+-fluxes suggest for the fact that an higher a_iNa^+ exists near the brush border than near the basal membrane, especially during glucose absorption. As is generally accepted that a_iNa^+ can stimulate the Na/K-pump [15, 25, 41, 42] in the concentration range found by us [15, 25, 39, 41, 42], it is not unwarranted to predict that this stimulation will be stronger close to the apical side of the cell than near the basal side of the cell. A direct consequence is that one expects to find in the interspace a variation in $a_{is}K^+$ from apical to basal end. This process does not necessarily evoke measurable electrical [8, 44, 47], Cl^- [23] or significant osmolarity gradients [23, 43] in cell or interspace, nor measurable gradients in a_iK^+ [47] or $a_{is}Na^+$. Only gradients for a_iNa^+ or $a_{is}K^+$ might be measurable. The extreme narrowness of the interspace in our preparation does not allow measurement of $a_{is}K^+$. The measurement of a_iNa^+ as a function of the depth of electrode penetration has not systematically been made during these investigations, but our impression was that there was a larger scatter in a_iNa^+ than in a_iK^+ or a_iCl^-.

The generation of these gradients will be strongly dependent on the structure of the epithelial compartments involved, and therefore these logical consequences of the pursuit of generally accepted descriptions of transepithelial transport can only be verified experimentally in epithelia with elongated cells and not in rather cuboidal cells (like for example those of Necturus gallbladder [12, 23, 43, 44]).

Acknowledgement. We thank Dr. A. van Rotterdam for his comments during this research, Dr. B. L. Roberts for his comments on the paper and correcting the English speling and grammar and H. van der Meyden and S. van Mechelen for the illustrations. The work was supported by the Netherlands Foundation for Biophysics with financial aid of the Netherlands Organisation for Advancement of Pure Science (ZWO).

References

1. Albus H, Bakker R, Siegenbeek van Heukelom J (1983) Circuit analysis of membrane potentials changes due to electrogenic sodium-dependent sugar transport in goldfish intestinal epithelium. Pflügers Arch 398:1–9
2. Albus H, Groot JA, Siegenbeek van Heukelom J (1979) Effects of glucose and ouabain on transepithelial electrical resistance and cell volume in stripped and unstripped goldfish intestine. Pflügers Arch 383: 55–66
3. Albus H, Lippens F, Siegenbeek van Heukelom J (1983) Sodium-dependent sugar and amino acid transport in isolated goldfish intestinal epithelium: Electrophysiological evidence against direct interactions at the carrier level. Pflügers Arch 398:10–17
4. Armstrong WMcD, Bixenman WR, Frey KF, Garcia-Diaz JF, O'Regan MG, Owens JL (1979) Energetics of coupled Na^+ and Cl^- entry into epithelial cells of bullfrog small intestine. Biochim Biophys Acta 551:207–219
5. Armstrong WMcD, Garcia-Diaz JF (1980) Ion-selective microelectrodes: Theory and technique. Fed Proc 739:2851–2859
6. Armstrong WMcD, Youmans SJ (1980) The role of bicarbonate ions and of cAMP in chloride transport by epithelial cells of bullfrog small intestine. Ann NY Acad Sci 341:139–155
7. Biagi B, Sohtell M, Giebisch G (1981) Intracellular potassium activity in the rabbit proximal straight tubule. Am J Physiol 241:F677–F686
8. Boulpaep EL, Sackin H (1980) Electrical analysis of intraepithelial barriers. In: Bronner F, Kleinzeller A, Boulpaep, E (eds) Current topics in membranes and transport, vol 13. Academic Press, New York, pp 169–197
9. Brown PD, Sepúlveda FV (1985) Potassium movements associated with amino acid and sugar transport in enterocytes isolated from rabbit jejunum. J Physiol (London) 363:271–285
10. Cardinal J, Lapointe J-Y, Laprade R (1984) Luminal and peritubular ionic substitutions and intracellular potential of the rabbit proximal convoluted tubule. Am J Physiol 247:F352–F364
11. Coles JA, Tsacopoulos M (1979) Potassium activity in photoreceptors, glial cells and extracellular space in the drone retina: changes during photostimulation. J Physiol (London) 290:525–549
12. Curci S, Frömter E (1979) Micropuncture of the lateral intercellular spaces of Necturus gallbladder to determine space fluid K^+ concentration. Nature 278:355–357
13. Diamond JM (1982) Transcellular cross-talk between epithelial cell membranes. Nature 300:683–685
14. Frömter E (1982) Electrophysiological analysis of rat renal sugar and amino acid transport. I. Basic phenomena. Pflügers Arch 393:179–189
15. Glitch HG, Push H, Venetz K (1976) Effect of Na and K ions on the active Na transport in guinea pig auricles. Pflügers Arch 365:29–36
16. Graf J, Giebisch G (1979) Intracellular sodium activity and sodium transport in Necturus gallbladder epithelium. J Membr Biol 47:327–355
17. Grasset E, Gunter-Smith P, Schultz SG (1983) Effects of Na-coupled alanine transport on intracellular K-activities and the K-conductance of the basolateral membranes of Necturus small intestine. J Membr Biol 71:89–94
18. Groot JA (1981) Cell volume regulation in goldfish intestinal mucosa. Pflügers Arch 392:57–66
19. Groot JA (1982) Aspects of the physiology of intestinal mucosa of the goldfish (Carassius Auratus L). Thesis, University of Amsterdam
20. Gunter-Smith PJ, Grasset, E, Schultz SG (1982) Sodium-coupled amino acid and sugar transport by Necturus small intestine: An equivalent electrical circuit analysis of a rheogenic co-transport system. J Membr Biol 66:25–39
21. Hudson RL, Schultz SG (1984) Sodium-coupled sugar transport: effects on intracellular sodium activities and sodium-pump activity. Science 224:1237–1239
22. Hyman D, Kaplan NM (1985) The difference between serum and plasma potassium. New Eng J Med 313:642
23. Ikonomov O, Simon M, Frömter E (1985) Electrophysiological studies on lateral intercellular spaces of Necturus gallbladder epithelium. Pflügers Arch 403:301–307
24. Johnson DC, Orlowitz L, Hitzig BM (1985) Differences between CSF and plasma Na^+ and K^+ activities and concentrations. Am J Physiol 248:R621–R626
25. Jørgensen PL (1980) Sodium and potassium ion pump in kidney tubules. Physiol Rev 60:864–917
26. Khuri RN (1979) Electrochemistry of the nephron. In: Giebisch G, Tosteson DC, Ussing HH (eds) Membrane transport of biology, vol IV. Springer, Berlin Heidelberg New York, pp 47–97
27. Lang F, Messner G, Wang W, Paulmichl M, Oberleithner H, Deetjen P (1984) The influence of intracellular sodium activity on the transport of glucose in proximal tubule of frog kidney. Pflügers Arch 401:14–21
28. Lau KR, Hudson RL, Schultz SG (1984) Cell swelling increases a barium-inhibitable potassium conductance in the basolateral membrane of Necturus small intestine. Proc Natl Acad Sci USA 81:3591–3594
29. Messner G, Koller A, Lang F (1985) The effect of phenylalanine on intracellular pH and sodium activity in proximal convoluted tubule cells of the frog kidney. Pflügers Arch 404:145–148
30. Messner G, Oberleithner H, Lang F (1985) The effect of phenylalanine on the electrical properties of proximal tubule cells in the frog kidney. Pflügers Arch 404:138–144
31. Meier PC, Lanter F, Ammann D, Steiner RA, Simon W (1982) Applicability of available ion-selective liquid membrane microelectrodes to intracellular ion activity measurements. Pflügers Arch 393:23–30
32. Samarzija I, Frömter E (1982) Electrophysiological analysis of rat renal sugar and amino acid transport III. Neutral amino acids. Pflügers Arch 393:199–209
33. Samarzija I, Hinton BT, Frömter E (1982) Electrophysiological analysis of rat renal sugar and amino acid transport II. Dependence on various transport parameters and inhibitors. Pflügers Arch 339:190–197
34. Schultz SG (1981) Potassium transport by rabbit descending colon in vitro. Fed Proc 40:2408–2411
35. Schultz SG (1981) Homocellular regulatory mechanisms on sodium transorting epithelia: Avoidance of extinction by "flush-through". Am J Physiol 241:F579–F590
36. Siegenbeek van Heukelom J, Albus H, Zuidema T (1982) Stimulation of the electrogenic Na/K-pump by transepithelial glucose transport in goldfish intestine. J Gen Physiol 80: 5a
37. Siegenbeek van Heukelom J, Dijkstra K, Ingen H van (1976) A versatile and reproducibly operating microelectrode puller. Med Biol Eng 3:644–652
38. Siegenbeek van Heukelom J, Van den Ham MD, Albus H, Groot JA (1982) Microscopical determination of the filtration permeability of the mucosal surface of the goldfish intestinal epithelium. J Membr Biol 63:31–39
39. Siegenbeek van Heukelom J, Zuidema T (1985) The influence of Ba^{2+} on membrane potential and K^+-induced depolarizations in goldfish intestinal epithelium. J Physiol (London) 366:92P
40. Siegenbeek van Heukelom J, Zuidema T, Kamermans M (1986) The role of the structure of epithelial compartments in transepithelial transport. In: Alvarado F, van Os CH (eds) Ion gradient-coupled transport; INSERM Symposium N. 26. Elsevier, Amsterdam
41. Smith MW (1967) Influence of the temperature acclimatization on the temperature-dependence and ouabain-sensitivity of goldfish intestinal adenosine triphosphatase. Biochem J 105: 65–71
42. Soltoff SP, Mandel LJ (1984) Active ion transport in the renal proximal tubule. II. Ionic dependence of the Na pump. J Gen Physiol 84:623–642
43. Spring KR, Hope A (1979) Fluid transport and dimensions of cells and interspaces of living Necturus gallbladder. J Gen Physiol 73:287–305
44. Suzuki K, Frömter E (1977) The potential and resistance profile of Necturus gallbladder cells. Pflügers Arch 371:109–117
45. Thomas RC (1978) Ion-sensitive intracellular microelectrodes. Academic Press, New York, London, San Francisco
46. White JF, Imon MA (1983) Effect of galactose on intracellular potential and sodium activity in urodele small intestine. Evidence for basolateral electrogenic transport. In: Gilles-Baillien M, Gilles R (ed) Intestinal transport: fundamental and comparative aspects. Springer, Berlin Heidelberg New York, pp 295
47. Zeuthen T (1978) Intracellular gradients of ion activities in the epithelial cells of the Necturus gallbaldder recorded with ion-selective microelectrodes. J Membr Biol 39:185–218
48. Zeuthen T, Monge C (1976) Electrical potentials and ion activities in the epithelial cell layer of the rabbit ileum in vivo. In: Kessler M (eds) Ion and enzyme electrodes in biology and medicine. Urban and Schwarzenberg, Munich, p 345
49. Zuidema T, Dekker K, Siegenbeek von Heukelom J (1985) The influence of organic counterions on junction potentials and measured membrane potentials. Bioelectrochem Bioenergetics 14:479–494
50. Zuidema T, Kamermans M, Siegenbeek van Heukelom J (1983) The role of the intercellular compartment during glucose absorption. Interstitial and intracellular potassium activities in goldfish intestinal epithelium. Gastroenterol Clin Biol 7:514
51. Zuidema T, Siegenbeek van Heukelom J, Kamermans M, Groot JA (1982) The transmembrane glucose evoked potential in goldfish (Carassius Auratus) intestinal epithelium and the role of the extracellular space. In: 4th Conf Eur Soc for Comp Physiol and Biochem Intestinal Transport: fundamental and comparative aspects. Sept 8–11 1982, Bielefeld, p 152
52. Zuidema T, Van Riel JW, Siegenbeek van Heukelom J (1985) Cellular and transepithelial responses of goldfish intestinal epithelium to chloride substitutions. J Membr Biol 88:293–304

Received January 16/Accepted April 28, 1986

[1] To visualize the meaning of this ratio: a cell with diameter equal to the width of a column in this Journal would have, in the same scale, a length exceeding one meter

during mucosal chloride substitution the relative cell volume decreases while during serosal substitutions it does not. The electrodiffusional permeability of the brush border membrane for chloride is so low that it is easily overlooked for two reasons. First: If 3 M KCl salt bridges are used as reference electrodes [60] the depolarization of the mucosal membrane is obscured by the shift of −4.1 mV to be expected for the cation-selective membrane in analogy to the shift observed with a potassium-sensitive microelectrode. Second, the reduction of a_iCl^- will lead to hyperpolarization overriding the depolarization. The initial depolarization after mucosal chloride substitution reflects the chloride permeability of both the mucosal membrane and the tight junction and is a weighed superposition of the depolarization of E_m, a hyperpolarization of E_s and a serosa-positive shunt diffusion potential.

The basolateral chloride permeability is approximately 20×10^{-6} cm sec^{-1} representing more than 30% of the total basolateral membrane conductance. This is the major reason why R_m/R_s decreases by serosal chloride substitution.

10. Conclusions for the Active Salt Transport of the Epithelium

In conclusion: the goldfish enterocyte possesses an electroneutral influx mechanism of chloride in the brush border membrane and a large chloride permeability in the basolateral membrane. The effective diffusional impedance of the basolateral membrane is higher than that of the brush border membrane, so that the cellular chloride activity is more influenced by the mucosal chloride activity than by the serosal activity.

If the stoichiometry of the mucosal coupling is 1 : 1 an extremely profitable configuration is present in the enterocyte since the energetics for uphill transport of chloride into the cell are minimized, as by this coupling no energy is necessary to overcome the electrical part (i.e., ψ_{mc}) of the electrochemical gradient. At the basolateral side this electrical part is used in a favorable way as here the chloride efflux is only coupled to other ions through the electrical gradient (principle of electroneutrality).

We thank Dr. B.L. Roberts for his comments on the paper and correcting the English spelling and grammar and H. van der Meyden for the illustrations. The work was supported by the Netherlands Foundation for Biophysics with financial aid of the Netherlands Organisation for Advancement of Pure Science (ZWO).

References

1. Albus, H., Bakker, R., Siegenbeek van Heukelom, J. 1983. Circuit analysis of membrane potentials changes due to electrogenic sodium-dependent sugar transport in goldfish intestinal epithelium. *Pfluegers Arch.* **398**:1–9
2. Armstrong, W.McD., Bixenman, W.R., Frey, K.F., Garcia-Diaz, J.F., O'Regan, M.G., Owens, J.L. 1979. Energetics of coupled Na^+ and Cl^- entry into epithelial cells of bullfrog small intestine. *Biochim. Biophys. Acta* **551**:207–219
3. Armstrong, W.McD., Garcia-Diaz, J.F. 1980. Ion-selective microelectrodes: Theory and technique. *Fed. Proc.* **39**:2851–2859
4. Baerentsen, H.J., Christensen, O., Thomsen, P.G., Zeuthen, T. 1982. Steady states and the effects of ouabain in the *Necturus* gallbladder epithelium: A model analysis. *J. Membrane Biol.* **68**:215–225
5. Baerentsen, H., Giraldez, F., Zeuthen, T. 1983. Influx mechanisms for Na^+ and Cl^- across the brush border membrane of leaky epithelia: A model and microelectrode study. *J. Membrane Biol.* **75**:205–218
6. Bakker, R., Dekker, K., Zuidema, T., Groot, J.A. 1982. Transepithelial Cl-transport in goldfish *Carassius auratus* intestinal mucosa and the effect of theophylline on fluxes and electrophysiology. 4th Conference of the European Society for Comparative Physiology and Biochemistry, Bielefeld (FRG) September 8–11, 1982
7. Bakker, R., Groot, J.A. 1984. cAMP-mediated effects of ouabain and theophylline on paracellular ion selectivity. *Am. J. Physiol.* **246**:G213–G217
8. Barry, P.H., Diamond, J.M. 1970. Junction potentials, electrode standard potentials, and other problems in interpreting electrical properties of membranes. *J. Membrane Biol.* **3**:93–122
9. Burckhardt, B.C., Frömter, E. 1981. Bicarbonate and hydroxylion permeability of the peritubular cell membrane of rat renal proximal tubular cells. *Pfluegers Arch.* **389**:R40
10. Christoffersen, G.R.J., Skibsted, L.H. 1975. Calcium ion activity in physiological solutions: Influence of anions substituted for chloride. *Comp. Biochem. Physiol.* **52A**:317–322
11. Cremaschi, D., James, P.S., Meyer, G., Rossetti, C., Smith, M.W. 1984. Developmental changes in intra-enterocyte cation activities in hamster terminal ileum. *J. Physiol. (London)* **354**:363–373
12. Dagostino, M., Lee, C.O. 1982. Neutral carrier Na^+- and Ca^{2+}-selective microelectrodes for intracellular application. *Biophys. J.* **40**:199–207
13. Duffey, M.E., Turnheim, K., Frizzell, R.A., Schultz, S.G. 1979. Intracellular chloride activities in rabbit gallbladder: Direct evidence for the role of the sodium-gradient in energizing "Uphill" chloride transport. *J. Membrane Biol.* **42**:229–245
14. Ellory, J.C., Ramos, M., Zeuthen, T. 1979. Cl^--accumulation in the plaice intestinal epithelium. *J. Physiol. (London)* **287**:12*P*
15. Field, M., Karnaky, K.J., Smith, P.L., Bolton, J.E., Kinter, W.B. 1978. Ion transport across the isolated intestinal mucosa of the winter flounder, *Pseudopleuronectes americanus*: I. Functional and structural properties of cellular and paracellular pathways for Na and Cl. *J. Membrane Biol.* **41**:265–293
16. Fisher, R.S. 1984. Chloride movement across basolateral membrane of *Necturus* gallbladder epithelium. *Am. J. Physiol.* **247**:C495–C500
17. Frizzell, R.A., Field, M., Schultz, S.G. 1979. Sodium-coupled chloride transport by epithelial tissues. *Am. J. Physiol.* **236**:F1–F8
18. Frömter, E. 1979. Solute transport across epithelia: What can we learn from micropuncture studies on kidney tubules? *J. Physiol. (London)* **288**:1–31
19. Garcia-Diaz, J.F., O'Doherty, J., Armstrong, W.McD. 1978. Potential profile, K^+ and Na^+ activities in *Necturus* small intestine. *Physiologist* **21**:41
20. Giraldez, F. 1984. Active sodium transport and fluid secretion in the gall-bladder epithelium of *Necturus*. *J. Physiol. (London)* **348**:431–455
21. Groot, J.A. 1981. Cell volume regulation in goldfish intestinal mucosa. *Pfluegers Arch.* **392**:57–66
22. Groot, J.A. 1982. Aspects of the Physiology of the Intestinal Mucosa of the Goldfish (*Carassius auratus* L). MultiCopy, Amsterdam
23. Groot, J.A., Albus, H., Siegenbeek van Heukelom, J. 1979. A mechanistic explanation of the effect of potassium on goldfish intestinal transport. *Pfluegers Arch.* **379**:1–9
24. Groot, J.A., Dekker, K., Van Riel, J.W., Zuidema, T. 1982. Intracellular ion concentrations and pH of stripped mucosa of goldfish (*Carassius auratus*) intestine in relation to Cl^- transport. 4th conference of the European Society for Comparative Physiology and Biochemistry, Bielefeld (FRG), September 8–11, 1982
25. Guggino, W.B., Boulpaep, E.L., Giebisch, G. 1982. Electrical properties of chloride transport across the *Necturus* proximal tubule. *J. Membrane Biol.* **65**:185–196
26. Halm, D., Krasny, E., Frizzell, R.A. 1982. Apical membrane potassium conductance in flounder intestine: Relation to chloride absorption. *Bull. Mount Desert Island Biol. Lab.* **21**:88–93
27. Henin, S., Smith, M.W. 1976. Electrical properties of pig colonic mucosa measured during early post-natal development. *J. Physiol. (London)* **262**:169–187
28. Hudson, R.L., Schultz, S.G. 1984. Sodium-coupled sugar transport: Effects on intracellular sodium activities and sodium-pump activity. *Science* **224**:1237–1239
29. Jacquez, J.A., Schultz, S.G. 1974. A general relation between membrane potential, ion activities and pump fluxes for symmetric cells in a steady state. *Math. Biosci.* **20**:19–26
30. Katz, U., Lau, K.R., Ramos, M.M.P., Ellory, J.C. 1982. Thiocyanate transport across fish intestine (*Pleuronectes platessa*). *J. Membrane Biol.* **66**:9–14
31. Laprade, R., Cardinal, J. 1983. Liquid junctions and isolated proximal tubule transepithelial potentials. *Am. J. Physiol.* **244**:F304–F319
32. Lee, C.O., Armstrong, W.McD. 1972. Activities of sodium and potassium ions in epithelial cells of small intestine. *Science* **175**:1261–1264
33. Liedtke, C.M., Hopfer, U. 1982. Mechanism of Cl^- translocation across small intestinal brush-border membrane: II. Demonstration of Cl^--OH^- exchange and Cl^- conductance. *Am. J. Physiol.* **242**:G272–G280
34. Meier, P.C., Lanter, F., Ammann, D., Steiner, R.A., Simon, W. 1982. Applicability of available ion-selective liquid membrane microelectrodes to intracellular ion activity measurements. *Pfluegers Arch.* **393**:23–30
35. Nellans, H.N., Frizzell, R.A., Schultz, S.G. 1973. Coupled sodium-chloride influx across the brushborder of rabbit ileum. *Am. J. Physiol.* **225**:467–475
36. Okada, Y., Irimajuri, A., Inouye, A. 1976. Intracellular ion concentrations of epithelial cells in rat intestine. Effects of external K and uphill transports of glucose and glycine. *Jpn. J. Physiol.* **26**:427–440
37. Okada, Y., Sato, T., Inouye, A. 1975. Effects of potassium ions and sodium ions on membrane potential of epithelial cells in rat duodenum. *Biochim. Biophys. Acta* **413**:104–115
38. Os, C.H. van, Wiedner, G., Wright, E.M. 1979. Volume flows across gallbladder epithelium induced by small hydrostatic and osmotic gradients. *J. Membrane Biol.* **49**:1–20
39. Reuss, L. 1979. Electrical properties of cellular transepithelial pathway in *Necturus* gallbladder: III. Ionic permeability of the basolateral cell membrane. *J. Membrane Biol.* **47**:239–259
40. Reuss, L. 1983. Basolateral co-transport in NaCl-absorbing epithelium. *Nature (London)* **305**:723–726
41. Reuss, L., Cheung, L.Y., Grady, T.P. 1982. Mechanisms of cation permeation across apical cell membrane of *Necturus* gallbladder: Effects of luminal pH and divalent cations on K^+ and Na^+ permeability. *J. Membrane Biol.* **59**:211–224
42. Reuss, L., Weinman, S.A. 1979. Intracellular ionic activities and transmembrane electrochemical potential differences in gallbladder epithelium. *J. Membrane Biol.* **49**:345–362
43. Rose, R.C., Schultz, S.G. 1971. Studies on the electrical potential profile across rabbit ileum: Effects of sugars and amino acids on transmural and transmucosal electrical potential differences. *J. Gen. Physiol.* **57**:639–663
44. Sackin, H., Boulpaep, E.L. 1981. Isolated perfused salamander proximal tubule: II. Monovalent ion replacement and rheogenic transport. *Am. J. Physiol.* **241**:F540–F555
45. Schultz, S.G. 1980. Basic principles of membrane transport. *In:* IUPAB Biophysics Series 1, Cambridge University Press, Cambridge-London-New York-New Rochelle-Melbourne-Sydney
46. Shindo, T., Spring, K.R. 1981. Chloride movement across the basolateral membrane of proximal tubule cells. *J. Membrane Biol.* **58**:35–42
47. Siegenbeek van Heukelom, J. 1978. The electrical characteristics of the absorptive goldfish intestinal epithelium. *Gastroent. Clin. Biol.* **2**:329
48. Siegenbeek van Heukelom, J., Van den Ham, M.D., Albus, H., Groot, J.A. 1981. Microscopical determination of the filtration permeability of the mucosal surface of the goldfish intestinal epithelium. *J. Membrane Biol.* **63**:31–39
49. Smith, P.L., Welsh, M.J., Stewart, C.P., Frizzell, R.A., Orellana, S.A., Field, M. 1981. Chloride absorption by the intestine of the winter flounder *Pseudopleuronectes americanus*: Mechanism of inhibition by reduced pH. *Bull. Mount Desert Island Biol. Lab.* **20**:96–101
50. Spring, K.R., Giebisch, G. 1977. Tracer Na fluxes in *Necturus* proximal tubule. *Am. J. Physiol.* **232**:F461–F470
51. Spring, K.R., Kimura, G. 1978. Chloride reabsorption by renal proximal tubules of *Necturus*. *J. Membrane Biol.* **38**:233–254
52. Turnberg, L.A., Bieberdorf, F.A., Morowski, S.G., Fordtran, J.S. 1970. Interrelationship of chloride, bicarbonate, sodium and hydrogen transport in human ileum. *J. Clin. Invest.* **49**:557–567
53. Waddell, W.J., Butler, T.C. 1959. Calculation of the intracellular pH from the distribution of 5,5-dimethyl-2,4-oxazolidinedione (DMO). Application to skeletal muscle of the dog. *J. Clin. Invest.* **38**:720–729
54. White, J.F. 1976. Intracellular potassium activities in *Amphiuma* small intestine. *Am. J. Physiol.* **231**:1214–1219
55. White, J.F. 1977. Activity of chloride in absorptive cells of *Amphiuma* small intestine. *Am. J. Physiol.* **232**:E553–E559
56. White, J.F. 1980. Bicarbonate-dependent chloride absorption in small intestine: Ion fluxes and intracellular chloride activities. *J. Membrane Biol.* **53**:95–107
57. Zeuthen, T. 1981. On the effects of amphotericin B and ouabain on the electrical potentials of *Necturus* gallbladder. *J. Membrane Biol.* **60**:167–169
58. Zeuthen, T., Monge, C. 1976. Electrical potentials and ion activities in the epithelial cell layer of the rabbit ileum in vivo. *In:* Ion and Enzyme Electrodes in Biology and Medicine. M. Kessler et al., editors. p. 345. Urban and Schwarzenberg, Munich
59. Zeuthen, T., Ramos, M., Ellory, J.C. 1978. Inhibition of

Student's-t-test. P>0.05 is considered not significant (n.s.).

Results

The effect of bilateral sodium substitutions on ψ_{mc} and a_iCl^-. Although it was reported earlier for goldfish intestinal epithelium that replacement of Na^+ by choline or NMDG (N-methyl-(D)-Glucamine) did not reduce significantly the intracellular chloride concentration ($[Cl^-]_i$) [23,24] we found that replacement of Na^+ by NMDG causes the intracellular chloride activity (a_iCl^-) and the membrane potential (ψ_{mc}) to decrease significantly (Table 1). Therefore the accumulation ratio R decreases from 4.0 to 1.8, an effect that should be expected when there is a coupling between sodium and chloride influx [17].

Table 1

	ψ_{mc} (mV)	a_iCl^- (meq/l)	$R = a_iI/(a_iI)_{eq}$	m,n
Control	-56.7 ± 1.0	39.4 ± 0.5	4.0	18,20
NMDG	-41.6 ± 0.7	31.8 ± 1.1	1.8	21,25

Measurements of ψ_{mc} and a_iCl^- in four epithelia during control and after 30–60 minutes of bilateral Na^+ to NMDG substitution; R is the intracellular accumulation ratio of chloride; m and n refer to the number of individual impalements with the indifferent electrode and the ion-selective electrode respectively.

The effect of furosemide.

Table 2

	ψ_{mc} (mV)	a_iCl^- (meq/l)	m,n
Control	-58.8 ±0.5	33.6 ± 1.8	15,14
Furosemide	-57.7 ± 0.6	35.0 ± 1.2	12,12

Measurements of ψ_{mc} and a_iCl^- in 2 epithelia during control and inthepresence of 1 mM of furosemide in the mucosal bathing solution.
m and n as defined at Table 1

The diuretic furosemide, reported to block Na,Cl-symport and Na,K,Cl-symport in other epithelia [22,38], is not effective in goldfish intestine. Neither the membrane potential, nor the intracellular chloride activity changes significantly (Table 2) [55]. In addition, in a number of separate experiments no changes could be observed in transepithelial potentials and resistances after the addition of either furosemide or the more potent loop-diuretic, bumetanide [31,43].

The effect of chloride substitutions on ψ_{mc} and a_iNa^+. Bilateral omission of Cl^- does not cause a significant reduction in intracellular sodium activity (Table 3), in clear contrast to e.g. renal tubule where in similar experiments a_iNa^+ decreased by 6-7 meq/l [38,50]. As reported also in Chapter III the membrane hyperpolarizes considerably. So, if a_iNa^+ is further from electrochemical equilibrium (R decreases from 0.017 to 0.011), this is due only to membrane hyperpolarization and not to a reduced influx of Na^+, as expected if the influxes of Na^+ and Cl^- were tightly coupled. Possibly an enhanced electrodiffusional influx of Na^+ and/or a reduction in Na/K-pump activity may account for the absence of the expected decrease in a_iNa^+.

Table 3

	ψ_{mc} (mV)	a_iNa^+ (meq/l)	$R= a_iI/(a_iI)_{eq}$	m,n
Control	-48.4 ± 1.1	12.2 ± 1.0	0.017	18,18
Cl-free	-61.4 ± 1.1	13.6 ± 2.2	0.011	12,14

Measurements of ψ_{mc} and a_iNa^+ in 3 epithelia under control conditions and after prolonged bilateral chloride to gluconate substitution. R, m and n as defined at Table 1

pH measurements in unstirred layers. If the mucosal surface of the goldfish intestine is approached with a miniature pH-electrode a small but very consistent step is observed in electrode potential (Figure 1) indicating a slightly alkaline mucosal microclimate [c.f. 33,46]. An opposite but larger step is observed at the serosal surface, suggesting a relatively acidic serosal microclimate (Table 4; cf Figure 1: right hand side).

Table 4

	ΔpH mucosal surface	n,N	serosal surface	n,N
Control	0.026±0.003	7,3	-0.108±0.009	13,3
Cl-free	-0.026±0.011	5,2	-0.042±0.002	5,1
HCO_3^-/CO_2-free	-0.037±0.012	10,1	-0.107±0.004	7,1

Steps in pH-signal of a miniature pH-electrode (ΔpH) on approaching the mucosal surface resp. the serosal surface in control bicarbonate buffer, chloride-free (isethionate for chloride substitution) bicarbonate buffer and Tris-Hepes buffer.
n refers to the number of registrations, N to the number of epithelia Significance was calculated with respect to control

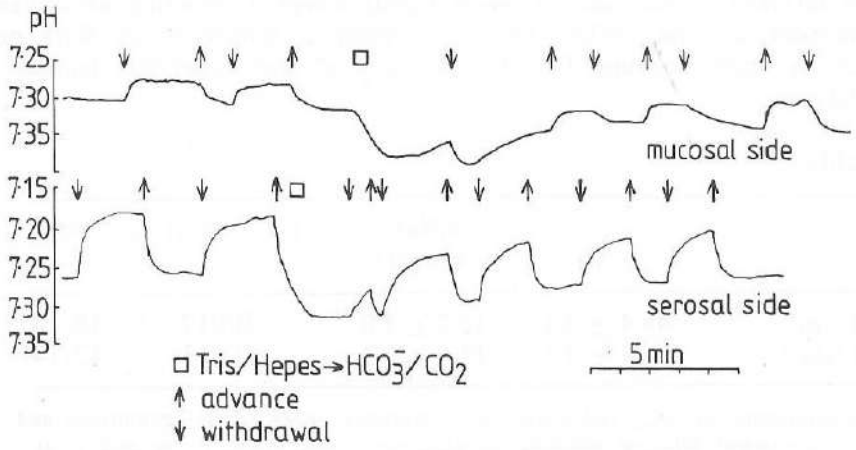

Fig. 1: pH gradients in the unstirred layers near the mucosal (upper recording) and serosal (lower recording) surface measured with a miniature pH electrode (diameter 1.2 mm) during the transition from bicarbonate-free (Tris/Hepes) to HCO_3^-/CO_2 buffers. The arrows indicate the advance of the electrode towards (↓), or withdrawal from the epithelium (↑), over a fixed distance of 0.6 mm, driven by an electronically controlled inchworm translator (Burleigh Instr.) (Note that a step of 0.017 pHu corresponds to an electrical potential difference of 1 mV)

After bilateral HCO_3^-/CO_2 substitution or chloride substitution the step reverses sign at the mucosal side (Figure 1). At the serosal side the step does not change significantly after bilateral HCO_3^-/CO_2 substitution but becomes smaller after chloride substitution (Table 4). Apparently transepithelial bicarbonate flux, proton flux or both change under these conditions in such a way that net acid transport is diminished or even abolished.

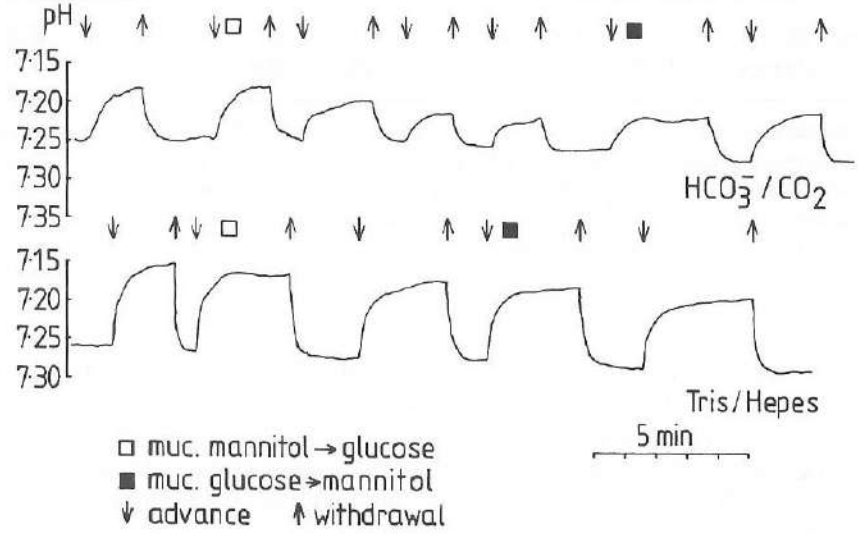

Fig.2: pH gradients in the serosal unstirred layers in mannitol solutions (■) and during glucose absorption (□), both in HCO_3^-/CO_2 buffers (upper recording) and Tris/Hepes buffers (lower recording). See also legends to Figure 1.

An interesting phenomenon was observed while measuring the serosal pH: the acidification is significantly decreased during glucose absorption in bicarbonate buffers, whereas this does not happen in Tris-Hepes buffer (Figure 2).

The effects of HCO_3^-/CO_2 substitution on ψ_{mc} and a_iCl^-. Table 5 (second column) shows that substitution of a HCO_3^-/CO_2 by a Tris/Hepes buffer of the same pH causes the membrane to depolarize significantly. In a separate experiment in which the extracellular chloride concentration was kept constant (normally Tris/Hepes buffers have a 20 mM higher chloride concentration to compensate for the difference in Hepes and bicarbonate concentration) the

intracellular chloride activity was not different from control value (fourth and fifth column).

Table 5

	ψ_{mc} (mV)	m	ψ_{mc} (mV)	a_iCl^- (meq/l)	m,n
Control	-54.2 ± 1.1	28	-49.2 ± 0.5	35.9 ± 1.5	8,6
Tris/Hepes	-46.0 ± 1.1	28	-45.3 ± 0.6	37.9 ± 1.3	7,6

Measurements of ψ_{mc} in HCO_3^-/CO_2 buffers as compared to Tris/Hepes buffers in 10 epithelia (second column). In another epithelium a_iCl^- was also measured (fourth and fifth column). The Tris/Hepes buffer in the latter case was adapted to contain approximately the same Cl^- concentration as the control solution (see text). m and n as defined in Table 1

The effects of pH_o on ψ_{mc}, a_iCl^- and pH_i. As reported in Chapter III (see also [23]) bilateral bicarbonate elevation results in an increase in intracellular pH, and consequently in $a_iHCO_3^-$, and in an hyperpolarization of the membrane. The intracellular chloride activity decreases slightly. The results are summarized in Figure 3, showing the actual driving forces for passive H^+ and Cl^- flux across the plasma membrane, namely the membrane potential (ψ_{mc}) and the chemical potential difference, expressed in the form of the the Nernst equilibrium potential: $E_I = \Delta\mu_I/z_IF$. Assuming that the membranes are highly permeable for CO_2 and that the dissociation rate of carbonic acid is sufficiently high, the electrochemical potential differences for H^+ and HCO_3^- can be equated so that the difference (E_{H^+} - E_{Cl^-}) is proportional to the driving force for HCO_3^-/Cl^- exchange.

In Figure 4 the same measurements are shown under bicarbonate-free conditions. Note that the difference (E_{H^+} - E_{Cl^-}) is larger than in Figure 3 but decreases also with increasing pH_o. Because of the absence of extracellular CO_2 a good determination of E_{HCO3^-} with the present methods is not possible.

Figure 3

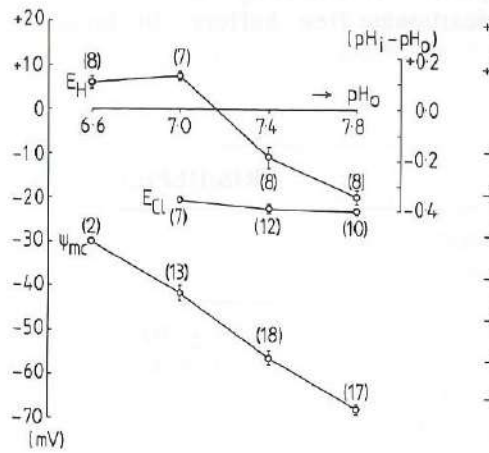

Figure 4

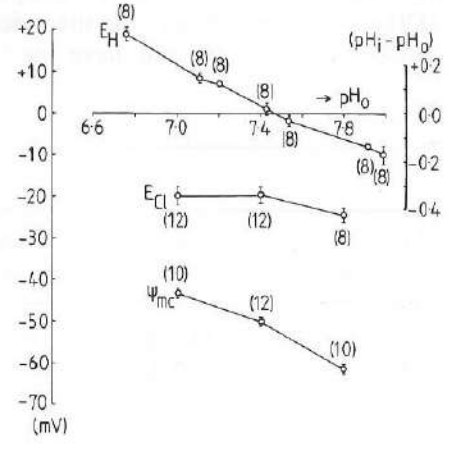

Fig.3: Transmembrane electrical (ψ_{mc}) and Nernst equilibrium potentials for H^+ (E_H) and Cl^- (E_{Cl}) as a function of pH of the bicarbonate-buffered bathing solutions. The data on E_H and ψ_{mc} are transposed from Chapter III (Table 4). The numbers in parentheses refer to the number of impalements with a normal 3M KCl filled microelectrode (ψ_{mc}) and with a chloride-selective microelectrode (E_{Cl}) in the same two epithelia or to the number of strips analysed with ^{14}C-DMO (E_H).

Fig. 4: Transmembrane electrical (ψ_{mc}) and Nernst equilibrium potentials for H^+ (E_H) and Cl^- (E_{Cl}) as a function of pH of the Tris/Hepes-buffered bathing solutions. The data on E_H are transposed from [23; Paper 3: Figure 3]. The numbers in parentheses refer to the number of impalements with a normal 3M KCl filled microelectrode (ψ_{mc}) and with a chloride-selective microelectrode (E_{Cl}) in the same two epithelia or to the number of strips analysed with ^{14}C-DMO (E_H).

The influence of pH_o on R_{ms} and GEP. Table 6 shows that with increasing pH the transmural resistance decreases while the GEP (transepithelial glucose evoked potential) increases. Qualitatively the same effects are measured with and without HCO_3^- (no data on GEP's in bicarbonate-free media were shown by lack of a sufficient number

of reliable data; see below). In the absence of HCO_3^-/CO_2 the preparations deteriorated often suddenly and irreversibly at the lower pH's, R_{ms} dropping to 25-50% of the control value and the GEP reducing to zero. This happened consistently if acetazolamide (Diamox) was added to the bicarbonate-free buffers. In bicarbonate buffers Diamox did not have such an effect.

Table 6

	HCO_3^-/CO_2		TRIS/HEPES
pH	R_{ms} (%)	GEP (%)	R_{ms} (%)
6.6	117 ± 3	80 ± 5	115 ± 10
7.0	110 ± 2	84 ± 7	111 ± 4
7.4	100	100	100
7.8	92 ± 1	114 ± 5	93 ± 1

The transmural resistance (R_{ms}) and glucose evoked potential (GEP) as a function of pH of the bathing solutions expressed in % of the control value (at pH=7.4). In the second and third column the values in HCO_3^-/CO_2 buffers are presented, in the fourth column those in Tris/Hepes buffers. GEP values in Tris/Hepes buffers are not shown (see text).

Mucosal chloride substitutions under bicarbonate-free conditions. Figure 5 shows a typical recording of the transepithelial responses, R_{ms} and ψ_{ms}, to mucosal chloride substitution in bicarbonate-free media. The electrodes were normal Ag-AgCl electrodes in contact with salt bridges containing control bathing solution. The salt bridge junctions give rise to large liquid junction potentials during chloride substitutions. For the resistance measurements these liquid junction potential artefacts are of no importance. For steady state measurements of the transepithelial potential accurate corrections for the liquid junction potential (l.j.p.) artefacts are possible (Chapter II).

Apart from the difference in transient, the steady state transepithelial diffusion potential (corrected for the l.j.p.) is significantly larger (+6.9 ± 0.6 mV (n=16)) in bicarbonate-free solutions than in control solutions (+2.9 ± 0.3 mV (see Chapter III)). Also R_{ms} increases considerably (from 15.5 ± 1.0 to 22.0 ± 2.4 Ωcm^2) in contrast to the responses in bicarbonate containing solutions, where R_{ms} did not change (Chapter III).

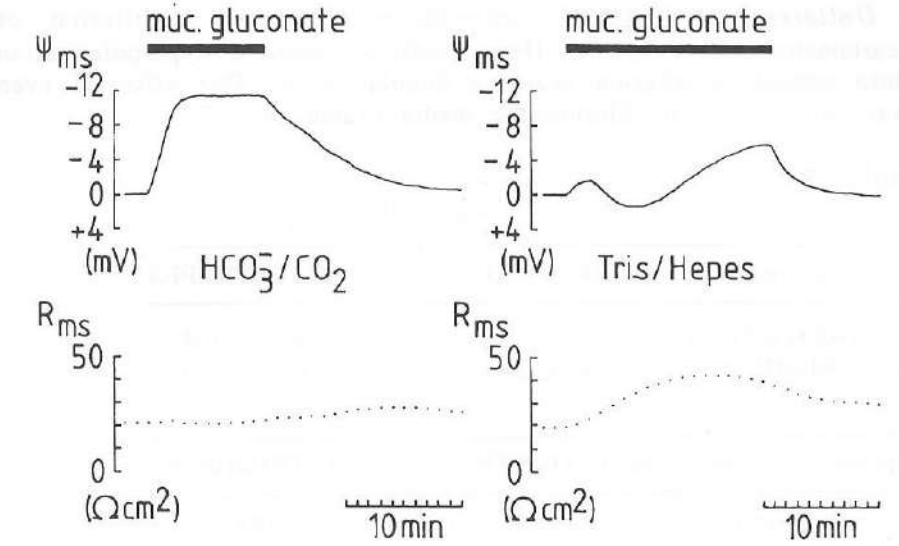

Fig. 5: Typical recordings of the transmural potential (ψ_{ms}) and resistance (R_{ms}) responses to mucosal chloride to gluconate substitution in HCO_3^-/CO_2 buffered solutions (left hand side) and during prolonged absence of HCO_3^-/CO_2 (right hand side). Resistances were measured at time intervals of 1 min. Reference electrodes were connected to the solutions with salt bridges filled with standard solution. The figures are not corrected for the large liquid junction potential artefacts introduced by these electrodes (approx. 13 mV; see Chapter II) as these can be expected to be almost identical in both situations.

Serosal bicarbonate variations and the use of SITS or DIDS. Variation of serosal HCO_3^- causes electrical changes qualitatively in agreement with a substantial electrodiffusional permeability for HCO_3^- (i.e. hyperpolarization after HCO_3^- elevation and depolarization after HCO_3^--reduction). A P_{HCO3-} was also demonstrated by Burkhart [9] in rat proximal tubule and was shown to be sensitive to SITS and acetazolamide [9,10,18]. We were not very successful in our experiments with SITS and DIDS because the membrane potentials tended to become unstable if we applied those drugs.

So, whereas DIDS and SITS may have an effect, the experiments reported in the previous paragraph show that acetazolamide definitely has an effect in goldfish intestine, but our results do not allow us to conclude that those drugs suppress P_{HCO3-}, as in rat proximal tubule [9,10].

Unilateral HCO_3^-/CO_2 substitutions. Mucosal substitution of bicarbonate buffers by Tris-Hepes buffers causes a hyperpolarization while serosal substitution causes a depolarization. This effect is even more pronounced in chloride-free media (Table 7).

Table 7

	ψ_{mc} (mV)	
with chloride	ser. HCO_3^-/CO_2	ser. TRIS/HEPES
muc. HCO_3^-/CO_2	-53.2 ± 1.5	-46.7 ± 0.9
muc. TRIS/HEPES	-59.0 ± 2.4	-43.4 ± 2.0
without chloride	ser. HCO_3^-/CO_2	ser. TRIS/HEPES
muc. HCO_3^-/CO_2	-71	-53
muc.TRIS/HEPES	-83 ± 1	-69 ± 1

Measurements of ψ_{mc} during unilateral and bilateral substitution by bicarbonate-free buffers as compared with control, both in chloride containing (upper table; 6 epithelia) and gluconate (chloride-free) solutions (lower table; 2 epithelia).

The effects of Ba^{2+} addition. In order to investigate the nature of the potassium permeability in goldfish enterocytes we studied the effects of Ba^{2+}, which is known to block certain potassium channels in other epithelia (e.g. [7,39]):

a. Intracellular concentrations, pH_i and cell water. The intracellular concentrations of the major ions as well as the intracellular pH (DMO) were measured in free-floating strips during control and in the presence of 5 mM of Ba^{2+} (Table 8). The measurements presented here include the measurements reported in Chapter III. Note that $[Na^+]_i$, $[Cl^-]_i$ and cell water are significantly increased. $[K^+]_i$ does not change significantly, nor does pH_i.

Table 8

	$[Na^+]$ (mM)	$[K^+]$ (mM)	$[Cl^-]$ (mM)	pH_0-pH_i	cw/dw
Control	46.3 ± 2.4	185.1 ± 5.3	53.0 ± 2.5	0.15 ± 0.03	2.93 ± 0.03
Ba^{2+}	60.3 ± 4.7	176.6 ± 6.5	61.8 ± 3.7	0.21 ± 0.05	3.11 ±0.05
	P<0.01	n.s	0.02<P<0.05	n.s	P<0.01

Intracellular ion concentrations, extracellular to intracellular pH-difference and cell water to dry weight ratio under control conditions and after the bilateral addition of 5 mM of Ba^{2+}.

b. Membrane potentials and unilateral Na/K substitutions. The effect of mucosal and serosal additions of Ba^{2+} on ψ_{mc} are shown in Figure 6.

Figure 6

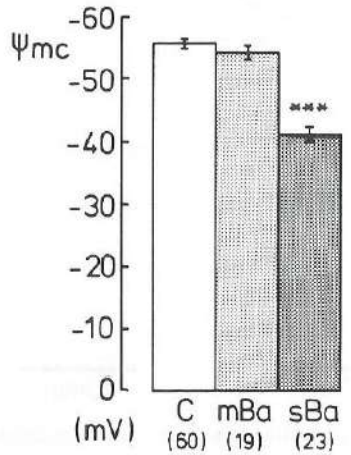

Figure 7

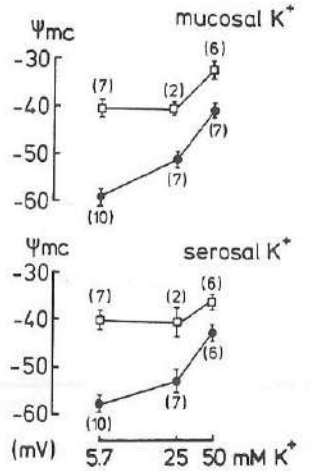

Fig. 6: The influence of 5 mM of Ba^{2+} in the mucosal bathing solution (mBa; $P > 0.1$) and in the serosal bathing solution (sBa; ***: $P < 0.001$) on ψ_{mc}. Numbers in parentheses indicate number of impalements in a total of 10 epithelia.

Fig. 7: The dependence of the membrane potential (ψ_{mc}) on the mucosal (upper diagram) and serosal potassium concentration (lower diagram) before (●) and after (□) isoosmotic substitution of 5 mM of barium for 10 mM of sodium. The total numbers of impalements in 4 epithelia are given in parentheses. Bars represent SEM.

It has been reported before [5,7] that the Ba^{2+}-sensitive channels are mainly located in the basolateral membrane. This is confirmed by the present experiments. On the other hand, Ba^{2+}-application to the serosal side also affects the responses of goldfish enterocytes to mucosal potassium elevations (Figure 7). Clearly the serosal addition of Ba^{2+} is almost equally effective in reducing both responses, suggesting that mucosal potassium elevation has a profound influence on the potassium concentration in the interspace [49].

c. Response of ψ_{ms} to mucosal chloride substitution. The presence of Ba^{2+} changes the transient response of the transepithelial potential to mucosal substitution of Cl^- by an impermeable anion. These kinds of responses are difficult to describe since they are seriously contaminated by salt bridge artefacts (Chapter II).

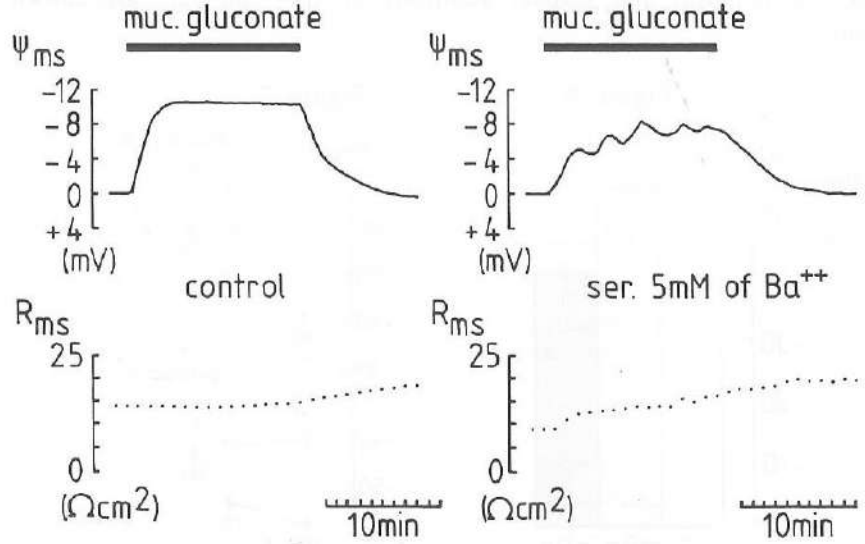

Fig.8: Typical recordings of the transmural potential (ψ_{ms}) and resistance (R_{ms}) responses to mucosal chloride to gluconate substitution in control solutions (left hand side) and in the presence of 5 mM of Ba^{2+} in the serosal bathing solution (right hand side). Resistances were measured at time intervals of 1 min. Reference electrodes were connected to the solutions with salt bridges filled with standard solution (see legends to Figure 5). No corrections are made for liquid junction potential artefacts in these figures.

It is clear, however, that after correction for these artefacts, the new steady state transepithelial diffusion potential is significantly larger than in control solutions (+5.6 ± 0.7 mV vs. +3.3 ± 0.9 mV; n=6) and that this steady state is reached later. A typical example of a response is shown in Figure 8 and is compared to the response in control solutions. The figure also shows the slow oscillations which frequently occur in these responses (cf [23], Paper 3: fig. 5). Note also the difference from Figure 5 in which the response to mucosal chloride substitution in bicarbonate-free media was shown.

d. Transepithelial Cl^--fluxes. Transepithelial Cl^-fluxes were measured with radioactively labeled chloride [3,23] under open-circuit conditions both in Ba^{2+} containing and control solutions (Table 9). Note that net transepithelial chloride transport is slightly reduced while the unidirectional fluxes are significantly increased.

Table 9

	J_{ms}	J_{sm} ($\mu mol/h.cm^2$)	J_{net}
Control	7.64 ± 0.34	4.62 ± 0.24	3.02 ± 0.42
Ba^{2+}	9.34 ± 0.66	7.54 ± 0.54	1.80 ± 0.86
	P<0.05	P<0.001	n.s.

Influence of Ba^{2+} on unidirectional chloride fluxes. The effect of Ba^{2+} was measured by adding bilaterally 5 mM of $BaCl_2$ after four 15 min periods (control) and continuing for another four 15 min periods. Measurements of J_{ms} and J_{sm} were performed on paired strips. Each value is the average of 31 to 36 measurements on 9 strips from 3 fishes.

e. The glucose evoked potentials .It has been reported that Ba^{2+} affects the repolarization phase in the transmembrane glucose evoked potential (Chapter IV, cf [32]). Here we show the averages of eight paired registrations of responses of ψ_{mc} and ψ_{ms} to mucosal glucose addition in control solutions and in Ba^{2+} containing solutions (Figure 9). Note the suppression of the repolarization by Ba^{2+}.

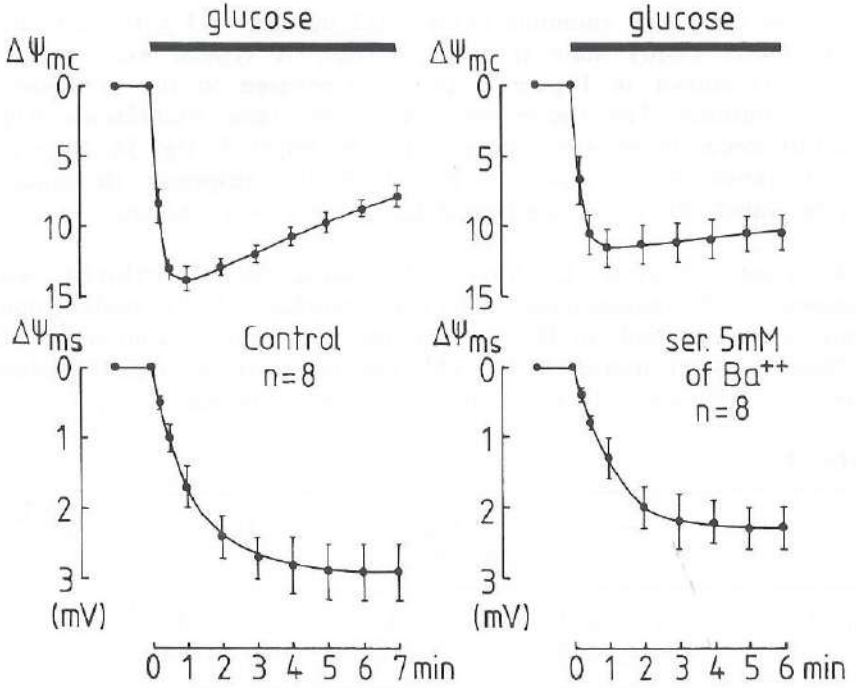

Fig. 9: Average responses of ψ_{mc} and ψ_{ms} to mucosal mannitol for glucose substitution measured under control conditions (left hand side) and in the presence of 5 mM of Ba^{2+} in the serosal bathing solution (right hand side).

Discussion

The double exchange mechanism. The net mucosa to serosa flux of chloride in goldfish intestine under normal conditions, being 3.1 ± 0.44 μmol/h.cm², reduces to only 0.33 ± 0.50 μmol/h.cm² after addition of 0.1 mM of ouabain and to 0.92 ± 0.50 μmol/h.cm² after substitution of sodium by choline [3,23] (cf [14]). This flux should be mainly transcellular because under control conditions the transepithelial potential is negligible (0.0 ± 0.1 mV, Chapter III [1]) and the chloride conductance of the paracellular pathway is small (approx. 10 mS/cm² [4]). Furthermore it is coupled in some way to the active transport of Na^+.

The intracellular accumulation of chloride, its reduction by sodium substitution (Table 1) and the direction of the net chloride flux from mucosa to serosa are strong evidence for the presence of an uphill secondary active chloride transport mechanism in the apical membrane energized in some way by the electrochemical sodium gradient. Such coupling mechanisms were demonstrated indeed in many epithelia and several alternatives were suggested: Na,Cl-symport [12,13,17], Na,K,(2)Cl-symport [22,37] and $Na^+/H^+ + HCO_3^-/Cl^-$-exchange [43,45,52]. The first and second mechanisms are reported to be inhibitible by furosemide or bumetanide [31,53], diuretics which do not seem to be effective in goldfish intestine (Table 2).

The third one supposes the mutual coupling, and possibly even driving [2], of Na^+/H^+ and HCO_3^-/Cl^- antiporters, by the dissociation equilibrium of intracellular H_2CO_3. This coupling is weaker than the obligatory 1:1 coupling of a Na^+,Cl^--symport and may explain why after sodium substitution some accumulation of chloride is still present (Table 1) and why after chloride substitution a_iNa^+ does not drop (Table 3). Further evidence for the existence of this parallel exchange mechanism in goldfish intestine are the relative acidification of the mucosal unstirred layers (Table 4) and the intracellular alkalinisation of 0.4 pHu after chloride substitution (Chapter III) and the intracellular acidification of 0.2 pHu after sodium substitution (reported by Groot et al [24]).

The role of HCO_3^-/CO_2. Although it is difficult to prove the intermediate role of the dissociation equilibrium of H_2CO_3 between the Na^+/H^+ and HCO_3^-/Cl^- antiporters this role is suggested by our experiments:

1. Omission of HCO_3^-/CO_2 in the bathing media causes the intracellular pH to increase by 0.2 pHu [24]. According to Table 5 a_iCl^- does not change while the membrane depolarizes significantly so that $\Delta\tilde{\mu}_{Cl^-}$, the driving force for Cl^- efflux, decreases. The difference between the electrochemical potentials for H^+ and Cl^-, therefore, increases. If the sodium gradient is the ultimate driving force indeed for transepithelial chloride transport, the 'impedance' of the link between $\Delta\tilde{\mu}_{H^+}$ and Cl^- efflux must be increased, which suggests a reduced availability of $a_iHCO_3^-$ from dissociation of H_2CO_3. The same argument applies to Figures 3 and 4 where ($E_{H^+} - E_{Cl^-}$) decreases with respect to E_{Cl^-} with increasing pH_i (or a_iHCO_3).
2. In the absence of HCO_3^-/CO_2, mucosal Cl^- substitution causes an important increase in R_{ms} (Figure 5). Since the partial chloride conductance of the tight junctions is small (<20%) [4], the interspace must contribute to this increase, as the interspace probably

collapses by inhibition of transepithelial solute transport. In the absence, therefore, of HCO_3^-/CO_2, coupling between Na^+ and Cl^- fluxes seems to be tighter, which is expected indeed when intracellular buffering capacity is reduced.

Basolateral anion permeabilities. One of the important outcomes of the calculation of Chapter III is the fact that the basolateral membrane possesses a substantial passive chloride permeability. The question how chloride leaves the cell serosally has been the subject of considerable debate. For example, in Necturus proximal tubule and also gallbladder a low basolateral chloride conductance was found which did not seem to allow sufficient chloride efflux to explain the transepithelial chloride flux [15,25,40,47]. It was necessary, therefore, to postulate that part of the Cl^--efflux across the basolateral membrane is non-rheogenic i.e. coupled to other ions by e.g. K^+,Cl^--symport, HCO_3^-/Cl^--exchange or a neutral Na^+,Cl^--pump [40,42]. Calculation of the basolateral chloride conductance (g_{Cl} = 3.86 mS/cm^2) from the chord conductance formula (Eq.1) and the ionic permeabilities of Table 5 in Chapter III, however, shows that the electrochemical potential for chloride across the basolateral membrane ($\Delta\tilde{\mu}_{Cl^-}/F$ = 30 mV) allows a basolateral efflux of approx. 115 $\mu A/cm^2$ of chloride, whereas the actually measured transepithelial chloride flux [3,23] is equivalent to approx. 90 $\mu A/cm^2$. So as yet there is no need to postulate a specialised transport mechanism in goldfish enterocytes. Baerentsen [2] arrived at a similar conclusion for Necturus gallbladder epithelium and argued that the basolateral chloride conductance is easily underestimated by serosal unstirred layers, the high potassium permeability of the basolateral membrane and, especially, the rheogenicity of the Na/K-pump (which was assumed to be electrically neutral by Reuss [44]). When a bicarbonate permeability of the basolateral membrane is not included in the formulae, a further underestimation is inevitable.

There is a number of reasons why we introduced a $(P_{HCO3^-})_{blm}$. First, from a theoretical standpoint the basolateral membrane should possess, apart from finite ionic permeabilities for K^+ and Cl^-, another permeability because the membrane e.m.f. under chloride-free conditions is much smaller than the Nernst equilibrium potential for K^+.

Whether a non-zero P_{Na+} or a non-zero P_{HCO3^-} is chosen,the conclusion that $(P_{Cl^-})_{blm}$ is large, is not affected. Second, the membrane potential responds to serosal HCO_3^- variations and unilateral HCO_3^-/CO_2 substitutions (Table 7) indicating such a rheogenic pathway for HCO_3^- or H^+ in the basolateral membrane. A third argument in favor of a rheogenic pathway for protons or bicarbonate ions, is that in HCO_3^-/CO_2-free media the proton equilibrium potential (E_{H+}) varies more strongly with the membrane potential (ψ_{mc}) than in HCO_3^-/CO_2-buffered media (see Figure 4). This is what one would expect when the buffering power of the intracellular medium is less than in bicarbonate-containing media. Rheogenic pathways for HCO_3^- or H^+ were also demonstrated by others in the peritubular membrane of rat proximal tubule [8,9,10,54] and salamander proximal tubule [6,34]. It was suggested by Boron and Boulpaep [6] that this basolateral HCO_3^- channel in Ambystoma proximal tubule is formed by a rheogenic $Na^+,2HCO_3^-$-symport but Burckhardt and Frömter [10] could not find evidence for such a symport mechanism in rat proximal tubule. Matsumura et al [34] argued that in Necturus proximal tubule, apart from the current-carrying $Na^+,(2)HCO_3^-/Cl^-$ exchanger postulated by Guggino et al [26], a second rheogenic bicarbonate pathway appears to be present as well. A detailed description of the bicarbonate pathway in goldfish intestine, therefore, cannot be given because the incompleteness of our data does not yet allow definite conclusions nor does it allow a profound comparison with reports from other authors, which suggest the existence of different, possibly even composite, mechanisms in different preparations.

Basolateral potassium recirculation. It is commonly accepted now that potassium accumulation in cells can be attributed to the Na/K-pump [28] which in epithelial cells is exclusively located in the basolateral membrane [51]. It is accepted also that in various leaky epithelia the basolateral membrane generally has a high potassium conductance (e.g [41,29] and Chapter III), which in fact is responsible for the larger part of the negative membrane potential. Considering this, the question arises how potassium is circulated across the basolateral membrane since, in order to cope with the total electrodiffusive efflux from the cell, the pump has to extract more potassium from the interspace than the cell can provide solely by electrodiffusive efflux into that space. The influx of sodium across the apical membrane in absorbing epithelia has been studied extensively in the past decades [16]. These studies have led to the assumption of the different sym- and anti-port mechanisms mentioned above,

responsible for the major part of the influx of sodium into the cell (Chapter VI, [20]), which, in steady state, is transferred almost completely into the interspace by the Na/K-pump.

This massive polar transport may generate electrochemical and osmotic gradients which directly or indirectly are responsible for net potassium absorption. This will be dealt with in more detail in the next chapter. Alternative mechanisms which could supply sufficient amounts of potassium in the interspace involve complicated transport systems in the cellular membranes themselves (Na,K,Cl$^-$- symport in the apical membrane, KCl-symport in the basolateral membrane), but as stated above we have no evidence for the existence of such mechanisms in goldfish intestine. It was suggested also that basolateral potassium conductance in epithelia is directly linked to the activity of the Na/K-pump [30,32,35]. Particularly when pump activity is enhanced during sugar or aminoacid absorption, such a mechanism may serve to supply sufficient extracellular potassium to the pump. Since Ba^{2+} was reported to block this potassium conductance, experiments with Ba^{2+} were carried out to investigate the nature of the potassium conductance and its relation to the Na/K-pump activity.

Bilateral Ba^{2+} application causes cell swelling and an increase in $[Na^+]_i$ (Table 6), suggesting that either the influx of Na^+ is increased or the efflux is decreased. Since the electrochemical driving force for Na^+ is reduced by the decrease of ψ_{mc}, the first possibility is unlikely, and therefore the activity of the Na/K-pump, responsible for Na^+ efflux, is probably reduced. The increases in cell water, $[Cl^-]_i$ and $[Na^+]_i$ and the depolarization of the cell membranes are all factors that are likely to stimulate, rather than inhibit the pump [27,33]. pH_i and $[K^+]_i$ do not change significantly and therefore do not seem to be the determining factors in this reduction. As Ba^{2+} reduces K^+ efflux, particularly into the interspace, it is conceivable that the potassium concentration in the lateral intercellular space is reduced and limits the pump rate (see Chapter IV).

It has been reported for other preparations [5,7,32] that the Ba^{2+}-sensitive potassium conductance is mostly located in the basolateral membrane. This is also true for goldfish enterocytes (Figure 6). On the other hand Ba^{2+}-application at the serosal side affects equally the responses of goldfish enterocytes to mucosal and to serosal potassium elevations (Figure 7). This suggests that mucosal potassium elevation exerts its depolarizing effect also indirectly, namely by permeation through the tight junction, increasing the intercellular potassium concentration and depolarizing the basolateral membrane. It should be pointed out that goldfish intestine is a leaky epithelium with a relatively large paracellular potassium conductance [1,48], so that even small electrochemical gradients may give rise to considerable transjunctional potassium fluxes. This is not the case for the paracellular chloride conductance which is reported to be low [4]. It is therefore remarkable that mucosal chloride substitution in the presence of Ba^{2+} has such a large effect on R_{ms} and ψ_{ms} (Figure 8). Since the unidirectional Cl^--fluxes are also increased it cannot be excluded that paracellular chloride conductance is increased in Ba^{2+} containing solutions at the cost of cation conductance. This would dissipate the osmotic gradient across the tight junctions and consequently reduce water and potassium influx across the mucosal barrier.

Serosal Ba^{2+} application suppresses the repolarization phase in the transmembrane GEP (Figure 9, see also Chapter IV). A similar effect was also reported by Lau et al [32] in Necturus small intestine, and was explained by the hypothesis of Grasset et al [21] that in the repolarization phase an -apparently Ba^{2+}-sensitive- conductance pathway is invoked by the enhanced action of the Na/K-pump (see also [30]). Compared to eg. Necturus small intestine the change in R_m/R_s ratio in goldfish intestine after mucosal glucose addition is only small [1]. Qualitatively, however, our results are in agreement with the findings of Grasset et al [21] in Necturus small intestine, of Frömter et al [18,19] in rat proximal tubule and Messner et al [36] in frog kidney, which all show a gradual increase in basolateral membrane conductance after an initial increase in apical membrane conductance. The opening of a substrate-induced sodium pathway is held responsible for the change in apical conductance. The increase in basolateral conductance is ascribed to an increase in potassium conductance. What elicits this increase is not clear at present. In his review article Lang [30] discussed several possibilities (intracellular pH changes by serosal bicarbonate influx, increase in intracellular aCa^{2+} by Na^+/Ca^{2+}-exchange, changes in a_iK^+), but arrived at the general conclusion that the basolateral potassium conductance is related to the pump activity and, more specifically, is sensitive to the potential difference across the basolateral membrane perse [30]. In our opinion there are two possible links between the apparent potassium conductance and pump activity:

First, according to the Nernst-Planck diffusion equations, basolateral potassium conductance is a function of $a_{is}K^+$ and ψ_{sc} while

the activity of the Na/K-pump is also likely to depend on these parameters. All these parameters are interrelated since the basolateral membrane e.m.f. itself depends to some extent on $a_{is}K^+$. We have presented direct and indirect evidence that in goldfish intestinal epithelium changes take place in $a_{is}K^+$ under various conditions, that influence basolateral potassium recirculation. We suggest, therefore, that, at least in our preparation, $a_{is}K^+$ plays a role in the regulation of basolateral potassium recirculation.

Second, the entry of glucose and sodium into the cell produces increases in a_iNa^+ (Chapter IV) and in cell volume (Chapter VI; [cf.11]) which lead to increased Na/K-pump activity. Salt deposit into the interspace should result in increased transepithelial water transport. This increased water transport can enhance transepithelial potassium flux in different ways: polarization and sweeping-away effects near the mucosal and serosal barriers, solvent drag, the opening of basolateral pores or other channels. In this way osmotic, or possibly electrochemical, gradients generated by the Na/K-pump itself can supply the extracellular potassium to be recirculated by the pump. These concepts will be dealt with further in Chapter VI.

The results presented in this chapter, therefore, led us to the conclusions that:

1. the apical membrane in goldfish enterocytes possesses the so-called double exchange mechanism, postulated also by others [43,45,52];
2. Na^+/H^+-exchange and HCO_3^-/Cl^--exchange are coupled by the dissociation equilibrium of carbonic acid;
3. the basolateral membrane possesses a rheogenic bicarbonate or H^+ pathway and a Ba^{2+}-inhibitible ionic permeability for potassium;
4. the potassium activity in the lateral intercellular space is extremely sensitive to events occurring at the mucosal barrier and may play a role in the modulation of pump activity.

References

1. Albus H, Bakker R, Siegenbeek van Heukelom J (1983) Circuit analysis of membrane potentials changes due to electrogenic sodium-dependent sugar transport in goldfish intestinal epithelium. Pflügers Arch. **398**: 1-9
2. Baerentsen HJ, Christensen O, Thomsen PG, Zeuthen T (1982) Steady state and the effects of ouabain in the Necturus gallbladder epithelium: A model analysis. J. Membrane Biol. **68**: 215-225
3. Bakker R, Dekker K, Zuidema T, Groot JA (1982) Transepithelial Cl^--transport in goldfish Carassius Auratus intestinal mucosa and the effect of theophylline on fluxes and electrophysiology. 4th Conference of the European Society for Comparitive Physiology and Biochemistry, Bielefeld (FRG) 8-11 September 1982
4. Bakker R, Groot JA (1984) cAMP-mediated effects of ouabain and theo-phylline on paracellular ion selectivity. Am. J. Physiol. **246**: G213-G217
5. Bello-Reuss E (1982) Electrical properties of the basolateral membrane of the straight portion of the rabbit proximal renal tubule. J. Physiol. (London) **326**: 49-63
6. Boron WP, Boulpaep EL (1983) Intracellular pH regulation in the renal proximal tubule of the salamander. Basolateral HCO_3^- transport. J. Gen Physiol. **81**: 53-94
7. Brown PD, Sepúlveda FV (1985) Potassium movements associated with amino acid and sugar transport in enterocytes isolated from rabbit jejunum. J. Physiol. (Lond) **363**: 271-285
8. Burckhardt BC, Frömter E (1981) Bicarbonate and hydroxylion permeability of the peritubular cell membrane of rat renal proximal tubular cells. Pflügers Arch. **389**: R40
9. Burckhardt BCh, Cassola AC, Frömter E (1984) Electrophysiological analysis of bicarbonate permeation across the peritubular cell membrane of rat kidney proximal tubule. II. Exclusion of HCO_3^--effects on other permeabilities and of coupled electroneutral HCO_3^--transport. Pflügers Arch. **401**: 43-51
10. Burckhardt BCh, Sato K, Frömter E (1984) Electrophysiological analysis of bicarbonate permeation across the peritubular cell membrane of rat kidney proximal tubule. I. Basic observations. Pflügers Arch. **401**: 34-42
11. Cardinal J, Lapointe JY, Laprade R (1984) Luminal and peritubular ionic substitutions and intracellular potential of the rabbit proximal convoluted tubule. Am. J. Physiol. **247**: F352-F364
12. Duffey ME, Thompson SM, Frizzell RA, Schultz SG (1977) Intracellular chloride activities and active chloride absorption in the intestinal epithelium of winter flounder. J. Membrane Biol. **50**: 331-341
13. Duffey ME, Turnheim K, Frizzell RA, Schultz SG (1979) Intracellular chloride activities in rabbit gallbladder. Direct evidence for the role of the sodium-gradient in energizing "uphill" chloride transport. J. Membrane Biol. **32**: 229-245
14. Field M, Karnaky KJ, Smith PL, Bolton JE, Kinter WB (1978) Ion transport across the isolated intestinal mucosa of the winter flounder, Pseudopleuronectes Americanus. I. Functional and structural properties of cellular and paracellular pathways for Na and Cl. J. Membrane Biol. **41**: 265-

293
15. Fisher RS (1984) Chloride movement across the basolateral membrane of Necturus gallbladder epithelium. Am. J. Physiol. **247**: C495-C500
16. Frizzell RA, Field M, Schultz SG (1979) Sodium-coupled chloride transport by epithelial tissues. Am. J. Physiol. **236**: F1-F8
17. Frizzell RA, Smith PL, Vosburgh E, Field M (1979) Coupled sodium-chloride influx across brush border of flounder intestine. J. Membrane Biol. **46**: 27-39
18. Frömter E (1979) Solute transport across epithelia: What can we learn from micropuncture studies on kidney tubules? J. Physiol. (London) **288**: 1-31
19. Frömter E (1982) Electrophysiological analysis of rat renal sugar and amino acid transport. I. Basic phenomena. Pflügers Arch. **393**:179-189
20. Graf J, Giebisch G (1979) Intracellular sodium activity and sodium transport in Necturus gallbladder epithelium. J. Membrane Biol. **47**: 327-355
21. Grasset E, Gunter-Smith P, Schultz SG (1983) Effects of Na-coupled alanine transport on intracellular K-activities and the K-conductance of the basolateral membranes of Necturus small intestine. J. Membrane Biol. **71**: 89-94
22. Greger R, Oberleithner H, Schlatter E, Cassola AC, Weidtke C (1983) Chloride activities in cells of isolated perfused cortical thick ascending limbs of rabbit kidney. Pflügers Arch. **399**: 29-34
23. Groot JA (1982) Aspects of the Physiology of the Intestinal Mucosa of the Goldfish (Carassius Auratus L). Thesis. MultiCopy Amsterdam
24. Groot JA, Dekker K, Van Riel JW, Zuidema T (1982). Intracellular ion concentrations and pH of stripped mucosa of goldfish (Carassius Auratus) intestine in relation to Cl^-transport. 4th Conference of the European Society for Comparative Physiology and Biochemistry, Bielefeld (FRG), September 8-11, 1982.
25. Guggino WB, Boulpaep EL, Giebisch G (1982) Electrical properties of chloride transport across the Necturus proximal tubule. J. Membrane Biol. **65**: 185-196
26. Guggino WB, London R, Boulpaep EL, Giebisch G (1983) Chloride transport across the basolateral cell membrane of the Necturus proximal tubule: Dependence on bicarbonate and sodium. J. Membrane Biol. **71**: 227-240
27. Hudson, R.L., Schultz, S.G. (1984) Sodium-coupled sugar transport: effects on intracellular sodium activities and sodium-pump activity. Science **224**: 1237-1239
28. Jørgensen PL (1980) Sodium and potassium ion pump in kidney tubules Physiol. Rev. **60**: 864-917
29. Kimura G, Spring KR (1980) Ionic conductance of the cell membranes and shunts of Necturus proximal tubules. In: Current topics in membranes and transport. Vol.13: Cellular mechanisms of renal tubular transport. E.L. Boulpaep (ed). Acad. Press. New York. Chapter 18
30. Lang F, Messner G, Rehwald W (1986) Electrophysiology of sodium coupled transport in proximal tubules. Am. J. Physiol. **250**: F953-F962
31. Larson M, Spring KR (1983) Bumetanide inhibition of NaCl transport by Necturus gallbladder. J. Membrane Biol. **74**: 123-129
32. Lau KR, Hudson RL, Schultz SG (1984) Cell swelling increases a barium-inhibitable potassium conductance in the basolateral membrane of Necturus small intestine. Proc. Natl. Acad. Sci. U.S.A. **81**: 3591-3594
33. Lucas ML, Lei FH, Blair JA (1980) The influence of buffer pH, glucose and sodium ion concentration on the acid microclimate in rat proximal jejunum in vitro. Pflügers Arch. **385**: 137-142
34. Matsumura Y, Cohen B, Guggino WB, Giebisch G (1984A) Electrical effect of potassium and bicarbonate on proximal tubule cells of Necturus. J. Membrane Biol. **79**: 145-152
35. Matsumura Y, Cohen B, Guggino WB, Giebisch G (1984B) Regulation of basolateral potassium conductance of the Necturus proximal tubule. J Membrane Biol. **79**: 153-161
36. Messner G, Oberleithner H, Lang F (1985) The effect of phenylalanine on the electrical properties of proximal tubule cells in the frog kidney. Pflügers Arch. **404**: 138-144
37. Musch MW, Orellana SA, Kimberg LS, Field M, Halm DR, Krasny EJ, Frizzell RA (1982) Na^+-K^+-Cl^--co-transport in the intestine of a marine teleost Nature **300**: 351-353
38. Oberleithner H, Lang F, Wang W, Giebisch G (1982) Effects of inhibition of chloride transport on intracellular sodium activity in distal amphibian nephron. Pflügers Arch. **394**: 55-60
39. Planelles G, Teulon J, Anagnostopoulos T (1981) The effects of Barium on the electrical properties of the basolateral membrane in proximal tubule. Naunyn-Schmiedeberg's Arch. Pharmacol. **318**: 135-141
40. Reuss L (1979) Electrical properties of cellular transepithelial pathway in Necturus gallbladder: III. Ionic permeability of the basolateral cell membrane. J. Membrane Biol. **47**: 239-259
41. Reuss L (1980) Ion conductances and electrochemical potential differences across membranes of gallbladder epithelium. In: Current topics in membranes and transport. Vol.13: Cellular mechanisms of renal tubular transport. E Boulpaep (ed). Acad. Press. New York. Chapter 14
42. Reuss L (1983) Basolateral KCl co-transport in a NaCl-absorbing epithelium. Nature **305**: 723-726
43. Reuss L (1984) Independence of apical membrane Na^+ and Cl^--entry in Necturus gallbladder epithelium. J. Gen. Physiol. **84**: 423-445
44. Reuss L, Bello-Reuss E, Grady TP (1979) Effects of ouabain on fluid transport and electrical properties of Necturus gallbladder. Evidence in favor of a neutral basolateral sodium transport mechanism. J. Gen. Physiol. **73**: 385-402
45. Seifter J, Kinsella JL, Aronson PS (1980) Mechanism of Cl transport in Necturus renal microvillus membrane vesicles (Abstract). Kidney Int. **19**: 257
46. Shiau YF, Fernandez P, Jackson MJ, McMonagle S (1985) Mechanisms maintaining a low pH microclimate in the intestine. Am. J. Physiol. **248**: G608-617
47. Shindo T, Spring KR (1981) Chloride movement across the basolateral membrane of proximal tubule cells. J. Membrane Biol. **58**: 35-42
48. Siegenbeek van Heukelom J (1978) The electrical characteristics of the absorptive goldfish intestinal epithelium. Gastroent. Clin. Biol. **2**: 329
49. Siegenbeek van Heukelom J, Zuidema T (1985) The influence of Ba^{2+} on membrane potential and K^+-induced depolarizations in goldfish intestinal epithelium. J. Physiol. (London) **366**: 92P
50. Spring KR, Kimura G (1978) Chloride reabsorption by renal proximal tubules of Necturus. J. Membrane Biol. **38**: 233-254
51. Stirling CE (1972) Radioautographic localization of the Na pump sites in rabbit intestine. J. Cell Biol. **53**: 704-714

Chapter VI

Epithelial compartments and transepithelial transport

Introduction

In this chapter we shall try to use the results from the previous chapters to provide a more coherent description of the transport modes that are compatible with these data. To that end this chapter is divided in the following sections.

1) Steady state analysis of fluxes for the major ions in the mannitol and glucose steady state, both in the presence and the absence of chloride, and a short discussion of the outcomes of this analysis.
2) A description in qualitative terms of the events in the transient period between the mannitol and glucose steady state, distinguishing the depolarization and repolarization phase.
3) In the first and second section a number of questions are raised concerning the possible existence of gradients of especially Na^+ in the transcellular route and of K^+ in the paracellular route. To find out whether such "cable-like" gradients can be modeled by a distributed description of the processes, a distributed model was implemented. The outcome of that study, as far as we carried it, is that such gradients can be obtained only with parameters that have extreme values. At the same time, however, one may question the choice of such parameters. We arrive at the conclusion, that potassium is reabsorbed by some, as yet unresolved, mechanism.
4) Because the previous sections mainly refer to fluxes, in this section the relation between the glucose-induced electrical changes, especially the repolarization of the membrane after the initial depolarization, and the fluxes is discussed.

SECTION 1: *The steady state fluxes*

From the data on intracellular activities, resistances, potentials of Chapter III and the ionic permeabilities that we derived (Chapter III: tables 5 and 6) net ion fluxes across the cellular membranes can be calculated with the Goldman-Hodgkin-Katz diffusion equation [38] using ion activities instead of concentrations (see Chapter III):

$$I_i = -\frac{P_i z_i F\psi}{RT}\left\{\frac{a_i^o - a_i^i \exp(z_i F\psi/RT)}{1 - \exp(z_i F\psi/RT)}\right\}$$

Steady state fluxes in mannitol solutions.

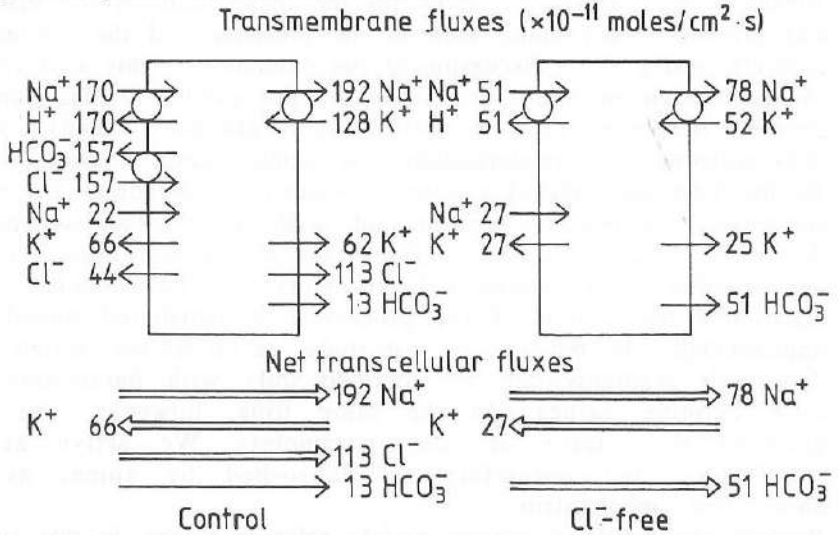

Fig. 1A and 1B: Calculated transmembrane and net transcellular ion fluxes in steady state mannitol conditions in the presence (1A) or absence of chloride (1B). It is assumed that total net current across each of both membranes is zero. Proton flux in one direction and bicarbonate flux in the opposite direction can not be distinguished because of the high permeability of the epithelium for CO_2.

Adding to the calculated electrodiffusional fluxes a parallel exchange of Na^+/H^+ (1:1) and HCO_3^-/Cl^- (1:1) in the apical membrane ([47] and Chapter V) and a rheogenic Na/K-pump (3:2) in the basolateral membrane, a picture can be constructed of ion fluxes if we assume the total transcellular ion fluxes to be electroneutral in the mannitol steady state. Consequently, this applies also to the electrical currents across the individual apical and basolateral membranes.

The transepithelial potential difference, normally being slightly negative (0 to -0.2 mV) in mannitol solutions, can be changed into a small positive one (+0.5 mV) by manipulations where the tight junction cation selectivity is lost ([6], cf.[2], figure 5). The small negative transepithelial potential difference in mannitol solutions is therefore interpreted as the sum of the positive transcellular potential, observed after the manipulation, and a slightly more negative potential, due to a small osmotic salt gradient over the tight junction (< 10 mM). In that case one should include the electrical current, associated with the positive transcellular potential, in the calculations but, being small, it is neglected (see also Chapter III, discussion section 7). In Figure 1A the steady state mannitol situation is shown under normal conditions and in Figure 1B the mannitol situation under chloride-free conditions.

Steady state fluxes during glucose absorption. The fluxes in the steady state glucose condition have been calculated in the same way as in the mannitol situation but without the condition that the total fluxes across each membrane are electroneutral. All measurements were made currentless and transcellular currents should be compensated by currents through the tight junction. From the fact that in the glucose situation $\psi_{ms} \approx E_1 = 2$ mV, one can calculate the charge transfer across the membranes. This makes it possible to calculate the glucose-cotransported Na^+-flux in the mucosal membrane. Maximum values of the glucose-induced sodium influx were calculated by Albus et al from the transient changes in E_m [1,3] to be 4.9 resp. 5.4 μmoles/cm^2.h, the first value being comparable to the value obtained here for the steady state which is the same in the presence and in the absence of chloride (4.6 resp. 4.7 μmoles/cm^2.h).

Inspection of all the above figures leads to the following conclusions and remarks:

1. In the mannitol situation the sodium extruded by the Na/K-pump mainly originates from the electroneutral influx mechanisms responsible for transepithelial salt transport [cf. 16], operating in the apical membrane (88% in control conditions and 65% in chloride-free conditions). So, there is massive transcellular transport of sodium, entering the apical membrane and leaving the cell all along the basolateral membrane.
2. Under all conditions net transcellular potassium flux is apparently directed towards the mucosa, so that potassium is exchanged transcellularly for sodium. Since most of the potassium is extracted

from the interspace this space would be depleted of potassium within about 20 seconds if the potassium was not replenished. The steady state elevation of a_sK^+ in control solutions, described in Chapter IV is therefore rather unexpected and needs clarification.

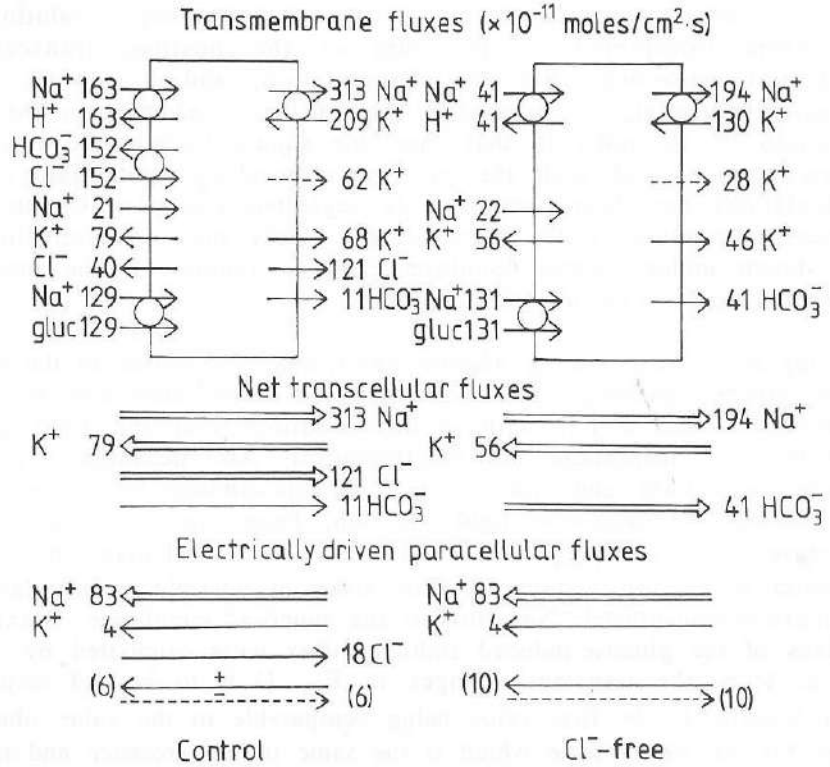

Fig. 2A and 2B: Calculated transmembrane and net transcellular ion fluxes in steady state glucose conditions in the presence (2A) or absence (2B) of chloride. In the figure the dotted arrow in the basolateral membrane represents the K^+-efflux that should be explained by an additional assumption (e.g. an increasing $(P_K)_{blm}$).

3. Both the calculated transcellular fluxes of sodium and of chloride exceed, as expected, the experimentally determined net transepithelial fluxes (J_{Na}= 0.92 nmoles/cm^2.s and J_{Cl} = 0.86 nmoles/cm^2.s [6]). Therefore, even in the mannitol steady state situation there must be transjunctional concentration gradients of Na^+ and Cl^- (under the assumption that E_l = 0 mV, P_{Na} = 100.10^{-6} cm/s and P_{Cl} = 25.10^{-6} cm/s; Chapter III) of approx. +10 mM. The difference in charge transfer is mainly compensated for by K^+-influx from mucosa to interspace. The transjunctional fluxes in the glucose absorbing steady state situation are also electrically driven.
4. In the mannitol situation the activity of the Na/K-pump is about halved by chloride-free solutions, while a_iNa^+ is not diminished. This leads to the question of what limits the pump activity under these conditions.
   It must be noted that in glucose conditions a_iNa^+ increased more with respect to the previous mannitol situation, and did not clearly stabilize (for figure 2B the value after 5 minutes was taken) while, on the other hand, in chloride solutions a_sK^+ is elevated with respect to a_oK^+ and in chloride-free solutions it is not.
5. The steady state fluxes for K^+ into and out of the cell during glucose absorption cannot be reconciled with the ionic permeabilities found for the mannitol control situation. A permanent surplus of K^+-influx would exist. As yet the most appealing explanation is that $(P_K)_{blm}$ has increased, an assumption that has also been put forward by others for other epithelia [7,11,17,22,25,27,32,39].

SECTION 2: *Functional description.*

Application of glucose to the mucosal side of the intestine stimulates the transepithelial transport of salt. Since under open circuit conditions this glucose absorption brings about a serosa-positive transepithelial potential but does not affect the transepithelial resistance, an increase in current, circulating through the epithelium, should take place. In addition, osmotic swelling of the cell by the influx of osmotically active material should be balanced by a supply of salt into the interspace. It was demonstrated that the increase in transepithelial potential was accompanied by a depolarization of the apical membrane, often followed by a partial repolarization. The depolarization is generally associated with the coupled sodium-glucose influx across the apical membrane, the repolarization with cellular processes leading to, or directly related to, activation of the basolaterally located Na/K-pump. The electrical responses are typical for intestine and renal tubule and are amply described, not only for goldfish intestine (Chapter I,IV; [1,2,3,42,43]) but also for different other preparations [8,13,17,22,25,26,32,36,48].

To delineate all interrelated processes that play a role in the glucose-induced electrical responses, the following recapitulation of findings of the studies by us and others [1,3,8,17,22,25,26,32,37] is

presented here in a schematic and condensed form.

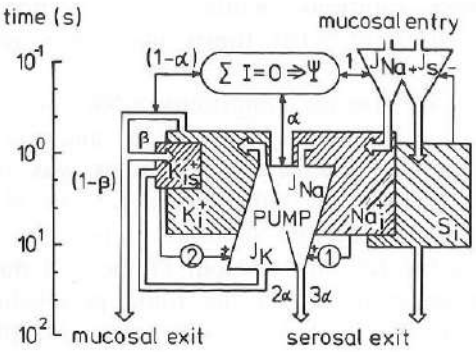

Fig. 3 :Schematic representation of the processes initiated by the coupled influx of sodium and glucose ($J_{Na} + J_S$) across the apical membrane of goldfish enterocytes. The vertical axis is an indicative logarithmic timescale and gives an indication of the delays and time constants of the processes depicted at that coordinate. Ψ represents the membrane potential (ψ_{mc}) which follows from the electro-neutrality principle $\Sigma I = 0$.
If the rheogenic influx of Na^+ is standardized at 1, α represents the fraction of this influx that is compensated electrically by the Na/K-pump and (1 - α) by electrodiffusion. β represents the fraction of the electrodiffusive fluxes entering the interspace in the form of K^+. Anion fluxes are not shown.
K_{is} is the potassium concentration in the interspace, K_i, Na_i and S_i are the intracellular concentrations of potassium, sodium and glucose respectively.
The stochiometry of the pump is indicated as $J_{Na} : J_K = 3 : - 2$; the arrows '1' and '2' represent stimulation of the Na/K-pump by Na_i^+ and K_{is}^+ resp.

Figure 3 depicts the processes contributing to the changes in the membrane potential after the onset of electrogenic Na^+-dependent absorption [40] in relation to their time constants. An indicative logarithmic timescale is plotted along the vertical axis. In most tissues a strict separation in time is not possible.

The first observable process is a depolarization of the mucosal membrane ($\psi_{mc} = \Psi$ in figure 3). Unstirred layers may obscure the response times of the faster membrane processes. The influx of electrical current loads the membrane capacitors (not shown). The time constant of this process is estimated by Frömter [13] to fall in the range of 10 ms. In the schematic representation of figure 3 the response time of the faster membrane processes is taken as 10^{-1} seconds.

The $\Delta\psi_{mc}$ thus induced in this time interval will be stabilized mainly by the following two processes:

A. electrodiffusional fluxes of ions - particularly K^+ - through the cell membranes (fraction 1 - α in figure 3). The fraction of these ionic fluxes entering the interspace in the form of potassium is denoted β.
B. A stimulation of the Na/K-pump as it transfers electrical charge out of the cell (3 Na^+ outwards versus 2 K^+ inwards: fraction α in the figure; [4,35,51]).

The response time of the Na/K-pump is reported to be short enough [12] to react within 1 second to changes in ion concentrations. The actual value of α, therefore, is a function of different parameters (see below), but will, theoretically, become equal to 1/3 in steady state (provided that the pump stoichiometry is 3:2).

The lateral intercellular space is the smallest relevant compartment in the tissue; in stripped goldfish intestine it occupies 4-8 % of the tissue volume while the total extracellular compartment is approximately 16 % [19]. So, the ion concentrations in this space are the first to change significantly, especially the concentrations of potassium: K_{is} in the figure. A depolarization of the mucosal membrane with 13 mV (i.e. $\Delta\psi_{mc}^{depol}$, cf. [1]) accounts for 60.10^{-11} moles/cm^2.s reduction of Cl^--efflux and for an increase of 81.10^{-11} moles/cm^2.s in K^+-efflux, of which 34.10^{-11} moles/cm^2.s (fraction β) is deposited in the interspace. At this moment the deficit of K^+-efflux into the interspace is therefore reduced which makes the intercellular potassium concentration increase initially by 0.28 mM/s. Since the changes in a_sK^+ are in the order of 1 to 2 meq/l, an indicative time for this process can be given as 10 seconds.

The increase in potassium activity ($a_{is}K^+$) may not only contribute to the decrease of ψ_{mc} (not shown) since it counteracts electrodiffusional potassium efflux through the highly conductive basolateral membranes, but also it may stimulate extracellularly the Na/K-pump according to its kinetic properties [14,15,44,45], as long as the original $a_{is}K^+$ is not maximally stimulatory (shown as stimulation "2"). It is possible that this effect is connected to the increase in $(P_K)_{blm}$. Considering other measurements [7,24,39], however, it is not likely that it is the sole source.

The next process is the increase in sodium concentration in the cell, Na_i^+ in figure 3, by the glucose-coupled sodium influx. As expected [3], our results show at 20 to 30 s after the onset of the glucose response a significant increase of the intracellular sodium activity a_iNa^+ (Chapter IV). After one minute, for instance, a_iNa^+ has increased already with approximately 2.5 meq/l. This stimulates the Na/K-pump intracellularly (shown as stimulation "1") but may also, together with the intracellular accumulation of glucose counteract further influx of sodium and glucose. Both effects tend to lead to a hyperpolarization of the membrane as net current influx decreases. It must be realised, however, that these effects apply equally to the chloride-free situation where the repolarization does not occur.

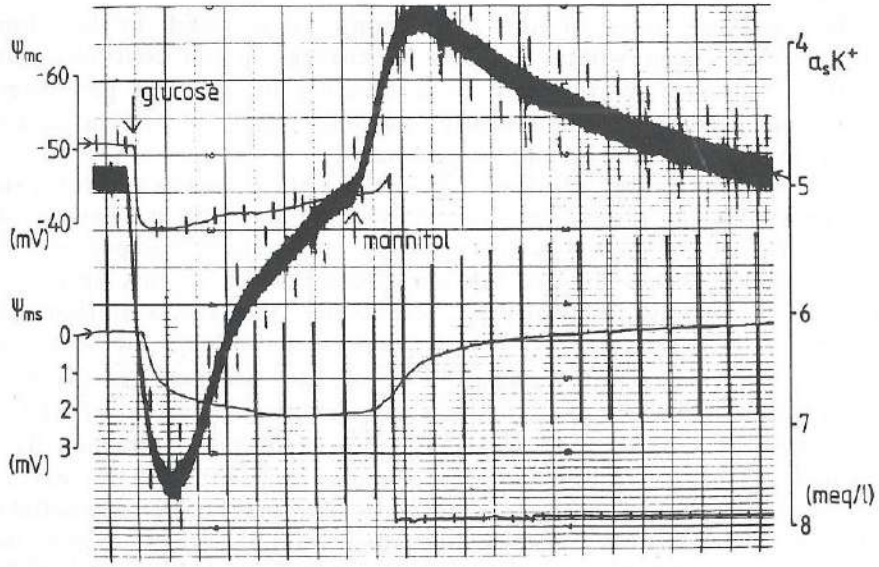

Fig. 4 : Typical simultaneous recordings of the responses of Ψ_{mc}, Ψ_{ms} and a_sK^+ to glucose for mannitol substitution in the mucosal medium, and back. The latter recording forms the signal of a potassium-selective microelectrode placed in the interstitium near the bottom of the cell with respect to the serosal voltage electrode, so that the recorded signal is a direct measure of the changes in a

Two other factors may contribute also to the repolarization. First, a decrease in $a_{is}K^+$ resulting from the stimulation of the Na/K-pump (not shown). Secondly, the increase in basolateral potassium conductance, postulated in other epithelia and mentioned in Section 1, in response to the mucosal sodium influx. These effects appear as a time-dependent increase in factor β.

So, using this pictorial representation (Figure 3) we predict that a_iNa^+ gradually increases after the onset of glucose absorption while $a_{is}K^+$ rises during the depolarization and decays in the repolarization phase. This is in agreement with the actual measurements of the changes in a_iNa^+ and a_sK^+ (see Chapter IV). The time course of a_sK^+, of which a typical example is shown in Figure 4, is considered to be a reflection of the changes in the interspace itself. Later we shall discuss this in more detail.

SECTION 3: *Diffusional analysis*

The observations from the previous paragraph and the additional information from the glucose-evoked responses prompted us to develop a semi-quantitative description aimed mainly at what occurs during the glucose-evoked responses. Whereas the basolateral membrane as a whole absorbs K^+, the same membrane apparently loses K^+ at the most basal side. A possible way to make this understandable is to assume that there are regional differences alongside the membrane. These differences may be interpreted as directly related with the geometry of the cell and its functional polarity.

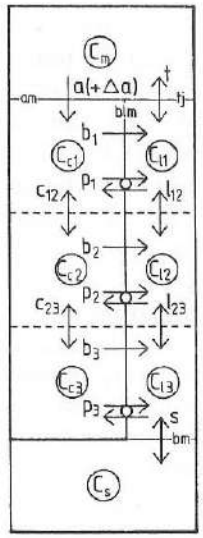

Fig. 5: Compartmental model used to calculate the intracellular sodium profile and the intercellular potassium profile under various conditions (for the meaning of the symbols: see Glossary of symbols)

The compartmental model depicted in Figure 5 was used to calculate the transcellular Na^+ and paracellular K^+ profile for a typical cell under control conditions and the changes in those profiles taking place after the onset of glucose absorption. The model consists of four major compartments: an intracellular compartment (C_c), an intercellular compartment (C_l), a mucosal bulk compartment (C_m) and a serosal bulk compartment (C_s). The latter two are of identical ionic composition. The simplest way to introduce distributive properties is to divide both C_c and C_l in three subcompartments: C_{c1}, C_{c2}, C_{c3}, resp. C_{l1}, C_{l2} and C_{l3}.

C_m is separated from C_{c1} by the apical membrane (am), and from C_{l1} by the tight junctions (tj). C_{ck} is separated from C_{lk} (k=1,2,3) by the basolateral membrane (blm) and C_{l3} from C_s by the basement membrane (bm). Six is the smallest number of subcompartments needed to demonstrate distributed properties in the epithelium. One can increase the number of intermediate compartments but this would not change the model calculations essentially. For convenience all volume and surface values (expressed in liters and cm^2 respectively) are related to one cell and fluxes expressed in units of 10^{-15} mmoles/s, thereby directly producing concentrations in mM and concentration changes in mM/s.

Figures 1 and 2 suggest that one can only get a fully explanatory model if one includes, in addition to the two cations Na^+ and K^+ used here, at least the fluxes and concentrations of H^+, Cl^-, HCO_3^- and in the glucose responses also glucose (cf. Fig. 3). This is not tried in this time-dependent model, for the simple reason that the number of parameters would become excessively large. However, we tried to make the Na^+ and K^+ values correspond with the steady state data, which do include the other ionic fluxes (Cl^--, H^+- and HCO_3^--), compensating the influx of Na^+. In fact the model is made primarily for explaining the responses of the cell to the rheogenic entrance of Na^+ through the Na^+-glucose cotransporter.

Glossary of symbols

C : compartments in the epithelium, identified by indices
k : number referring to the subcompartment, k=1 most apical compartment, k=2 intermediate compartment, k=3 most basal compartment
V_c resp V_{ck} : volume of C_c resp. C_{ck}: cf eq. 9
V_l resp. V_{lk} : volume of C_l resp. C_{lk}: cf. eq. 10

Na_c resp Na_k : Na-concentration in cell. compartment C_c resp C_{ck}
K_l resp K_k: K-concentration in interspace compartment C_l resp C_{lk}
K_o : K-concentration in C_m and C_s: 5.7 mM
a : steady state electrodiff. Na-influx across am
Δa : glucose-coupled Na-influx into C_{c1} across am
b : electrodiffusional K-flux from C_c to C_l
b_k : electrodiffusional K-flux from C_{ck} to C_{lk}
Δb : glucose-induced increase of b
c_{12} resp. c_{23} : Na-diff.rate $C_{c1} \Rightarrow C_{c2}$ and $C_{c2} \Rightarrow C_{c3}$
l_{12} resp. l_{23} : K-diff.rate $C_{l1} \Rightarrow C_{l2}$ and $C_{l2} \Rightarrow C_{l3}$
p : current though Na/K-pump from C_c to C_l(mmoles/s)
p_k : the same between C_{ck} and C_{lk}
(So, active Na-fluxes through the pump are given by 3p resp $3p_k$; the active K-flux by -2p resp. $-2p_k$)
p_{max} : maximal value of p
Δp : glucose-induced increase of p
$K_{m,Na}$ resp. $K_{m,K}$: kinetic parameters (K_m-values) of the Na/K-pump (for intracellular Na resp. extracellular K) (mM)
s : K-flux from C_{l3} into C_s across bm
t : K-flux from C_m into C_{l1} across tj
α : fraction elec. uncomp. Na^+-flux through the Na/K-pump: ratio p:a (in steady state α =1/3)
β : b as fraction of total electrodiff. K^+-efflux ratio b:2p in steady state

Equations

The ion concentrations in the six subcompartments obey the following equations:

(1) $dNa_1/dt = (a - 3p_1 - c_{12})/V_{c1}$

(2) $dNa_2/dt = (c_{12} - 3p_2 - c_{23})/V_{c2}$

(3) $dNa_3/dt = (c_{23} - 3p_3)/V_{c3}$

(4) $dK_1/dt = (t + b_1 - 2p_1 - l_{12})/V_{l1}$

(5) $dK_2/dt = (l_{12} + b_2 - 2p_2 - l_{23})/V_{12}$

(6) $dK_3/dt = (l_{23} + b_3 - 2p_3 - s)/V_{13}$

Further we use (for explanation see below):

(7) $p = p_1 + p_2 + p_3$

with $p_k = \frac{p_{max}/3}{(1 + (K_{m,Na}/Na_k))^3.(1 + (K_{m,K}/K_k))^2}$ (mmoles/s)

(8) $b_k = b/3$

(9) $V_{ck} = V_c/3$

(10) $V_{lk} = V_l/3$

The equations are solved numerically by iterative calculations taking the increments of time $\Delta t = 0.1$ s.

Estimations and assumptions

$V_c = 700.10^{-15}$ l: The volume of a typical cell is calculated by simplifying the cell to a rectangular block with apical surface of 5 µm x 5 µm and height of 70 µm. Further it is multiplied with the estimated value 0.4, to obtain the relative volume freely accessible for diffusion.

$V_l = 140.10^{-15}$ l: The volume of the intercellular space per cell is derived from the above cell dimensions and an interspace width of 0.2 µm extracellular space at the basal end of the cell between cell and basement membrane is neglected.

Na_c and K_l resp. Na_k and K_k: The intracellularly and intercellularly measured single ion activities presented in this thesis were divided by 0.73 (the activity coefficients of Na^+ and K^+ in standard biological solutions) to obtain concentration values. So, Na_c = 15 mM (in normal steady state), a value much smaller than the chemically determined intracellular sodium concentration (approx. 50 mM; see e.g. Table 3). As has been discussed before, this discrepancy is nearly always found on determining a_iNa^+. It is generally assumed that a part of the total intracellular sodium content is sequestrated or compartmentalized.

$a = 220.10^{-15}$ mmoles/s: calculated from the resting Cl^- (and HCO_3)-efflux according to Figure 1A (1.92 nmoles/s.cm^2 serosal epithelial area) and corrected for the serosal to mucosal surface ratio (4.7 [42]) with the additional assumption that approx. 50% of the cells is actually absorbing. This last assumption is based on the experimental evidence from other folded epithelia (resembling goldfish intestine): In hamster intestine, for instance, only the enterocytes in the top third of the villus transport sugars and aminoacids [23]. In rabbit small intestine it was shown that villus tip enterocytes contained over twice the number of sodium pumps found in the crypts [34]. Also the increase in membrane potentials from crypt to villus top in hamster terminal epithelium seems to indicate such an increasing sodium pump activity along the crypt-villus axis [10].

$\Delta a = 175.10^{-15}$ mmoles/s which, calculated like a, is equivalent to 5.5 µmoles/cm^2.h. This is in fact the value given by Albus et al [3] which is an upper estimate and is slightly larger than the value according to Figure 2A, which corresponds to $\Delta a = 134.10^{-15}$ mmoles/s per absorbing cell. In first approximation a(glucose) = a(mannitol) + Δa; small deviations due to changes in membrane potential are neglected (see Figure 1).

$b = \beta(a - p)$ in the steady state the electrodiffusional efflux of K^+ into the interspace, that, together with the the excess cationic efflux through the pump (-p), is balanced by basolateral Cl^- and HCO_3^- efflux. In mannitol steady state condition β would be expected to be approx. 0.5 since $(P_K)_{am} = (P_K)_{blm}$ and $\psi_{mc} = \psi_{sc}$. At the onset of glucose absorption β will be transiently reduced to even 0.25. In the calculations we varied this value in order to see what is the dependency of the outcome on the choice of this parameter (see further discussion).

$c_{k,k+1} = 330.10^{-15}.(Na_k - Na_{k+1})$ (mmoles/s): The diffusion coefficient of NaCl in free solutions ($1.4.10^{-5}$ cm^2/s), is reduced in cytoplasm by a factor 4.5 (in analogy to e.g. the apparent diffusion coefficient D(KCl) in frog ventricular strips [9]). For simplicity it is assumed that the one-dimensional Fick's diffusion equation can be applied: $J = -D.A.\Delta C/\Delta x$.

$l_{k,k+1} = 32.10^{-15}.(K_k - K_{k+1})$ (mmoles/s): The diffusion coefficient of KCl in free solutions ($1.7.10^{-5}$ cm^2/s) is reduced by a factor 4.5 (in analogy to e.g. cortical tissue where the apparent extracellular D(KCl) was decreased by a factor 4 to 6 [31]).

p_{max} is normally chosen between 450.10^{-15} and 900.10^{-15} mmoles/s; $K_{m,Na}$ = 13 mM; $K_{m,K}$ = 1.5 mM: The Na/K-pump is assumed to be rheogenic with coupling ratio 3:-2 [1,51], to be evenly distributed over the basolateral membrane and to obey higher order Michaelis-Menten kinetics [4,29] according to Equation 7. K_m-values and maximum ATP-ase activity (p_{max}) are chosen to fall in the range reported in literature [4,44,45] and to produce proper values for Na_i. Electrical stimulation of the pump [cf. 37] is not included in the model calculations.

$t = 7.10^{-15}.(K_o - K_1)$ (mmoles/s): In Chapter II the P_K of the tight junction was given as 125.10^{-6} cm/s. Since ψ_{ms} is small this value is only corrected for the mucosal to serosal surface amplification (4.7).

$s = 12.10^{-15}.(K_3 - K_o)$ (mmoles/s): Serosal series resistance is approx. 5 Ωcm^2 [1]; if that barrier is not ion-selective t_K = 0.022 or P_K = 200.10^{-6} cm/s which is corrected in the same way as t.

Since the water permeability of the mucosal barrier is large ($P_f > 65.10^{-3}$ cm/s related to serosal surface [42]) and cell swelling remains restricted to less than 5 % (see Table 4), volume corrections are not included in this semi-quantitative model.

Results and discussion

The steady state mannitol situation. In the steady state mannitol situation the total influx of sodium should be equal to the rate of active extrusion as there are no other important efflux mechanisms for sodium. Similarly, the net efflux and active influx of potassium should cancel. As $(P_K)_{am} = (P_K)_{blm}$ approx. 1/3 of the total Na^+-influx is the K^+-flux entering the interspace (b). In total, 2/3 of the total Na^+-influx into the cell enters the interspace as a rheogenic contribution, i.e. is not compensated electrically during the membrane transport-step itself: 1/3 through the pump, and 1/3 through K^+-efflux. In the mannitol steady state this is compensated for by Cl^--(and HCO_3^-)-fluxes. Solving the equations (1) to (10), while varying β between 0.5 and 1.0 and adjusting p_{max} in order to keep Na_i more or less constant, one finds the intercellular potassium concentrations as given in Table 1.

Table 1

β	Na_1 (mM)	Na_2 (mM)	Na_3 (mM)	K_1 (mM)	K_2 (mM)	K_3 (mM)
0.50	15.4	15.0	14.7	1.8	1.7	2.1
0.60	15.4	15.0	14.7	2.5	2.4	2.9
0.70	15.4	15.0	14.7	3.3	3.2	3.6
0.80	15.4	15.0	14.7	4.1	4.0	4.3
0.90	15.4	15.0	14.7	4.9	4.9	5.0
1.00	15.3	14.9	14.7	5.7	5.7	5.8

Calculated steady state concentration profiles for intracellular Na^+ and intercellular K^+ with increasing values of β (see text)

Table 2

D_c(NaCl) (cm^2/s)	D_l(KCl) (cm^2/s)	Na_1 (mM)	Na_2 (mM)	Na_3 (mM)	K_1 (mM)	K_2 (mM)	K_3 (mM)
3.10^{-6}	4.10^{-6}	15.3	14.9	14.7	5.7	5.7	5.8
6.10^{-7}	4.10^{-6}	16.7	14.7	13.7	5.5	5.7	5.9
6.10^{-7}	8.10^{-7}	16.8	14.7	13.7	5.3	5.8	6.0

Calculated steady state concentration profiles for intracellular Na^+ and intercellular K^+ for different intracellular (D_c) and intercellular (D_l) salt diffusion coefficients.

A small increase in K and decrease in Na is observed when comparing the basal and the apical compartments. The value of K_3 is to be associated with a_sK^+, which was measured in Chapter IV. Since $a_sK^+ > a_oK^+$ (a_oK^+ = 4.2 meq/l), K_3 should be larger than K_o (K_o = 5.7 mM). Apparently the calculations produce too low a value for K_3. A simple method to make cable-like features more readily apparent is by lowering the diffusion coefficients in the model.

Table 2 gives the profiles for intracellular free Na and intercellular K calculated under the original assumptions (column 2); under the assumptions that only the intracellular salt diffusion coefficient (D_c(NaCl)) is further reduced by a factor 5 (for β = 1.00) (column 3); or that the intercellular salt diffusion coefficient (D_l(KCl)) is also reduced by this factor (column 4).

Whether such low apparent diffusion coefficients should be

considered realistic is left open, but they produce gradients similar to values that have been reported in rabbit enterocytes [2,52] and in gallbladder epithelial cells [50,51].

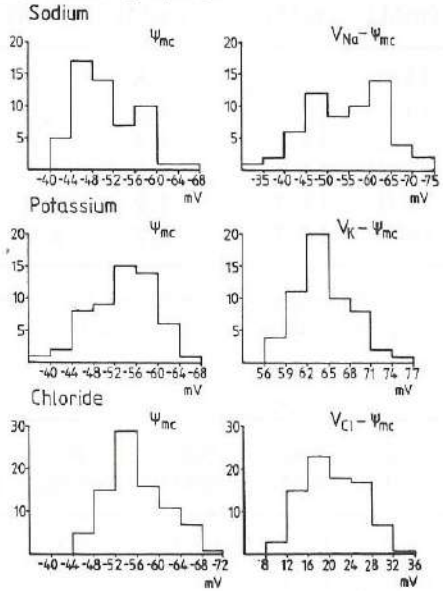

Fig. 6 :Frequency histograms of membrane potential (ψ_{mc}) and the difference of ion potential (V_I) and ψ_{mc} for goldfish epithelial cells. The latter is in fact the uncorrected transmembrane Nernst equilibrium potential and is normally used to calculate intracellular ion activity with the Nicolsky-Eisenman equation (Chapter II: eq. 6). Membrane potentials and ion potentials (V_I) were paired by taking simultaneous or almost simultaneous (within a few minutes) recordings from nearby cells. Number of observations on ordinate refers to the number of impaled cells. Note the differences in scale factors.

Although we have no direct experimental evidence for the existence of a large intracellular sodium gradient in goldfish enterocytes, histograms of intracellular ion potentials ($E_I - \psi_{mc}$) show a rather large spread for the sodium-selective microelectrodes compared to the potassium or chloride-selective and potential recording microelectrodes (Figure 6). This could be due to the fact that such an intracellular activity gradient for sodium exists.

The glucose-induced changes. The sequence of processes following the onset of glucose absorption was already described in figure 3. In contrast to the control situation, the glucose-coupled sodium-influx is

entirely rheogenic, and electroneutrality of fluxes across the individual membranes is no more conserved. Electroneutrality of the cell interior, however, demands that compensatory ionic fluxes start to flow. The two processes that are immediately available for this purpose are enhancement of K^+-efflux and reduction of Cl^--efflux. The increase in electrodiffusional efflux of potassium into the interspace (Δb) is responsible for a transient increase in intercellular potassium concentration (K^+_{is} in Figure 3 and K_I in model).

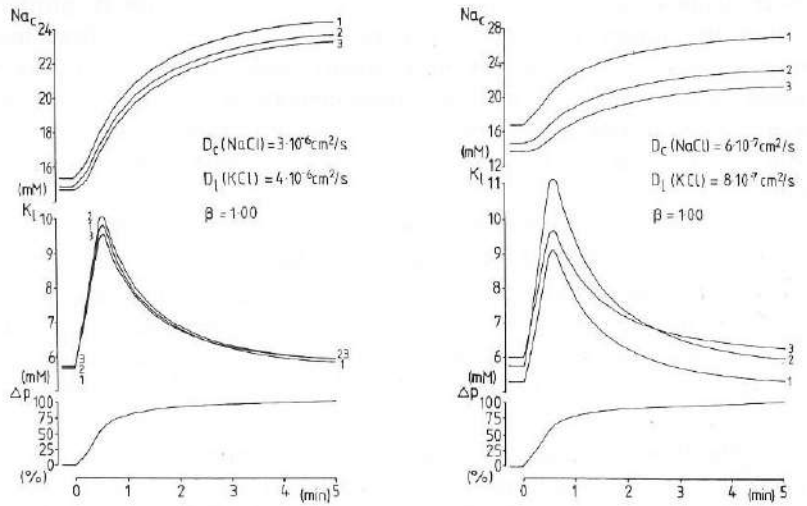

Fig. 7A: Model calculations of the changes in intracellular sodium, intercellular potassium concentrations and pump activity after a step in rheogenic sodium influx across the apical membrane (Δa). Numbers 1, 2 and 3 refer to the subcompartment (see Glossary of symbols). For details see text.
Fig. 7B: The same as 7A, but now assuming a considerable reduction in salt diffusion coefficients D_c(NaCl) and D_I(KCl).

The time constant of this process is much shorter than the time constant of the changes in intracellular sodium concentration.(Na^+_i in Figure 3, Na_c in model). The increase in K_I stimulates the Na/K-pump already to a degree dependent on the setting and kinetic properties of the pump. Electrical stimulation of the pump is not included. Due to the strongly enhanced influx of sodium ions across the brushborder membrane during glucose absorption, the average Na_c increases. The Na/K-pumps are stimulated further by this rise in Na_c and subsequently the Na/K-pump starts to drain more and more K^+ from the interspace. As apical Na^+-influx continues, a new steady state will eventually be reached for Na_c and K_I.

In Figures 7 two examples are shown of model calculations of the changes in intracellular sodium and intercellular potassium profile. Parameter β was taken constant and equal to 1.00. This value is higher than expected from the membrane properties but was taken in order to get a_sK^+ (corresponding to K_3) in the measured range (see further discussion). The difference between 7A and 7B is that in the second figure the diffusion coefficients of NaCl and KCl are reduced, so that steeper gradients are obtained for both profiles (cf. Table 2). In the lower panels the activation of the Na/K-pump (Δp) is plotted. It shows that the pump is quickly stimulated already in the first minute and only slowly approaches its new steady state. If the pump is also stimulated electrically - by the depolarization of the basolateral membrane- this initial stimulation will be even more outspoken.

From these (and similar not shown) results one can conclude the following:

1. It is impossible to model the process in such a way, that values for K_3 are found, equal to or larger than K_0, unless β is close to 1. Intuitive arguments show that this is not amazing. In figures 1 and 2 a deficit of K^+-fluxes into the interspace is observed. The supply of K^+ to the interspace might come from the serosal, the mucosal compartment or the cell. Since a_sK^+ is not reduced, suppletion from the serosal compartment can be excluded.
   If the interspace potassium would be replenished through the tight junctions, a transjunctional K^+ concentration gradient in the control situation would be needed of at least -6 mM ($P_K = 125.10^{-6}$ cm/s; Chapter III). In glucose steady state an even larger, rather unrealistic, gradient would be needed. Moreover, in these cases large aK^+-gradients would exist in the interspace, requiring unrealistically low salt diffusion coefficients (Table 2).
   As a matter of fact we measured (not reported in previous Chapters) an elevated aK^+ in the mucosal unstirred layers (a_mK^+) near the bottom of the interfold space (7.1 $\pm$ 0.6 meq/l equivalent with a concentration of 9.7 $\pm$ 0.7 mM, n=14 in six epithelia vs 4.2 meq/l resp. 5.7 mM in the bathing solution). Similar elevations have also been measured by White [49] in Amphiuma intestine, Cremaschi in hamster intestine [10], Lucas in rat jejunum [30] and Zeuthen in rabbit small intestine (in vivo) [52]. The elevated a_mK^+, however, does not apply to the same region in the epithelium as the a_sK^+ measurements and is therefore irrelevant to the present problem.
   Suppletion of K^+ by the cell would imply that the cell absorbs K^+ from the mucosal compartment. This is only possible if the cell has a facilitated electroneutral K^+-efflux mechanism in the basolateral membranes (for in stance KCl-symport or K^+/H^+-antiport) and an energized K^+-influx mechanism in the apical membrane (for instance Na,K,Cl-symport). If it exists, then the latter mechanism is not sensitive to furosemide or bumetanide (cf. Chapter V). Such symport systems would lead to reabsorption of K^+ and therefore counteract the mucosal efflux suggested by figures 1 and 2. This would correspond to a value of factor β which is larger than 0.5.
2. The question could be raised whether there is some systematic error in the determination of a_sK^+. In order to exclude physico-chemical errors we studied the behaviour of the K^+-sensitive microelectrodes thoroughly (Chapter II), and are confident that such errors can be excluded. Shifts due to the presence of localized negative charges (Donnan-effects) should also have been observed with Na^+- and Cl^--sensitive microelectrodes, and are not. The argument can be raised that the K^+-sensitive microelectrode possibly induced some damage to the epithelium on its way to the basal compartment, and for the time of the measurements a small excess K^+ diffused out of the cells. If, for instance, a small number of damaged cells is supported, through intercellular gap junctions by their neighbouring cells, this might have escaped our observation. With the available measuring techniques we cannot fully exclude this possibility although we do not consider it likely, since the average membrane potential in nearby cells is not affected by the insertion of the potassium-selective microelectrode into the interstitium (Chapter IV).
3. Since the parameter β is reduced immediately after the onset of glucose absorption (mainly by reduction in Cl^--efflux) while it increases again in the repolarization phase (a.o. by the increase in $(P_K)_{blm}$) the size and time course of the transients in Na_c and K_l in Figure 7 will become more in accordance with the experimental results of Chapter IV if β is allowed to vary. Modeling this properly, however, would require more knowledge of the characteristics of the Na/K-pump, which is still the most unspecified component in the description. At this stage we consider it therefore not opportune to do so.

SECTION 4: *The glucose-induced potential changes..*

In the calculations above, electroneutrality was maintained by the condition that influxes and effluxes of electrical charges sum to zero. However, we can also draw conclusions about the glucose-induced depolarization of ψ_{mc}.The actual size of this depolarization depends on what fraction of this current is balanced by the 'shunt' through the other ionic pathways and what through the stimulated Na/K-pump. During the repolarization phase changes occur not only in the pump current (p) and K^+ diffusion (b), but also possibly in the amount of rheogenic entry itself (Δa). Changes in parameters which may be responsible for the repolarization are therefore:

1. net stimulation of the Na/K-pump by increasing a_iNa^+,
2. reduction of Na^+-influx by dissipation of the transmembrane sodium gradient,
3. increase in membrane conductance(s), especially the potassium conductance.

Recently Bakker [5] showed that the change in ψ_{ms} after glucose addition in goldfish intestine is already complete during the depolarization phase of ψ_{mc}. Since both R_{ms} and ψ_{ms} do not change any more, circular current remains constant during the repolarization. This is remarkable since it implies that, if the rheogenic Na/K-pump is stimulated significantly during the repolarization phase, the conductance of the basolateral membrane increases in parallel, which suggests a link between these quantities.

In a recent review article [24] Lang discussed the possible mechanisms leading to the repolarization in proximal tubule cells. Like others [17,39] he ascribed the repolarization mainly to an increase in basolateral membrane conductance, but concluded that the basolateral potassium conductance and the basolateral membrane potential are in fact mutually dependent. In his opinion the $(Na^+ + K^+)$-ATP-ase may be involved, possibly by the fact that both the potassium conductance and the pump activity depend on the intracellular potassium activity. He considers it possible that the basolateral potassium conductance is part of the $(Na^+ + K^+)$-ATP-ase [39] but admits that this idea is still speculative.

The changes in R_m/R_S-ratio after glucose addition are small in goldfish intestine [1], in comparison with many other preparations [8,17,20,22,25,26,32]. The initial decrease in this ratio is usually

interpreted as the opening of a glucose-induced sodium conductance in the apical membrane and the increase in the repolarization phase as the increase in the basolateral potassium conductance [7,17,22,25,32,39], caused by pH_i or a_iCa^{2+} changes, by cell swelling or by activation of the Na/K-pump itself. In goldfish enterocytes, the initial decline in R_m/R_S after exposure to glucose was 18 % and in the repolarization phase this ratio returned to the pre-glucose value [1]. This value fits well within the flux data of section 1 (Figures 1A and 2A), if it is assumed that $(P_K)_{blm}$ increases from 34.10^{-6} cm/s to 65.10^{-6} cm/s and $G_{Na,gluc}$ = 1.35 mS/cm^2.

From our experiments (Chapter IV) it appeared that the repolarization is generally susceptible to manipulations affecting basolateral potassium recirculation: e.g. serosal Ba^{2+} addition and unilateral potassium elevation (see Chapter IV). Also prolonged potassium depletion of the bathing solutions leads to instability and often absence of the repolarization (Albus: unpublished results, cf. [24]). This is indeed compatible with the assumption that the repolarization is at least partly due to an increase in apparent basolateral potassium conductance.

Regarding the role of the Na/K-pump: the repolarization is suppressed by blocking the pump by ouabain [1]. The repolarization, therefore, is certainly linked to the pump activity. As discussed earlier, we measured significant changes in a_sK^+, which, considering the dimensions of the interspace and the diffusion rate of potassium, are likely to reflect the changes in the interspace itself. (It is peculiar that, at least to our knowledge, nobody else in literature, makes reference to the possible role of $a_{is}K^+$ in stimulating the pump in the first phase after the onset of glucose absorption.) The effects of these changes on pump rate and on passive basolateral potassium efflux respectively are opposite and their electrogenic contribution to the membrane potential may therefore cancel partly. Note, however, that under chloride-free conditions the repolarization is usually completely absent (see Chapter IV), while the changes in a_iNa^+ and a_sK^+, except for a small difference in time courses, are similar to those under control conditions. There is no reason to assume that the pump is not stimulated under these circumstances, so that apparently stimulation of the pump does not necessarily lead to hyperpolarization. An explanation for this could be that under chloride-free conditions the intracellular Ca^{2+} [39] is no more in its regulatory traject for the basolateral potassium conductance [39]. This, however, is certainly not the only possible explanation.

The effect of glucose absorption on cell water, Na^+ content and $[Na^+]_i$

According to Lau et al [28] cell swelling per se forms the 'signal' that results in an increase in a Ba^{2+}-sensitive potassium conductance in the basolateral membrane [7,17,27].

Table 3

	cell water/ dry weight (kg/kg)	Na^+ content/ dry weight (mmoles/kg)	$[Na^+]i$ (mM)
Mannitol	3.92 ± 0.03	163 ± 6	49 ± 2
Glucose	4.05 ± 0.04	177 ± 7	52 ± 2
	P<0.01	n.s.	n.s.
Mannitol (Cl^--free)	3.56 ± 0.03	130 ± 3	43 ± 1
Glucose (Cl^--free)	3.66 ± 0.03	143 ± 3	46 ± 1
	P<0.05	P<0.01	P<0.05

Influence of glucose on cell water, Na^+ content and Na^+ concentration in normal and chloride-free solutions. Extracellular space was assumed to be 15% throughout [cf.23]. Each value is the average of 30 strips from 5 fishes.

The conductance increase is therefore considered to be a 'volume regulatory response' to cell swelling. To test whether this is true we investigated the influence of chloride on the glucose-induced cell swelling.

Chemical analysis of mucosal strips (for methods see Chapter III), incubated for half an hour in glucose containing solutions shows that Na content increases, compared to paired control strips incubated in mannitol solutions (Table 3). Since "tissue water/dry weight"-ratio is also increased, $[Na^+]_i$ is not significantly different from control. This applies to the normal situation but the difference in chloride-free conditions is also very small.

We mentioned above that a_iNa^+ increases immediately after the onset of glucose absorption (Chapter IV) and it increases more in Cl^--free media. Cell swelling, reducing again the intracellular sodium concentration, seems to be a secondary response to the influx of

osmotically active material. It apparently occurs more slowly in Cl^--free media. In these solutions the repolarization of the membrane is absent. Considering the time course of $a_{is}K^+$, however, stimulation of the pump is as fast as in normal situations. We therefore suggest that replacing chloride by an impermeable anion leads to a decreased net epithelial solute transport [18,46], because cation flux can not anymore be compensated for by anions. Without a sufficiently large anion flux not only the net basolateral NaCl-flux and volume flow will stop, but also the recirculation of potassium related to this transport.

During serosal Ba^{2+} application the ability to replenish potassium in the interspace is also reduced. Because $[Na^+]_i$ and cell water are increased (Chapters IV and V) one may conclude that the pump is inhibited, but now, in contrast to the Cl^--free situation, ψ_{mc} is decreased. The major factor determining the pump rate under these conditions therefore seems to be $a_{is}K^+$. This suggests a role also for $a_{is}K^+$ in stimulating the Na/K-pump immediately after the onset of glucose absorption. In the second phase this is gradually taken over by a_iNa^+. We suggest that this extracellular stimulation helps the cell to prevent too sudden and large changes in volume in response to mucosal addition of substrate.

Another finding was reported by Lau et al [28], namely that a moderate increase in osmolarity of the substrate containing solution also reduces the spontaneous repolarization. We know that the general effect of mucosal hyperosmolarity is that it produces an increase in transepithelial resistance by narrowing the interspace [33,42,43], an effect that can be reversed partly by mucosal addition of glucose [43]. The interpretation is that increased mucosal sodium influx stimulates the Na/K-pump, which by sodium extrusion increases the osmolarity, and therefore the volume of the interspace. Most probably, therefore, during the repolarization phase an increased water influx takes place into the interspace, partly through the basolateral membrane. Simultaneous increase in mucosal osmolarity stops this water flow and suppresses the repolarization. It appears that in goldfish intestine approximately 30 mosmoles/l is the gradient making up for the concentrative action of glucose absorption. The opposite effect is observed when ouabain is used [2,43]; then glucose absorption - in part reversibly - increases R_{ms}.

So, apparently, the mechanism that causes the repolarization requires a properly functioning Na/K-pump; it needs Cl^- (as permeable anion) to back up Na^+-transport, it needs a substantial K^+-permeability to transfer charge across the basolateral membrane and

it needs a high water permeability (P_f, cf. [42]) to back up the NaCl-transport. Provided that all these prerequisites are available glucose absorption stimulates the Na/K-pump, enhances the solute concentration in the interspace and therefore induces transepithelial water transport. This increased water transport, in its turn, stimulates basolateral potassium efflux by increasing the apparent potassium conductance, thus alleviating the need for K^+ in the interspace.

In conclusion, our experimental results and model calculations are compatible with the following explanations:

1. The repolarization is caused by stimulation of the Na/K-pump.
2. The rheogenicity of the pump itself may contribute to the repolarization, but the main factor seems to be the opening of a potassium conductance pathway associated with the pump.
3. The repolarization is abolished when the basolateral extrusion of cations is not accompanied by the extrusion of anions, normally chloride ions.
4. The repolarization it at least partly due to increased transcellular water transport in response to solute transport.
5. The interspace forms the venting valve that closes and opens the transepithelial transport route.
6. By this function, therefore, the osmotic and - by consequence - hydraulic pressure difference between the cells and the interspace plays the role of "mediator" in transepithelial transport to prevent "flush-through" [39].

References

1. Albus H, Bakker R, Siegenbeek van Heukelom J (1983) Circuit analysis of membrane potentials changes due to electrogenic sodium-dependent sugar transport in goldfish intestinal epithelium. Pflügers Arch. **398**: 1-9
2. Albus H, Groot JA, Siegenbeek van Heukelom J (1979) Effects of glucose and ouabain on transepithelial electrical resistance and cell volume in stripped and unstripped goldfish intestine. Pflügers Arch. **383**: 55-66
3. Albus H, Lippens F, Siegenbeek van Heukelom J (1983) Sodium-dependent sugar and amino acid transport in isolated goldfish intestinal epithelium: Electrophysiological evidence against direct interactions at the carrier level. Pflügers Arch. **398**: 10-17
4. Baerentsen HJ, Christensen O, Thomsen PG, Zeuthen T (1982) Steady state and the effects of ouabain in the Necturus gallbladder epithelium: A model analysis. J. Membrane Biol. **68**: 215-225

5. Bakker R (1986) Feedback on potassium permeability by sodium-glucose cotransport in fish intestine. In: (Eds) F. Alvarado and C.H. van Os. Ion gradient-coupled transport; Inserm. Symp. No. 26. Elsevier Science Publishers, Amsterdam, p. 249
6. Bakker R, Groot JA (1984) cAMP-mediated effects of ouabain and theophylline on paracellular ion selectivity Am. J. Physiol. **246**: G213 -217
7. Brown PD, Sepúlveda FV (1985) Potassium movements associated with amino acid and sugar transport in enterocytes isolated from rabbit jejunum. J. Physiol. (Lond) 363: 271-285
8. Cardinal J, Lapointe JY, Laprade R (1984) Luminal and peritubular ionic substitutions and intracellular potential of the rabbit proximal convoluted tubule. Am. J. Physiol. **247**: F352-F364
9. Cleeman L, Gaughan MJ (1984) Measurements of intracellular ^{42}K diffusion in frog ventricular strips. Pflügers Arch. **401**: 101-103
10. Cremaschi D, James PS, Meyer G, Rossetti G, Smith MW (1984) Developmental changes in intra-enterocyte cation activities in hamster terminal epithelium. J. Physiol **354**: 363-373
11. Diamond JM (1982) Transcellular cross-talk between epithelial cell membranes. Nature **300**: 683-685
12. Forbusch B.III (1982) Time resolved Na efflux with a single turnover of the Na pump in membrane vesicles from dog kidney. J. Gen. Physiol. **80**: 15a-16a
13. Frömter E (1982) Electrophysiological analysis of rat renal sugar and amino acid transport. I. Basic phenomena. Pflügers Arch. **393**: 179-189
14. Gadsby DC (1980) Activation of electrogenic Na^+/K^+ exchange by extracellular K^+ in canine cardiac Purkinje fibers. Proc. Natl. Acad. Sci. USA **77**: 4035-4039
15. Glitch HG, Push H, Venetz K (1976) Effect of Na and K ions on the active Na transport in guinea pig auricles. Pflügers Arch. **365**: 29-36
16. Graf J, Giebisch G (1979) Intracellular sodium activity and sodium transport in Necturus gallbladder epithelium. J. Membrane Biol. **47**: 327-355
17. Grasset E, Gunter-Smith P, Schultz SG (1983) Effects of Na-coupled alanine transport on intracellular K-activities and the K-conductance of the basolateral membranes of Necturus small intestine. J Membrane Biol. **71**: 89-94
18. Green R, White SJ (1984) The effect of luminal anion substitution on fluid absorption from the proximal convoluted tubule of the anaestetized rat. J. Physiol. (Lond) **358**: 109P
19. Groot JA (1982) Aspects of the physiology of intestinal mucosa of the goldfish (Carassius Auratus L), Thesis, University of Amsterdam
20. Gunter-Smith PJ, Grasset E, Schultz SG (1982) Sodium-coupled amino acid and sugar transport by Necturus small intestine: An equivalent electrical circuit analysis of a rheogenic co-transport system. J Membrane Biol. **66**: 25-39
21. Gupta BL, Hall TA, Naftalin RJ (1978) Microprobe measurement of Na, K and Cl concentration profiles in epithelial cells and intercellular spaces of rabbit ileum. Nature **272**: 70-73
22. Hudson RL, Schultz SG (1984) Sodium-coupled sugar transport: effects on intracellular sodium activities and sodium-pump activity. Science **224**: 1237-1239
23. Kinter WB, Wilson TH (1965) Autoradiographic study of sugar and aminoacid absorption by everted sacs of hamster intestine. J. Cell Biol. **25**: 19- 39

24. Lang F, Messner G, Rehwald W (1986) Electrophysiology of sodium coupled transport in proximal tubules. Am. J. Physiol. **250**: F953-F962
25. Lang F, Messner G, Wang W, Paulmichl M, Oberleithner H, Deetjen P (1984) The influence of intracellular sodium activity on the transport of glucose in proximal tubule of frog kidney. Pflügers Arch. **401**: 14-21
26. Lapointe J, Laprade R, Cardinal J (1984) Transepithelial and cell membrane electrical resistances of the rabbit proximal convoluted tubule J. Physiol. **247**: F637-F649
27. Lau KR, Hudson RL, Schultz SG (1984) Cell swelling increases a barium-inhibitable potassium conductance in the basolateral membrane of Necturus small intestine. Proc. Natl. Acad. Sci. USA **81**: 3591-3594
28. Lau KR, Hudson RL, Schultz SG (1986) Effect of hypertonicity on the increase in basolateral conductance of Necturus small intestine in response to Na^+-sugar cotransport. Biochim. Biophys. Acta **855**: 193-196
29. Lew VL, Ferreira HG, Mauro T (1979) The behaviour of transporting epithelial cells. I. Computer analysis of a basic model. Proc. R. Soc. London B. **206**: 53-83
30. Lucas ML, Cannon MJ (1983) Measurement of Na^+ ion concentration in the unstirred layer of small intestine by polymer Na^+ sensitive electrodes. Biochim. Biophys. Acta **730**: 41-48
31. Lux HD, Neher E (1973) The equilibration time course of $[K^+]_o$ in cat cortex. Exp. Brain Res. **17**:190-205
32. Messner G, Oberleithner H, Lang F (1985) The effect of phenylalanine on the electrical properties of proximal tubule cells in the frog kidney. Pflügers Arch. **404**: 138-144
33. Reuss L, Finn AL (1977) Effects of luminal hyperosmolality on electrical pathways of Necturus gallbladder. Am. J. Physiol. **232**(3): C99-C108
34. Rowling PJE, Sepúlveda FV (1984) The distribution of Na^+,K^+-ATPase along the villus-crypt axis in rabbit small intestine. Biochim. Biophys. Acta **771**: 35-41
35. Sackin H, Boulpaep EL (1983) Rheogenic transport in the renal proximal tubule. J. Gen. Physiol. **82**: 819-851
36. Samarzija I, Frömter E (1982) Electrophysiological analysis of rat renal sugar and amino acid transport III. Neutral amino acids. Pflügers Arch. **393**: 199-209
37. Schultz SG (1977) Sodium-coupled solute transport by small intestine: a status report. Am. J. Physiol. **233**: E249-E254
38. Schultz SG (1980) Basic principles of membrane transport. IUPAB Biophysics series 1, Cambridge University press, Cambridge, London, New York, New Rochelle, Melbourne, Sydney.
39. Schultz SG (1981) Homocellular regulatory mechanisms in sodium transporting epithelia: avoidance of extinction by "flush-through". Am. J. Physiol. **241**: F579-F590
40. Schultz SG, Curran PF (1970) Coupled transport of sodium and organic solutes. Physiol. Rev. **50**: 637-718
41. Siegenbeek van Heukelom J (1986) Physiological aspects of absorption and secretion in intestine. Vet. Res. Commun. **10**: 341-354
42. Siegenbeek van Heukelom J, van den Ham MD, Albus H, Groot JA (1981) Microscopical determination of the filtration permeability of the mucosal surface of the goldfish intestinal epithelium. J. Membrane Biol. **63**: 31-39
43. Siegenbeek van Heukelom J, van den Ham MD, Dekker K (1982) The modulation by glucose transport of the electrical responses to hypertonic solutions of the goldfish intestinal epithelium. Pflügers Arch. **395**: 65-70
44. Smith MW (1967) Influence of the temperature acclimatization on the temperature-dependence and ouabain-sensitivity of goldfish intestinal Adenosine Triphosphatase. Biochem. J. **105**: 65-71
45. Soltoff SP, Mandel LJ (1984) Active ion transport in the renal proximal tubule. II. Ionic dependence of the Na Pump. J. Gen. Physiol. **84**: 623-642
46. Tormey JMcD, Diamond JM (1967) The ultrastructural route of fluid transport in rabbit gallbladder. J. Gen. Physiol. **50**: 2031-2060
47. Turnberg LA, Bieberdorf FA, Morowski SG, Fordtran JS (1970) Interrelationship of chloride, bicarbonate, sodium and hydrogen transport in human ileum. J. Clin. Invest. **49**: 557-567
48. Wanke E, Carbone E, Testa PL (1979) K^+ conductance modified by a titratable group accessible to protons from from the intracellular side of squid axon membrane. Biophys. J. **26**: 319-324
49. White JF (1976) Intracellular potassium activities in Amphiuma small intestine. Am. J. Physiol. **231**: 1214-1219
50. Zeuthen T (1978) Intracellular gradients of ion activities in the epithelial cells of the Necturus gallbladder recorded with ion-selective microelectrodes. J. Membrane Biol. **39**: 185-218
51. Zeuthen T (1981) On the effects of Amphotericin B and ouabain on the electrical potentials of Necturus Gallbladder. J. Membrane Biol. **76**: 167-169
52. Zeuthen T, Monge C (1976) Electrical potentials and ion activities in the epithelial cell layer of the rabbit ileum in vivo. In: Kessler M. et al (ed) Ion and enzyme electrodes in Biology and Medecine. Urban and Schwarzenberg, Munich, p. 345

Chapter VII.

General discussion and concluding remarks

In this chapter a number of aspects are discussed which were not dealt with elsewhere.

Ionic activities in leaky epithelia

Regarding the experimental results, the activities and the electrical parameters measured by us in goldfish intestine match well with values reported in the literature for other leaky epithelia. The relative completeness of data obtained by our group allows us to give a more detailed description of the mechanisms involved in transepithelial salt and sugar transport, which may apply also to other, less amply investigated, intestinal preparations.

In Table 1 measurements of ionic activities in goldfish intestine reported in this thesis are compared with values found in the literature for other intestinal preparations. At this time the only other intestinal preparations for which values for the three major ions Na^+, K^+ and Cl^- are reported in literature are amphibian intestines (Armstrong et al [3], White et al [37]). The ionic activities in these preparations are comparable with those found by us but the membrane potential is generally much lower. This may be due to species differences, differences in preparation and perfusion techniques or to differences in compositions of the bathing solutions.

The influence of the bathing solutions is illustrated, for instance, by the observation that the membrane potential depends on the presence of HCO_3^-/CO_2 and varies strongly with pH and $[K^+]$ (Chapter V). This is one of the major problems in comparing results of different authors: the lack of standardization in the composition of bathing solutions. For this reason a column is added indicating -if known- the presence or absence of HCO_3^-/CO_2 in the bathing solutions. Chloride-free media or different pH's are indicated as well.

Table 2 summarizes data found in the literature on the ionic activities in two other leaky epithelia, gallbladder and kidney. Both ionic activities and membrane potentials in goldfish intestine are similar to those found in Necturus gallbladder. This last preparation is thoroughly investigated by a great number of research groups (see

Table 2) and stands often model for transport studies in leaky epithelia.

Table 1

	a_iK^+ (meq/l)	a_iNa^+ (meq/l)	a_iCl^- (meq/l)	ψ_{mc} (mV)	HCO_3^-/CO_2	Ref
Plaice	--	--	38	-34	+	[11]
	--	--	32	-45	+	[20]
Sole	--	--	35	-33	+	[42]
Goldfish	93	11	35	-53	+	[this thesis]
Winter Flounder	--	--	24	-69	+ (pH=8.0)	[10]
	82	--	22	-65	+ (pH=8.0)	[31]
	56	--	35	-44	+ (pH=7.2)	[id]
Bullfrog	80	18	33	-34	-	[3]
	--	--	34	(-34)	+	[4]
	85	14	--	-45	? Cl-free	[23]
Amphiuma	57-73	17	33	-28--37	+	[37]
winter anim.	42	--	19	-37	-	[35,36]
	44	--	--	-40	- Cl-free	[id]
summer anim.	--	--	28-37	-24--33-	-	[id]
Necturus	108	6	--	-35	?	[13]
	67	--	--	-31	-	[15]
	--	12	--	-27	-	[19]
Rabbit						
small intest *(in vivo)*	40-160	--	10-80	-5--35	?	[41]
ileum	--	--	30-80	-5--30	?	[18]
Hamster						
ileum	113	31	--	-35	+	[8]

Intracellular ionic activities of K^+, Na^+ and Cl^- and membrane potentials found in literature for different intestinal preparations. The sixth columnn indicates whether the bathing solutions contain bicarbonate (+) or not (-). When different pH's or chloride-free solutions were used this is indicated.

Since there are also other similarities (e.g. R_m/R_s ratio, tight junction selectivity; [26,28]) it is tempting to draw conclusions by analogy about the membrane properties of goldfish intestinal epithelium. There are, however, several important differences: e.g. gallbladder epithelium has a positive transepithelial potential under control conditions (1-3 mV), does not possess symporters for Na^+ and

sugars or amino acids and has a relatively simple geometry, since the cells are almost cuboidal and are arranged in flatsheets.

Table 2

	a_iK^+ (meq/l)	a_iNa^+ (meq/l)	a_iCl^- (meq/l)	ψ_{mc} (mV)	HCO_3^-/CO_3	Ref.
Gallbladder						
Necturus	49-141	8-39	28-58	-28--56	+	[39]
	87	22	35	-65	+	[29]
	--	11	20	-70	+	[27]
	101	13	25	-67	+	[12]
	99	8	19	-68	-	[id]
	92	15	20	-55	+	[14]
Rabbit	--	--	35	-49	?	[10]
	52	--	--	-61	+	[24]
	73	--	--	-64	+	[17]
Proximal Tub.						
Necturus	59	20	19	-59	?	[21]
	57	30	24	-62	+	[32]
Frog	64	14	14	-57	+	[34]
Triturus	--	--	11	-60	+	[38]
	--	--	22	-60	-	[id]
Rat	--	--	13	-71	+	[7]
Distal Tub.						
Amphiuma	--	12	--	-83	?	[25]
	47	16	--	--	?	[21]
CTAL						
Rabbit	--	--	26	-69	-	[16]

Intracellular ionic activities of K^+, Na^+ and Cl^- and membrane potentials found in litterature for different gallbladder and kidney preparations
See legends of Table 1. CTAL = Cortical Thick Ascending Limb of Henle's Loop.

Like intestine, the proximal tubule transports glucose and aminoacids, but differs strongly in membrane potentials, intracellular activities of potassium and chloride (Table 2) and in geometry of the cells. The tubular shape of the preparation allows quick variations in the test solutions. Unstirred layers are almost absent on both sides of the epithelium. Comparison with intestinal preparations, therefore, can only be made if these differences are taken into account. The simple geometry and the resulting absence of substantial unstirred layers in gallbladder and kidney preparations may be the reason why the membrane potentials are larger then in intestinal preparations. In

this connection it is important to note that reduction of the unstirred layers has always been one of our main concerns. Our technique of stripping off the underlying musculature [2], the choice of our preparation as well as the construction of our perfusion system were aimed at minimizing unstirred layer effects. Low membrane potentials were usually accompanied by unstable recordings and have been discarded for that reason. After inspection they could normally be attributed to a low viability of the preparation or to faults in the measuring or perfusion system.

Ion substitution experiments and the physicochemical properties of the substituents. In Chapter II the results were reported of an investigation into the origin of an artifactual electrode potential change on substitution to solutions containing large organic anions. The conclusion was that one can equally well suppose that the effect per se is due to a reduction in single ion activities of the anorganic cations or that processes near the reference electrode, similar to the Pallman effect in micellar structures, introduce this potential change. We concluded, however, that for accurate measurements one can get around this difficulty of interpretation by using reversible cation-selective electrodes as reference electrode in analogy to the Ag/AgCl electrode commonly used during cation substitution experiments. In this way not only are transient phenomena no longer obscured by electrode artefacts (see Chapter II: Figure 1) but also steady state measurements can be performed without a correction for those artefacts. The latter statement can be substantiated as follows:

In the analysis of the chloride substitution experiments in Chapter III potentials and conductances were assumed to obey the Nernst-Planck diffusion equations. The zero-current potentials were described by the extended form of the Goldman-Hodgkin-Katz equation (see Chapter III: Eq. A1-A6). The electrode potentials of the ion-selective microelectrode are given by the Nicolsky-Eisenman equation (Chapter II: Eq. 6). According to those equations a cation-selective electrode, as a reference electrode, and the cell membrane both behave as cation-selective membranes, so that the contribution of a changing single cation activity (or activity coefficient) is cancelled to a degree relative to the permselectivities of both membranes (and for unilateral substitutions also to the R_m/R_s-ratio of the electrical equivalent circuit). Artefacts inherent in the use of liquid junction type reference electrodes are thereby excluded.

An example can illustrate this more adequately: if the single ion activities of the cations in chloride-free solutions were reduced by the theoretical maximum of 15 % (corresponding to -4 mV change in electrode potential), and a cation-selective electrode is used as a reference electrode, the permeabilities of the apical membrane as calculated for goldfish intestine in Chapter III do not change ($(P_{Cl}/P_K)_{am}$ = 0.21 and $(P_{Na}/P_K)_{am}$ = 0.025). The calculated permselectivity of the basolateral membrane (which is less cation-selective) changes only slightly: $(P_{Cl}/P_K)_{blm}$ from 0.59 to 0.60 and $(P_{HCO3}/P_K)_{blm}$ from 0.23 to 0.19 (see Chapter III: Table 6). This means that different interpretations do not lead to significantly different conclusions about the permselectivity of the membranes. If no correction had been made for either a liquid junction artifact or a reduction in single ion activity, the membrane potential in chloride-free solutions would have been overestimated by -4 mV, leading to a different permselectivity of the membranes: $(P_{Cl}/P_K)_{am}$ changes from 0.21 to 0.25, $(P_{Na}/P_K)_{am}$ from 0.025 to 0.016; $(P_{Cl}/P_K)_{blm}$ does not change significantly (0.59) and $(P_{HCO3}/P_K)_{blm}$ decreases from 0.23 to 0.15.

Secondary active transport in leaky epithelia. There is now ample evidence that transport of a large number of ions and organic solutes in absorptive epithelia is mediated by membrane-bound 'secondary active' transport mechanisms energized by the electrochemical sodium gradient, which itself is generated by active extrusion of sodium by the Na/K-pump. The number and complexity of such transport systems postulated in recent literature are already quite impressive and are still growing. We are somewhat reluctant, however, to postulate too easily such a transporter by analogy with similar mechanisms in other preparations as long as this is not supported by direct experimental evidence or by other independent techniques. Therefore we did not want to make our conclusions dependent on the question whether, for instance, the sym- and antiporters for KCl and rheogenic bicarbonate transport in the basolateral membrane exist (see Chapters III and V). The different mechanisms for NaCl and proton transport in the apical membrane, however, are well established now and have been tested with a variety of experimental techniques. This is also true for sodium-glucose and aminoacid symport in the apical membrane. In the models presented in Chapters III and VI we therefore restricted ourselves to these two 'secondary active' mechanisms and included further an active exchange pump (Na/K-pump) and 'passive' transport of water, ions and solute.

Rheogenicity of the Na/K-pump. Rather essential in our analysis (Chapter III) is the assumption that the basolateral Na/K-pump is rheogenic, i.e. that it carries net charge out of the cell. This assumption is derived from the ouabain experiments in glucose-transporting tissue by Siegenbeek and Bakker [30] and Albus et al [1; Fig.4, Table 3] which show a rapid initial depolarization of approx. 10 mV in ψ_{mc} after ouabain poisoning. In non-transporting tissue the effect is smaller and fuses with other depolarizing processes, such as the increase of the intracellular potassium concentration. A prudent estimation of the initial change would be approx. 5 mV.

This depolarization would be in accordance with the present analysis (see Chapter III) which accounts for a rheogenic contribution of 5.2 mV in E_a (i.e. the Goldman-Hodgkin-Katz potential for the apolar cell; Chapter III: Eq. 4) or 8.9 mV in E_s, provided that the pump ratio is r = 3/2 as in excitable tissues (e.g. [33], cf. [40]). Reuss et al [28] argued that the pump in Necturus gallbladder is not rheogenic because they did not find an immediate depolarization after ouabain poisoning. This is in contrast to Baerentsen et al [5] who found a clear depolarization (6.3 mV within 10 s) in the same preparation if connective tissue was carefully removed. Furthermore Reuss' arguments depend strongly on the calculation of the net transcellular Na flux from fluid transport measurements for which values are reported in the range of 3-25 $\mu l.cm^{-2}.h^{-1}$ [5], and on the value of the basolateral membrane resistance estimated from the apparent membrane resistance ratio, a value taken four times lower by Baerentsen et al [5] in order to fit the other circuit parameters.

Osmolarity in the intercellular compartment. The analysis of the chloride substitution experiments in Chapter III led us to the assumption that E_l is negligible. On the other hand we suggested (Chapter VI) that a standing salt concentration gradient in the interspace -as in the model of Diamond and Bossert [9]- is responsible for sustained transepithelial water transport. Since the tight junctions are cation-selective a transjunctional salt concentration gradient would give rise to a small serosa-negative diffusion potential. The presence of such a diffusion potential is suggested indeed by the experiments of Bakker and Groot [6] who increased the paracellular chloride conductance, by the application of theophylline or ouabain (see also Albus et al [2]). In order to explain this apparent contradiction it is necessary to realise that the tight junction potential is a diffusion potential between the mucosal solution and the apical

side of the interspace. The mucosal solution may be well stirred at the top of the folds but it is not between the folds, especially low down in the interfold space where the potassium activity is elevated substantially (Chapter VI). In addition to this, E_l also reflects the contributions of gradients in the interspace itself while the experimental ψ_{ms} may further contain the series contributions of gradients within the mucosal solution and across the serosal barrier. The potassium elevation in the mucosal unstirred layer (Chapter VI) in particular counteracts the effect of intercellular hyperosmolarity. Using the Goldman-Hodgkin-Katz equation with a permselectivity for the tight junctions as given in Chapter III (Table 6) one can calculate easily that each meq/l of mucosal potassium elevation compensates (in E_l) for roughly 2 mOsm of intercellular hyperosmolarity. As a consequence, an osmolarity gradient across the tight junctions does not necessarily lead to a non-zero E_l. On the other hand, the assumption of a serosa-negative E_l, which is abolished by bilateral chloride substitution leads to large discrepancies in calculated and measured R_m/R_s-ratio (see Chapter III). This makes us confident that our assumption that E_l is negligible, is correct.

Glucose evoked responses and the properties of the Na/K-pump. The electrical phenomena associated with glucose transport have been discussed extensively in the work of Albus et al [1,2] and in Chapters IV and VI of this thesis. We concluded that the transmembrane GEP is not simply the sum of two successive rheogenic events, one in the apical membrane and one in the basolateral membrane, shunted by the resistances of the equivalent electrical network of Chapter I (Figure 4). We can not describe the sequence of processes quantitatively mainly because we still do not know exactly how the Na/K-pump is kinetically stimulated, how it behaves electrically and what other ionic pathways are connected with it [cf. 22]. Apart from this missing link, which demands a more multidisciplinary investigation, we were able to identify at least qualitatively the succession of processes responsible for most of the major experimental results on glucose absorption reported in this thesis : the transient changes in ionic activities, both intracellular and extracellular, and the disappearance of the repolarization under various experimental conditions.

References

1. Albus H, Bakker R, Siegenbeek van Heukelom J (1983) Circuit analysis of membrane potentials changes due to electrogenic sodium-dependent sugar transport in goldfish intestinal epithelium. Pflügers Arch. **398**: 1-9
2. Albus H, Groot JA, Siegenbeek van Heukelom J (1979) Effects of glucose and ouabain on transepithelial electrical resistance and cell volume in stripped and unstripped goldfish intestine. Pflügers Arch. **383**: 55-66
3. Armstrong WMcD, Bixenman WR, Frey KF, Garcia-Diaz JF, O'Regan MG, Owens JL (1979) Energetics of coupled Na^+ and Cl^- entry into epithelial cells of bullfrog small intestine. Biochim. Biophys. Acta **551**: 207-219
4. Armstrong WMcD, Youmans SJ (1980) The role of bicarbonate ions and of cAMP in chloride transport by epithelial cells of bullfrog small intestine. Ann. N. Y. Acad. Sci. **341**: 139-155
5. Baerentsen HJ, Christensen O, Thomsen PG, Zeuthen T (1982) Steady states and the effects of ouabain in Necturus gallbladder epithelium: A model analysis. J. Membrane Biol. **68**: 215-225
6. Bakker R, Groot JA (1984) cAMP-mediated effects of ouabain and theophylline on paracellular ion selectivity. Am. J. Physiol. **246**: G213-G217
7. Cassola AC, Mollenhauer M, Froemter E (1983) The intracellular chloride activity of rat proximal tubular cells. Pflügers Arch. **399**:259-265
8. Cremaschi D, James PS, Meyer G, Rossetti C, Smith MW (1984). Developmental changes in intra-enterocyte cation activities in hamster terminal ileum. J. Physiol. **354**:363-373
9. Diamond JM, Bossert WN (1968) Functional consequences of ultrastructural geometry in "backwards" fluid-transporting epithelia. J. Cell Biol. **37**: 694-702
10. Duffey ME, Turnheim K, Frizzell RA, Schultz SG (1979) Intracellular chloride activities in rabbit gallbladder. Direct evidence for the role of the sodium-gradient in energizing "uphill" chloride transport. J. Membrane Biol. **32**: 229-245
11. Ellory JC, Ramos M, Zeuthen T (1979) Cl^--accumulation in the plaice intestinal epithelium. J. Physiol. (London) **287**:12P
12. Fisher RS, Spring KR (1984) Intracellular activities during volume regulation by Necturus gallbladder. J. Membrane Biol. **78**:187-199
13. Garcia-Diaz JF, O'Doherty J, Armstrong WMcD (1978) Potential profile, K^+ and Na^+ activities in Necturus small intestine. Physiologist **21**:41
14. Giraldez F (1984) Active sodium transport and fluid secretion in the gall-bladder epithelium of Necturus. J. Physiol. **348**: 431-455
15. Grasset E, Gunter-Smith P, Schultz SG (1983) Effects of Na-coupled alanine transport on intracellular K-activities and the K-conductance of the basolateral membranes of Necturus small intestine. J. Membrane Biol. **71**: 89-94
16. Greger R, Oberleithner H, Schlatter E, Cassola AC, Weidtke C (1983) Chloride activities in cells of isolated perfused cortical thick ascending limbs of rabbit kidney. Pflügers Arch. **399**:29-34
17. Gunter-Smith PJ, Grasset E, Schultz SG (1982) Sodium-coupled amino acid and sugar transport by Necturus small intestine: An equivalent electrical circuit analysis of a rheogenic co-transport system. J. Membrane Biol. **66**: 25-39
18. Henriques de Jesus C, Ellory JC, Smith MW (1975) Intracellular chloride activities in the mucosal epithelium of rabbit terminal ileum. J. Physiol. (London) **244**:31P-32P
19. Hudson, R.L., Schultz, S.G. (1984) Sodium-coupled sugar transport: effects on intracellular sodium activities and sodium-pump activity. Science **224** : 1237-1239
20. Katz U, Lau KR, Ramos MMP, Ellory JC (1982) Thiocyanate transport across fish intestine (Pleuronectes platessa). J. Membrane Biol. **66**: 9 -14
21. Khuri RN (1979) Electrochemistry of the nephron. In (Giebisch G, Tosteson DC, Ussing HH, Eds) Membrane Transport of Biology, Vol IVA, Springer, Berlin, Chapter II
22. Lang F, Messner G, Rehwald W (1986) Electrophysiology of sodium coupled transport in proximal tubules. Am. J. Physiol. **250**: F953-F962
23. Lee CO, Armstrong WMcD (1972) Activities of sodium and potassium ions in epithelial cells of small intestine. Science **175**:1261-1264
24. Meyer G, Henin S, Cremaschi D (1981) Cell K^+ activity in rabbit gallbladder. Bioelectr. Bioenerg. **8**:576-579
25. Oberleithner H, Lang F, Wang W, Giebisch G (1982) Effects of inhibition of chloride transport on intracellular sodium activity in distal amphibian nephron. Pflügers Arch. **394**:55-60
26. Os CH van, Slegers JFG (1975) Electrical potential profile of gallbladder epithelium. J. Membrane Biol. **24**:341-363
27. Reuss L (1984) Independence of apical membrane Na^+ and Cl- entry in Necturus gallbladder epithelium. J. Gen. Physiol. **84**:423-445
28. Reuss L, Bello-Reuss E, Grady TP (1979) Effects of ouabain on fluid transport and electrical properties of Necturus gallbladder. Evidence in favor of a neutral basolateral sodium transport mechanism. J. Gen. Physiol. **73**:385-402
29. Reuss L, Weinman SA (1979) Intracellular ionic activities and transmembrane electrochemical potential differences in gallbladder epithelium. J. Membrane Biol. **49**:345-362
30. Siegenbeek van Heukelom J, Bakker R (1979) Electrogenic processes in membranes of the goldfish intestine. Gastroenterol. Clin. Biol. **3**: 170
31. Smith PL, Welsh MJ, Stewart CP, Frizzell RA, Orellana SA, Field M (1981) Chloride absorption by the intestine of the winter flounder Pseudopleuronectes americanus: Mechanism of inhibition by reduced pH. Bull. M.D.I.B.L. **20**: 96-101
32. Spring KR, Kimura G (1978) Chloride reabsorption by renal proximal tubules of Necturus. J. Membrane Biol. **38**: 233-254
33. Thomas RC (1972) Electrogenic sodium pump in nerve and muscle cells. Physiol. Rev. **52**: 563-594
34. Wang W, Messner G, Oberleithner H, Lang F, Deetjen P (1984) The effect of ouabain on intracellular activities of Na^+, K^+, Cl^-, H^+ and Ca^{2+} in proximal tubules of frog kidneys. Pflügers Arch. **401**:6-13
35. White JF (1976) Intracellular potassium activities in Amphiuma small intestine. Am. J. Physiol. **231**:1214-1219
36. White JF (1977) Activity of chloride in absorptive cells of Amphiuma small intestine. Am. J. Physiol. **232**:E553-E559
37. White JF, Burnup K, Ellingsen D (1986) Effect of sugars and aminoacids on

amphibian Cl^- transport and intracellular Na^+, K^+ and Cl^- activity. Am. J. Physiol **250**: G109-117
38. Yoshitomi K, Hoshi T (1983) Intracellular Cl^- activity of the proximal tubule of Triturus kidney: dependence on extracellular ionic composition and transmembrane potential. Am. J. Physiol. **245**:F359-F366
39. Zeuthen T (1978) Intracellular gradients of ion activities in the epithelial cells of the Necturus gallbladder recorded with ion-selective microelectrodes. J. Membrane Biol. **39**: 185-218
40. Zeuthen T (1981) On the effects of Amphotericin B and ouabain on the electrical potentials of Necturus Gallbladder. J. Membrane Biol. **76**: 167-169
41. Zeuthen T, Monge C (1976) Electrical potentials and ion activities in the epithelial cell layer of the rabbit ileum in vivo. In: Kessler M et al, (ed) Ion and enzyme electrodes in Biology and Medicine. Urban and Schwarzenberg, Munich, p 345
42. Zeuthen T, Ramos M, Ellory JC (1978) Inhibition of active chloride transport by piretanide. Nature (London) **273**:678-680

Summary

One of the most important properties of intestinal epithelium is that it is able to transport considerable amounts of salts and nutrients from the intestinal lumen towards the blood against a concentration gradient. This transport goes along with water transport in order to maintain the tonicity of the transported fluid. Much is known already, albeit mainly qualitatively, about the mechanisms reponsible for the coupling. The pivoting element in all explanations of active transepithelial transport is the action of the so-called Na/K-pump, or more biochemically described ($Na^+ + K^+$)-ATPase located in the basolateral membrane of the enterocyte. This pump maintains the unequal distribution for sodium and potassium across the cell membrane.

Specialized coupling mechanisms in the membranes utilize the energy accumulated in the concentration differences (i.e. the chemical potential differences across the membrane) in order to transport sugars, amino acids and ions either into or out of the cell. The polarity of these mechanisms in the different membrane aspects of the enterocyte results in transcellular transport. In that respect the high potassium permeability of the cell membranes is of importance, since it is ultimately the origin for the second driving force available: the potential across the cell membrane. This membrane potential provides the driving force for rheogenic transport, i.e. transport that by its own action carries electrical charges across the membrane. Finally, local differences in osmolarity, both intracellular and extracellular, resulting from solute transport, provide the osmotic pressure differences which are the driving force for water transport.

In this thesis electrophysiological experiments and model calculations are reported which are aimed to characterize and quantify a number of the above mechanisms for energy transduction in goldfish intestine. A number of the experiments were carried out with ion-sensitive microelectrodes. This thesis studies in detail the transport of glucose and chloride and should be considered a part of the research program of the group Membrane Physiology, with the following publications: H. Albus [1-5], R. Bakker [6-9], J.A. Groot [10-16] and J. Siegenbeek van Heukelom [17-22].

In **Chapter 1** a brief description is given of the preparation followed by a review of the historical background of our research. Three major lines of research can be distinguished: the development

of models for water transport, for sugar and amino acid transport and, more recently, for chloride transport. Within this historical context the possibilities for electrophysiological work with conventional and ion-selective microelectrodes are discussed and the aims of the present investigation are summarized as follows:

- the determination of permeabilities of the plasma membranes by measurement and analysis of membrane potentials and intracellular ion activities, both under control conditions and during unilateral and bilateral ion substitutions;
- the identification of ion fluxes, resulting from active rheogenic transport of sodium with glucose and of the coupling mechanisms between mucosal cotransport systems and the basolateral Na/K-pump. This is done by measurement and analysis of membrane potentials, intracellular and interstitial ion activities, before, during and after the onset of glucose absorption under various experimental conditions.

In addition to these aims it became necessary to investigate experimentally and theoretically what the ion-selective electrodes are actually measuring, both in the cell and in the biological solutions used by us, in order to eliminate, if possible, artefacts and ambiguities in interpretation. This chapter is completed by a section about materials and techniques and a glossary of symbols.

In **Chapter 2** one of the above mentioned ambiguities is scrutinized in order to explain the change of about - 4 mV observed when potentials were measured with cation selective microelectrodes with respect to a salt bridge during substitutions of chloride by organic anions (like glucuronate or gluconate). Such potential changes are equivalent to a decrease of about 15 % in the apparent cation activity without a measurable change in concentration. Measurements of the osmotic values of these solutions (both with freezing point depression and by vapor pressure) did not provide evidence to explain this phenomenon as due to ion association. Electrode artefacts near the ion selective microelectrode could also be excluded. In consequence, the effect must come from the junction of the reference electrode or from a decrease in ion activity coefficient that cannot be explained by any existing theory. There are no thermodynamical grounds for a choice between these two alternative explanations, though it is unlikely that the last explanation is the only one. Therefore, the measurement of the potassium activity for instance in chloride-free solution is always wrought with uncertainties. The actual conclusion for the measurements of membrane potentials was that during chloride substitutions a salt bridge connection between the experimental solutions and the reference electrode is not the best approach. One can better use a cation selective electrode as reference or carry out appropriate corrections.

Chapter 3 describes a comprehensive study of the permeability properties of the apical and basolateral cell membranes. Measurements are presented of membrane potentials, transepithelial potentials and intracellular ion activities of Na^+, K^+ and Cl^-. Values for the transepithelial resistance and resistance ratio of apical and basolateral membrane (R_m/R_s) under control conditions are also presented. Similar measurements were executed in bilateral chloride-free solutions, while electrical measurements during unilateral chloride substitutions are also included. Cell volume, intracellular pH and ion concentrations of Na^+, K^+, Cl^- were determined under control and bilateral chloride-free conditions. Finally, intracellular chloride activities and concentrations were measured during unilateral chloride-substitutions.

From the analysis of these results, using electrical equivalent circuits and, for the estimation of the permeability ratio's an adapted version of the Goldman-Hodgkin-Katz equation, one can conclude that an electroneutral chloride influx exists in the apical membrane. The calculations lead to the surprising conclusion that the relative permeability of basolateral membrane for chloride is large. The results also substantiate the existence of a considerable permeability for bicarbonate in the basolateral membrane.

The membrane potential of goldfish intestinal epithelium responds in a very characteristic manner to mucosal glucose addition. This response consists of a fast depolarization followed by a slower repolarization. During this response a permanent increase in intracellular Na^+-activity is measured. At the same time a transient elevation of K^+-activity in the submucosal (interstitial) space just underneath the cellular layer is observed. In normal, chloride-containing solutions, the K^+-activity measured there appears also to be elevated permanently with respect to the bathing solutions. These measurements, as well as the measurements of the intracellular K^+- and Cl^--activities are presented in **Chapter 4**.

Omission of chloride from the bathing media leads to a considerable hyperpolarization and, at the same time, reduction of the submucosal K^+-activity. Now, addition to the mucosal medium of glucose does not induce a repolarization, but intracellular Na^+-activity increases more and the transient elevation of K^+-activity in the

interstitial space still occurs. Both serosal addition of Ba^{2+} (5 mM), and unilateral increase of the K^+-activity depolarize the membrane and suppress the repolarization.

The discussion in this chapter directs the attention to possible explanations for these effects and can be summarized as follows:

The explanation, generally accepted in the literature, stating that basolateral K^+-conductance increases, is also applicable here. In particular, the sensitivity for serosal Ba^{2+} confirms this. The results do not exclude the possibility that the K^+-conductance is coupled in some way to the activity of the Na/K-pump, that augments as well. The permanently elevated submucosal K^+-activity during control conditions might be explained by the possibility that ion concentration gradients exist in the cell and in the lateral interspace.

The results described in **Chapter 5** are directly connected with those of the previous two chapters.

Firstly experiments are presented, substantiating the relation between the Na^+- and Cl^--influx across the mucosal membrane. The way of coupling can also be outlined: an exchange of Na^+ and H^+ together with an exchange of HCO_3^- and Cl^-, intracellularly coupled with each other by the dissociation-equilibrium of H_2CO_3.

The existence of the bicarbonate permeability in the basolateral membrane, mentioned earlier, could be substantiated experimentally. Its precise character has not been determined.

Finally, the effects of serosally added Ba^{2+} on cellular properties and characteristics have been investigated further chemically. It could be shown that Ba^{2+} suppresses the basolateral K^+-conductance, which in turn changes the intercellular K^+-activity and thereby the activity of the Na/K-pump.

In order to understand more fully the consequences of the results, particularly from Chapter 4, the ion fluxes between the various compartments are more quantitatively analyzed in **Chapter 6.** Special attention is directed towards the relationship between the transport properties and the specially elongated structure of the epithelial cells in goldfish intestine.

The first step is the translation of the permeability data and potentials to fluxes across the membranes, both in the presence and absence of chloride and in transporting and non-transporting preparations. From the calculation of the balance of fluxes it appears that a net K^+-flux from serosa to mucosa is to be expected, which is

not in direct agreement with the observations (Chapter 4) that in the submucosal space an elevated potassium activity is measured. In addition, an increased basolateral K^+-conductance can be deduced from the flux calculations, especially when the epithelium is transporting. This is in agreement with the explanation for the secondary repolarization after mucosal glucose addition mentioned before.

Using a simple relationship diagram the succession of processes starting with the rheogenic influx of Na^+ and glucose has been delineated. The next step is the use of a semi-quantitative model, named the diffusional model. This model takes into account the diffusion velocities in the elongated compartments in the epithelium and the possibility that fluxes across the basolateral aspects of the cell membrane might vary depending on the distance from the tight junction (and -vice versa- the basal membrane). The enterocytes are very elongated and separated by a very narrow interspace, or lateral intercellular space, that makes contact with the mucosal solution through the tight junctions and with the serosal solution via the basal membrane. Data from this thesis and reasonable estimations from the literature are used to calculate the concentration profiles for Na^+ in the cell and for K^+ in the interspace in steady state and as a function of time after the onset of the glucose evoked changes.

The conclusion is that the submucosal K^+-activity and its response to glucose addition can only be explained quantitatively with additional assumption concerning the K^+-permeability of the basolateral membranes. The permeability changes might occur due to modulation by transepithelial water transport. This water transport in its turn is driven by the osmotic gradients due to active solute transport. This assumption is the more attractive as it can also explain the susceptibility of the repolarization for several experimental procedures.

In **Chapter 7** we compare our data concerning intracellular ion activities with those from a variety of other leaky epithelia as similar measurements in other other fish enterocytes are scarce. This chapter ends with a recapitulation of a number of essential assumptions, discussed in previous chapters, that need more explanation, such as the osmolarity in interspace and the rheogenicity of the Na/K-pump.

References

1. Albus H (1983) Intestinal transport of monosaccharides and neutral amino acids. An electrophysiological study. Academisch proefschrift. Universiteit van Amsterdam
2. Albus H, Bakker R, Siegenbeek van Heukelom J (1983) Circuit analysis of membrane potentials changes due to electrogenic sodium-dependent sugar transport in goldfish intestinal epithelium. Pflügers Arch. **398**: 1-9
3. Albus H, Groot JA, Siegenbeek van Heukelom J (1979) Effects of glucose and ouabain on transepithelial electrical resistance and cell volume in stripped and unstripped goldfish intestine. Pflügers Arch. **383**: 55-66
4. Albus H, Lippens F, Siegenbeek van Heukelom J (1983) Sodium-dependent sugar and amino acid transport in isolated goldfish intestinal epithelium: Electrophysiological evidence against direct interactions at the carrier level. Pflügers Arch. **398**: 10-17
5. Albus H, Siegenbeek van Heukelom J (1976) The electrophysiological characteristics of glucose absorption of the goldfish intestine as compared to mammalian intestines. Comp. Biochem. Physiol. **54A**: 113-119
6. Bakker R (1985) Electrophysiology of fish intestine. In: Transport processes, Iono and osmoregulation. (Eds. R. Gilles and M. Gilles-Baillien). Springer-Verlag, Heidelberg. pp 240-250.
7. Bakker R (1986) Feedback on potassium permeability by sodium-glucose cotransport in fish intestine. In: (Eds) F. Alvarado and C.H. van Os. Ion gradient-coupled transport; Inserm. Symp. No. 26. Elsevier Science Publishers, Amsterdam, p. 249
8. Bakker R, Dekker K, Zuidema T, Groot JA (1982) Transepithelial Cl-transport in goldfish Carassius Auratus intestinal mucosa and the effect of theophylline on fluxes and electrophysiology. 4th Conference of the European Society for Comparitive Physiology and Biochemistry, Bielefeld (FRG) 8-11 September 1982
9. Bakker R, Groot JA (1984) cAMP-mediated effects of ouabain and theophylline on paracellular ion selectivity. Am. J. Physiol. **246**: G213-G217
10. Groot JA (1981) Cell volume regulation in goldfish intestinal mucosa. Pflügers Archiv **392**: 67-71
11. Groot JA (1982) Aspects of the Physiology of the Intestinal Mucosa of the Goldfish (Carassius Auratus L). Thesis University Amsterdam. MultiCopy Amsterdam
12. Groot JA, Albus H, Bakker R, Dekker K (1983) Changes in sugar trans port and electrophysiological characteristics of intestinal preparations of temperature acclimated goldfish (Carassius auratus L.). J. Compar. Physiol. **151**: 163-170
13. Groot JA, Albus H, Bakker R, Siegenbeek van Heukelom J, Zuidema T (1983) Electrical phenomena in fish intestine. In: Intestinal transport (ed. M. Gilles-Baillien and R. Gilles), Springer-Verlag, Heidelberg. pp 321-340.
14. Groot JA, Albus H, Siegenbeek van Heukelom J (1979) A mechanistic explanation of the effect of potassium on goldfish intestinal transport. Pflügers Archiv **379**: 1-9
15. Groot JA, Bakker R, Dekker K, Oosterhuis W (1986) Modulation of transepithelial ion permeability by neurohumoral agents: comparison of fish and rat intestine. In: "Ion gradient-coupled transport" (eds. F. Alvarado and C.H. van Os), Elsevier Sci. Publ. pp 411-414.
16. Groot JA, Dekker K, Van Riel JW, Zuidema T (1982). Intracellular ion concentrations and pH of stripped mucosa of goldfish (Carassius Auratus) intestine in relation to Cl-transport. 4th Conference of the European Society for Comparitive Physiology and Biochemistry, Bielefeld (FRG), September 8-11, 1982.
17. Siegenbeek van Heukelom J (1978) The electrical characteristics of the absorptive goldfish intestinal epithelium. Gastroent. Clin. Biol. **2**: 329
18. Siegenbeek van Heukelom J (1986) Physiological aspects of absorption and secretion in intestine. Vet. Res. Commun. **10**:341-354.
19. Siegenbeek van Heukelom J, van den Ham MD, Albus H, Groot JA (1981) Microscopical determination of the filtration permeability of the mucosal surface of the goldfish intestinal epithelium. J. Membrane Biol. **63**: 31-39
20. Siegenbeek van Heukelom J, van den Ham MD, Dekker K (1982) The modulation by glucose transport of the electrical responses to hypertonic solutions of the goldfish intestinal epithelium. Pflügers Arch. **395**: 65-70
21. Siegenbeek van Heukelom J, Zuidema T (1985) The influence of Ba^{2+} on membrane potential and K^{+}-induced depolarizations in goldfish intestinal epithelium. J. Physiol. **366**: 92P
22. Siegenbeek van Heukelom J, Zuidema T, Kamermans M (1986) The role of the structure of epithelial compartments in transepithelial transport. In: Ion Gradient-Coupled Transport; INSERM Symposium No. 26, Editors: F. Alvarado and C.H. van Os, Elsevier Science Publishers B.V., Amsterdam
23. Zuidema T, Dekker K, Siegenbeek van Heukelom J (1985) The influence of organic counterions on junction potentials and measured membrane potentials. Bioelectrochem. Bioenerg. **14**: 479-494
24. Zuidema T, Groot JA, Siegenbeek van Heukelom (1981) Chloride transport in goldfish intestinal epithelium. 4th Meeting European Intestinal Transport Group, 30 aug. - 2 sept. Berlin.
25. Zuidema T, Kamermans M, Siegenbeek van Heukelom J (1983) The role of the intercellular compartment during glucose absorption. Interstitial and intracellular potassium activities in goldfish intestinal epithelium. Gastroenterol. Clin. Biol. **7**: 514
26. Zuidema T, Kamermans M, Siegenbeek van Heukelom J (1983) Interstitial and intracellular potassium activities during glucose absorption in goldfish intestinal epithelium. Arch. Int. Physiol. Biochim. **91**: P5
27. Zuidema T, Kamermans M, Siegenbeek van Heukelom J (1986) Influence of glucose absorption on ion activities in cells and submucosal space in goldfish intestine. Pflügers Arch. **407**: 292-298
28. Zuidema T, Siegenbeek van Heukelom J, Kamermans M, Groot JA (1982) The transmembrane glucose evoked potential in goldfish Carassius Auratus L. intestinal epithelium and the role of the extracellular space. 4th conference of the European Society for Comparative Physiology and Biochemistry, Bielefeld (FRG) 8-11 September 1982.
29. Zuidema T, Van Riel JW, Siegenbeek van Heukelom J (1985) Cellular and transepithelial responses of goldfish intestinal epithelium to chloride substitutions. J. Membrane Biol. **88**: 293-304

Samenvatting

Eén van de belangrijkste eigenschappen van darmepitheel is, dat het in staat is aanzienlijke hoeveelheden zouten en voedingsstoffen tegen een koncentratiegradiënt in van het darmlumen (mucosa) naar het bloed (serosa) te transporteren. Dit gaat gepaard met watertransport, zodanig dat de toniciteit van de getransporteerde vloeistof min of meer konstant blijft. Over de mechanismen die hiervoor verantwoordelijk zijn, is, althans kwalitatief, al veel bekend. Essentieel in alle, meer recente, verklaringen van 'aktief' epitheliaal transport is de werking van de zgn. Na/K-pomp in het basolaterale membraan, die een ongelijke verdeling onderhoudt voor Na^+- en K^+-koncentraties binnen en buiten de cel. Gespecialiseerde koppelingsmechanismen maken gebruik van de energie opgeslagen in deze koncentratieverschillen (de chemische potentiaal van de betrokken ionen) om suikers, aminozuren en ionen de cel in of juist uit te drijven. Door het polaire karakter van deze mechanismen ontstaat transcellulair stoftransport. Hierbij speelt ook de relatief hoge kaliumpermeabiliteit van de celmembranen een belangrijke rol, die immers het chemisch potentiaalverschil van K^+ over de membranen via de membraanpotentiaal beschikbaar maakt als drijvende kracht voor rheogeen transport d.w.z. deeltjestransport waarbij netto lading wordt verplaatst. De lokale verschillen in osmolariteit, binnen en buiten de cel, die het gevolg zijn van stoftransport, leveren tenslotte de osmotische drukverschillen die drijvende kracht zijn voor watertransport.

In dit proefschrift wordt verslag gedaan van elektrofysiologische experimenten en modelberekeningen die erop gericht zijn een aantal van de bovenstaande mechanismen voor energieoverdracht in de goudvisdarm verder te karakteriseren en te kwantificeren. Daarbij is, wat de experimentele kant betreft, gebruik gemaakt van ionselektieve mikroelektroden. Het onderzoek vormt een onderdeel van het onderzoeksprogramma van de groep membraanfysiologie van de vakgroep Algemene Dierkunde waarvan reeds eerder publikaties verschenen van H. Albus [1-5], R. Bakker [6-9], J.A. Groot [10-16] en J. Siegenbeek van Heukelom [17-22]. Voor verwijzingen: zie Engelstalige samenvatting.

In **Hoofdstuk 1** wordt na een korte bespreking van het door ons gebruikte preparaat, een overzicht gegeven van de historische achtergronden van ons onderzoek, waarbij drie hoofdlijnen worden onderscheiden: de ontwikkeling van modellen voor watertransport,

voor suiker- en aminozuurtransport en, het meest recent, voor chloridetransport. Binnen deze historische kontekst wordt vervolgens besproken waar de aangrijpingspunten liggen voor elektrofysiologisch werk met behulp van gewone en ion-gevoelige mikroelektroden en worden de doelstellingen van het onderhavige onderzoek samengevat:

- de bepaling van de permeabiliteitseigenschappen van de plasmamembranen door meting en analyse van membraan-potentialen en intracellulaire aktiviteiten, zowel onder kontrole-kondities als tijdens unilaterale en bilaterale ionsubstituties.
- de identifikatie van ionbewegingen die het gevolg zijn van aktief rheogeen transport van Na^+ en glucose en van de koppelingsmechanismen tussen mucosale cotransportsystemen en de basolaterale Na/K-pomp; dit alles door meting en analyse van membraanpotentialen, intracellulaire en interstitiële aktiviteiten, voor, tijdens en na het begin van glucose-absorptie, onder diverse experimentele kondities.
- daarnaast bleek in de praktijk een theoretisch en experimenteel onderzoek noodzakelijk naar wat de door ons gekonstrueerde ion-gevoelige mikroelektrode feitelijk meet, zowel in de cel als in biologische oplossingen, om artefacten en dubbelzinnige interpretaties zoveel mogelijk te elimineren.

Het hoofdstuk wordt afgesloten met enige paragrafen over gebruikte methoden en technieken en een lijst van veelvuldig gebruikte symbolen.

In **Hoofdstuk 2** wordt de oorzaak onderzocht van een verandering in circuitpotentiaal van ongeveer -4 mV bij kontrolemetingen met kation-gevoelige mikroelektroden in chloride-vrije oplossingen (chloride gesubstitueerd door grote organische anionen zoals glucuronaat of gluconaat). Dit impliceert een daling van ca. 15% in de schijnbare kationaktiviteit in zulke oplossingen, hoewel de totale kationkoncentratie gelijk is gehouden. Uit osmolariteitsmetingen wordt gekonkludeerd dat er geen reden is om aan te nemen dat sprake is van sterke ion-associatie. Ook kunnen elektrode-artefacten van de iongevoelige elektrode redelijkerwijs worden uitgesloten zodat het effekt is terug te brengen tot een elektrode-artefact aan het kontaktoppervlak van de referentie-elektrode en/of tot een afname van de kation-aktiviteiten in de betrokken oplossingen. Op theoretische gronden kan daartussen niet worden gekozen, zodat de meting van bijv. de K^+-aktiviteit in een chloride-vrije oplossing altijd een element van onzekerheid bevat. Het betekent wel dat bij meting van de membraanpotentiaal gedurende chloridesubstituties een referentie-elektrode verbonden door een zoutbrug aanzienlijke artefacten veroorzaakt die slechts kunnen worden voorkomen door direkt een kation-gevoelige referentie-elektrode te gebruiken, of althans achteraf daarnaar te korrigeren.

Hoofdstuk 3 beschrijft een uitgebreid onderzoek naar de permeabiliteitseigenschappen van de beide celmembranen. Metingen worden gepresenteerd van membraanpotentialen, transepitheliale potentialen, intracellulaire ionaktiviteiten van Na^+, K^+ en Cl^- alsmede van transepitheliale weerstand en weerstandsratio R_m/R_s onder kontrolekondities. Dezelfde metingen zijn gedaan bij dubbelzijdige chloridevervangingen, terwijl de elektrische metingen bovendien zijn uitgevoerd bij eenzijdige chloridevervangingen. Celvolume, intracellulaire pH en ionenkoncentraties van Na^+, K^+ en Cl^- zijn bepaald onder kontrolekondities en bij tweezijdige chloridevervanging. Tenslotte zijn intracellulaire chloride-aktiviteit en -koncentratie ook nog gemeten bij enkelzijdige chloridevervanging.

Uit de analyse van deze resultaten met behulp van een elektrisch equivalent circuit en evaluatie van de permeabiliteitsverhoudingen met een aangepaste vorm van de Goldman-Hodgkin-Katz-vergelijking kan worden gekonkludeerd tot een elektroneutraal chloride influxmechanisme in het mucosaal membraan. Van de berekende permeabiliteiten is het meest opvallend de hoge permeabiliteit voor chloride in het basolaterale membraan. Bovendien wordt een niet te verwaarlozen permeabiliteit voor bicarbonaat gevonden in het basolaterale membraan.

De membraanpotentiaal van goudvisdarmepitheel vertoont een zeer karakteristieke responsie op mucosale aanbieding van glucose. Deze responsie bestaat uit een snelle depolarizatie die wordt gevolgd door een langzamere repolarizatie. Tijdens deze responsie treedt een blijvende verhoging op in de Na^+-aktiviteit in de cel en een transiente verhoging in de K^+-aktiviteit in de submucosale (interstitiële) ruimte, juist achter de cel, welke trouwens ook in kontrolesituatie al enigszins is verhoogd t.o.v. de badmedia. Deze metingen, alsmede die van de intracellulaire K^+- en Cl^--aktiviteit worden gepresenteerd in **Hoofdstuk 4.**

Weglating van chloride uit de badmedia heeft een aanzienlijk hyperpolarizatie tot gevolg met een gelijktijdige verlaging van de submucosale K^+-aktiviteit. Bij aanbieding van glucose blijft nu de repolarizatie achterwege. Wel vertonen de intracellulaire Na^+-

aktiviteit en de interstitiële K^+-aktiviteit de normale verhoging.

Zowel serosaal aangeboden barium (5 mM), als eenzijdige K^+-verhoging depolarizeert het membraan en onderdrukt de eerder genoemde repolarizatie.

De diskussie in dit hoofdstuk richt zich op de mogelijke verklaringen van deze effekten en kan als volgt worden samengevat:

De in de literatuur vrij algemeen aanvaarde verklaring voor de repolarizatie, n.l. een toename van de relatieve K^+-geleidbaarheid van het basolaterale membraan, is ook hier toepasbaar. Vooral het feit dat deze Ba^{2+}-gevoelig is, bevestigt deze opvatting. Het is niet onmogelijk dat de K^+-geleidbaarheid op enigerlei wijze is gekoppeld aan de aktiviteit van de Na/K-pomp, welke immers ook toeneemt. De permanente verhoging van de submucosale K^+-aktiviteit onder kontrolekondities roept vragen op over het bestaan van koncentratiegradiënten niet alleen buiten, maar ook binnen de cel.

De resultaten beschreven in **Hoofdstuk 5** sluiten direkt aan op de bevindingen in de voorgaande twee hoofdstukken.

Eerst worden de experimenten gepresenteerd, die de koppeling aantonen tussen Na^+- en Cl^--influx over het mucosale membraan. Bovendien wordt met deze resultaten de manier waarop deze koppeling plaats vindt verklaard: een uitwisseling van Na^+ en H^+ en een uitwisseling van HCO_3^- en Cl^-, die intracellulair met elkaar zijn verbonden door het dissociatie-evenwicht van H_2CO_3.

Het bestaan van de al eerder genoemde bicarbonaatpermeabiliteit van het basolaterale membraan wordt experimenteel ondersteund, hoewel het precieze karakter hiervan niet kan worden vastgesteld.

Tenslotte worden de effekten bestudeerd van serosale Ba^{2+}-aanbieding op een aantal grootheden en karakteristieke responsies. Aangetoond wordt dat Ba^{2+} inderdaad de basolaterale K^+-geleidbaarheid onderdrukt, welke, waarschijnlijk door zijn invloed op de intercellulaire K^+-aktiviteit, in belangrijke mate de aktiviteit van de Na/K-pomp bepaalt.

Om een beter inzicht te krijgen in de konsekwenties van de resultaten van met name hoofdstuk 4 wordt in **Hoofdstuk 6** meer kwantitatief ingegaan op de ion-fluxen tussen de verschillende kompartimenten en wordt de eventuele relatie onderzocht met de struktuur van de epitheelcellen in goudvisdarm.

Allereerst worden uit de gegevens over permeabiliteits-eigenschappen en potentialen de fluxen berekend over de verschillende membranen, in de aan- en in de afwezigheid van chloride, voor wel-

en voor niet-glucose-transporterend epitheel. Uit de balans blijkt dat netto transcellulair K^+-transport van serosa naar mucosa moet worden verwacht, hetgeen niet direkt in overeenstemming is met waarnemingen dat aan de voet van de cellen de extracellulaire K^+-aktiviteit is verhoogd (Hoofdstuk 4). Wel wijzen de resultaten op een toename van de basolaterale K^+-geleidbaarheid in glucose-transporterend epitheel die mogelijk in verband kan worden gebracht met de al eerder genoemde sekundaire repolarizatie van de membraanpotentiaal na glucose-aanbieding.

Daartoe wordt vervolgens aan de hand van een eenvoudig pijldiagram de opeenvolging van processen besproken die begint met de rheogene influx van Na^+ en glucose. De processen worden verder geanalyseerd met een semi-kwantitatief model. Dit 'diffusiemodel' houdt rekening met eindige diffusiesnelheden in langgerekte kompartimenten, en met de mogelijkheid dat fluxen van het ene naar het andere kompartiment niet homogeen verdeeld zijn over het grensvlak tussen die kompartimenten. Epitheelcellen zijn immers zeer langgerekt en worden gescheiden door een zeer nauwe tussenruimte, de intercellulaire ruimte, die kontakt maakt met de mucosale vloeistof via de tight junctions en met de serosale vloeistof via het basale membraan. Door ons gemeten grootheden en redelijke schattingen uit de literatuur worden gebruikt om transepitheliale koncentratieprofielen te berekenen van intracellulair Na en extracellulair K in steady state en als funktie van de tijd na glucose-aanbieding.

De konklusie is dat de submucosale verhoging van de K^+-aktiviteit en de responsie hiervan op glucoseaanbieding alleen kwantitatief verklaard kunnen worden met extra aannames over de basolaterale K^+-geleidbaarheid. Deze zou bijvoorbeeld gemoduleerd kunnen worden door transcellulair watertransport. Dit watertransport wordt op zijn beurt weer gedreven door osmotische gradiënten die ontstaan door aktief stoftransport. Deze aanname is des te aantrekkelijker omdat daarmee tevens de gevoeligheid van de repolarizatie voor diverse experimentele ingrepen kan worden verklaard.

In **Hoofdstuk 7** worden, aangezien er in het algemeen weinig bekend is over ion-aktiviteiten in vissedarm, de door ons gevonden aktiviteiten in goudvisdarmepitheel vergeleken met literatuurwaarden voor andere lekke epithelia. Tenslotte worden enige vrij essentiële aannames besproken uit eerdere hoofdstukken die nog toelichting behoefden, zoals bijv. de osmolariteit in de intercellulaire ruimte en de rheogeniciteit van de Na/K-pomp.

Stellingen

behorende bij het proefschrift
"Monovalent ions and glucose absorption in goldfish intestine"
door T. Zuidema

I. De afwijking in elektrode-potentiaal van kation-gevoelige elektroden in oplossingen met grote anorganische anionen kan op soortgelijke wijze verklaard worden als het Pallman-effekt.
(J.Th.G. Overbeek (1953), J. Colloid Sci. **8**: 593-607; dit proefschrift)

II. Het negeren van zoutbrug-artefacten bij elektrofysiologische metingen tijdens ion-substituties met grote anorganische ionen kan aanleiding geven tot foutieve interpretaties. Aan dit probleem wordt in de elektrofysiologische literatuur te weinig aandacht gegeven.
(Dit proefschrift)

III. Normeringsafspraken voor fysiologische media zouden de vergelijkbaarheid van experimentele resultaten bevorderen en de experimentele fysiologie een meer kwantitatief karakter verlenen.

IV. Bij de interpretatie van de membraandepolarizaties ten gevolge van K^+-verhoging in de peritubulaire badvloeistof dient rekening te worden gehouden met de tijdelijke verhoging van de intercellulaire K^+-aktiviteit bij luminale aanbieding van suikers.
(G. Messner et al (1985), Pflügers Arch. **404**: 138-144; dit proefschrift)

V. De vergelijkingen 34, 35 en 40 van het artikel "Electrical analysis of intraepithelial barriers" van Boulpaep en Sackin zijn onjuist en nodeloos ingewikkeld.
(E.L. Boulpaep, H Sackin (1980), In: Current topics in Membranes and Transport Vol. 13, Ch. 12; A.van Rotterdam pers.comm.)

VI. Het woord potentiaal heeft in de elektrofysiologische literatuur nieuwe betekenissen gekregen die afwijken van de fysische definitie.

VII. Een visuele stimulus van afwisselend scherpe en onscherpe, doch verder gelijke, patronen geeft bij de mens aanleiding tot relatief eenvoudige occipitale Visual Evoked Potentials (VEP's) die zich goed lenen voor objektieve bepaling van de gezichtsscherpte.
(O. Estévez U., pers. comm.)

VIII. Verlofregelingen voor onderwijspersoneel moedigen allerminst aan tot nascholing en zelfstudie.

IX. Het systeem van schoolonderzoeken als onderdeel van de eindexamens in het voortgezet onderwijs is inefficiënt, vormt een onnodige belasting van de leerling en verstoort het leerproces.

X. Hantering van het begrip "mantel"-zorg is misleidend wanneer dit betekent dat gehandicapten en hun huisgenoten in de kou worden gezet door een tekort aan professionele thuiszorg.

XI. Een provinciale overheid die een voor wielrenners aantrekkelijk rijwielpad aanlegt in een traditioneel wandelgebied voor hondenliefhebbers veroorzaakt animositeit en is terecht de gebeten hond (Visserspad, Overveen-Zandvoort).

XII. Het is een hoopvolle gedachte dat een systeem van apart-heid, fysisch gezien, een geringe entropie bezit.

XIII. Marathonlopers en promovendi hebben veel gemeen. Alleen krijgen de laatsten zelden de gelegenheid hun persoonlijke tijd te verbeteren.